PNAMP Special Publication: Remote Sensing Applications for Aquatic Resource Monitoring

Results of a Special Session at the
2008 ASPRS Annual Conference

Cover: This image shows true color digital imagery draped over a LiDAR derived 1st return model of Trail Creek, Oregon. The 3-D view also shows vector layers identifying stream bankfull (red), flood-prone (green), and valley floor (blue) elevations created from a LiDAR bare earth model. Image courtesy of Russ Faux, Watershed Sciences.

PNAMP Special Publication: Remote Sensing Applications for Aquatic Resource Monitoring

Editors:
Jennifer M. Bayer
Jacquelyn L. Schei

Pacific Northwest Aquatic Monitoring Partnership
in association with
Puget Sound Region of the American Society
for Photogrammetry and Remote Sensing

Suggested citation formats:

Entire publication
Bayer, J.M., and Schei, J.L., eds., 2009, PNAMP Special Publication: Remote Sensing Applications for Aquatic Resource Monitoring, Pacific Northwest Aquatic Monitoring Partnership, Cook, Washington, 100 p.

Chapter within the publication
Kinzel, P.J., 2009, Advanced tools for River Science: EAARL and MD_SWMS, *in* Bayer, J.M., and Schei, J.L., eds., PNAMP Special Publication: Remote Sensing Applications for Aquatic Resource Monitoring, Pacific Northwest Aquatic Monitoring Partnership, Cook, Washington, chap. 3, p. 17-26.

Contents

Acknowledgments

Thanks to the contributors to the conference session and this publication and to the American Society for Photogrammetry and Remote Sensing (ASPRS) for hosting the session at their 2008 Annual Conference. Conference organizers, presenters, and expert panel discussion participants included Mike Beaty, Jennifer Bountry, Mimi D'Iorio, Peter Eldred, Russ Faux, Ralph Garono, Ralph Haugerud, Dan Isaak, Paul Kinzel, Jim McKean, Melinda Moeur, Amar Nayegandhi, Ken Tiffan, Nancy Tubbs, Paul Wagner, and Keith Wolf. Thanks to Rick Champion, Tom Frost, Deanna Jacobsen, Frank McCormick, and Keith Wolf for conducting peer review of the papers included in this publication.

In addition, we thank the session helpers and the Puget Sound Region of ASPRS for their support.

We thank the Pacific Northwest Aquatic Monitoring Partnership (PNAMP) Steering Committee for their support and the entities that provide funding for PNAMP coordination.

Special thanks to Keith Wolf for proposing and facilitating the collaboration between PNAMP and the ASPRS Puget Sound Region that yielded not only this product but also a great start to future collaborations and also for his assistance with the executive summary.

Executive Summary

Each year millions of dollars are spent to monitor the status and trend of natural resources and determine the effectiveness of restoration programs in the Pacific Northwest. Although there is increasing consensus among regional, Federal, private, State, Tribal, and stakeholder organizations with respect to the need for integrated and standardized monitoring information, funding for these activities is stagnant or decreasing. As a result, there is an increasing need to improve the efficiency and cost effectiveness of monitoring programs.

Natural resource managers currently largely rely on traditional assessment methods to determine watershed health, habitat condition and the behavior and status of individual animals or groups of animals. The information collected is then used in many diverse biological and ecological science and policy forums, often with significant management implications. Although current programs use various techniques to assess population status and trends and habitat condition, the statistical design and methods associated with these programs often address a limited number, or, individual hypotheses. In some cases, the information provided using these methods is not sufficient to understand sources of data variability or causative mechanisms, or to aid in the selection of corrective actions if needed. Similarly, these programs are unable to provide regionally comparable or spatially relevant information. We believe it is essential to improve our ability to gather comparable data, examine the suitability of current designs and methods to address regional monitoring needs, and to consider new tools and resources to complement traditional approaches.

Thus, the Pacific Northwest Aquatic Monitoring Partnership (PNAMP) has recognized a need to improve the availability of information about remote sensing applications that are used in the monitoring arena. This is one of several monitoring tools, but it is a powerful addition to existing methods. To this end, and as an outlet for information about some current uses of remote sensing in the Pacific Northwest, PNAMP hosted a special session at the 2008 American Society for Photogrammetry and Remote Sensing (ASPRS) Annual Meeting. The special session, titled “Remote Sensing Applications for Aquatic Resource Monitoring,” was intended to share some current applications of remote sensing techniques in aquatic resource monitoring and to raise awareness in the remote sensing community of the need for improved remote sensing applications.

The session included 11 presentations of current applications of remote sensing in aquatic resource monitoring, which provide the basis for the papers included in this volume. The session concluded with an expert panel discussion that focused on current technologies and needs these technologies address. In addition, participants were asked to discuss other potential uses of current technologies and the development of new tools and their application in the monitoring arena. Much of the expert panel discussion, session presentations, and papers in this volume addressed three varieties of airborne LiDAR (LIght Detection And Ranging) instrument; thus, we offer a brief description of these technologies as part of the introduction to the expert panel discussion (chapter 12, this volume). We note these three central topics are part of several remote sensing data acquisition methods; other methods include satellite imagery, and some ground-based methods.

As a result of the special session, PNAMP has started a greater dialog among its members about remote sensing applications in aquatic resource monitoring and affiliations with experts in the field of remote sensing. This dialog suggests that as advances in remote-sensing technology are improving the quality and quantity of topographic data available, there is strong likelihood that more precise and cost-effective data can be collected in coordination with traditional ground survey-based habitat assessment techniques. PNAMP would like to continue to facilitate these discussions, to include a comparison of the cost, benefits, and tradeoffs of remote sensing technique integration with ground surveys. It is our hope that this dialog will increase awareness, expand the use of remote sensing techniques in aquatic resource monitoring, and create impetus for development of new remote sensing applications. In 2009, PNAMP will work with the American Fisheries Society’s Washington and British Columbia Chapter to host a larger regional symposium that builds upon the impetus and depth-of-knowledge approach that began with ASPRS and PNAMP remote sensing specialists.

In closing, there is a fundamental need to improve information available to natural resources managers and decision processes. Categorical investigations to inform ecosystem-driven scientific effort and especially management decisions by State, Federal, and Tribal governments are complex and numerous. Although some monitoring questions are unique to particular agencies and organizations, the need for comprehensive and efficient collection of information on metrics and indicators on all or certain aspects of the status and trend of fish, habitat, and watershed health is common to entities involved in monitoring in the Pacific Northwest. By applying well-coordinated monitoring approaches, technical and fiscal resources can be more effectively shared among interested parties, data can be shared, resulting information can provide increased scientific credibility, and allow greater accountability to stakeholders. In particular, economies of scale, shared interests, and multiple-use data suggest that it would be good to pool monitoring funds from multiple agencies for acquisition of remotely-sensed data. PNAMP will strive to provide leadership through the development and advancement of recommendations and agency level agreements that are considered for adoption by the participating agencies to this end.

This page left intentionally blank

Chapter 1.—EAARL: An Airborne LiDAR System for Mapping Coastal and Riverine Environments

Amar Nayegandhi[1], C.W. Wright[2], and J.C. Brock[3]

Abstract

LiDAR, an acronym for Light Detection and Ranging, is an active remote sensing technique that determines the distance between the sensor and the target by accurately measuring the round-trip time of a pulse of laser energy (Wehr and Lohr, 1999). The Experimental Advanced Airborne Research Lidar (EAARL) is an airborne LiDAR system that provides unique capabilities to survey coral reefs, nearshore benthic habitats, coastal vegetation, and sandy beaches (Wright and Brock, 2002). Operating in the blue-green portion of the electromagnetic spectrum, the EAARL is specifically designed to measure submerged topography and adjacent coastal land altitudes in a single scan of transmitted laser pulses (fig. 1). Four main features separate the EAARL from traditional airborne bathymetric LiDAR: (1) a relatively short (1.3 ns) laser pulse, (2) a radically narrowed receiver field-of-view (FOV)(1.5–2 mrad), (3) digitized signal temporal backscatter amplitude waveforms, and (4) software as opposed to hardware implementation of real-time signal-processing elements. The short pulse and narrow FOV are beneficial in coastal environments to determine bare-Earth topography under short vegetation, as well as in riverine environments where large changes in topography occur over a very small area. The small receiver FOV rejects ambient light and

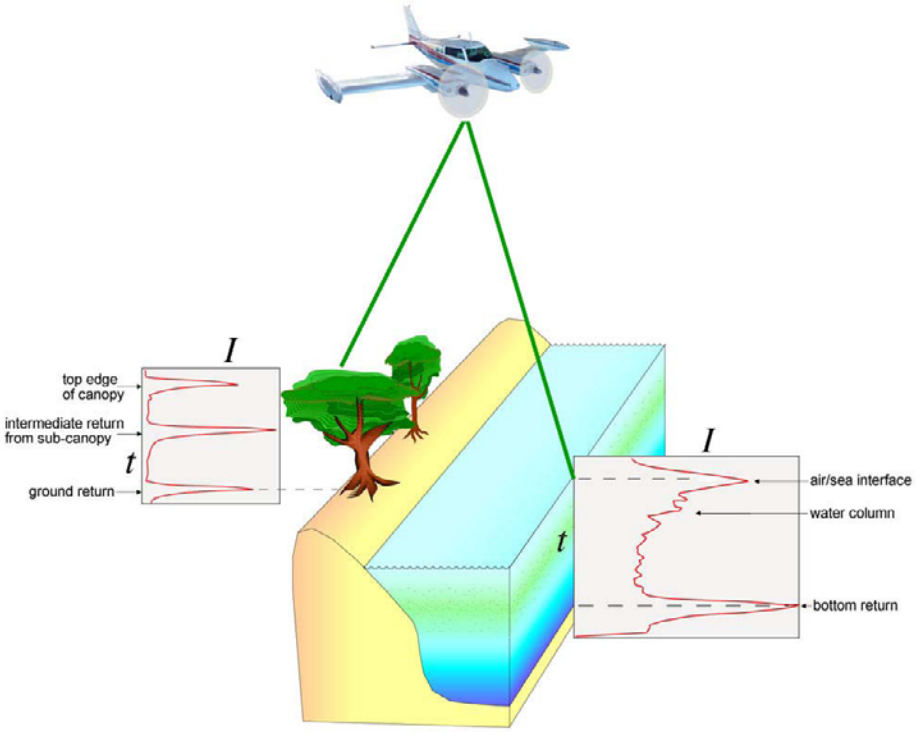

Figure 1. The EAARL system senses and records LiDAR backscatter returned to the sensor (*I*) in a series of equal time intervals (*t*) at 1 nanosecond resolution, thereby enabling the seamless characterization of sub-aerial and submerged topography.

[1]Jacobs Technology, Inc. Contracted to U.S. Geological Survey, 600 4th St. South, St. Petersburg, FL 33701. anayegandhi@usgs.gov

[2]U.S. Geological Survey, 600 4th St. South, St. Petersburg, FL 33701. wwright@usgs.gov

[3]U.S. Geological Survey, Coastal and Marine Geology Program, Reston, VA 20192. jbrock@usgs.gov

multiplies scattered photons from the water column and bottom-reflected backscatter (Feygels et al., 2003), thereby ensuring relatively high contrast and short duration of the bottom return signal. The EAARL system can accommodate a large signal dynamic range, thereby making it suited to mapping topography over a variety of reflective surfaces in the coastal zone, ranging from bright sand to dark submerged sea-bottom.

EAARL uses a very low-power, eye-safe laser pulse, in comparison to a traditional bathymetric LiDAR system that allows for a much higher pulse-repetition frequency (PRF) and significantly less laser energy per pulse (approximately 1/70th) than do most bathymetric LiDARs. The laser transmitter produces up to 10,000 short-duration (1.3 ns), low-power (70 µJ), 532-nm-wavelength pulses each second. The energy of each laser pulse is focused in an area roughly 20 cm in diameter when operating at a 300-m altitude. Based on test flights over typical Caribbean coral reef environments, EAARL has demonstrated penetration to greater than 25 m, and can routinely map coral reefs ranging in depth from 0.5 to 20 m below the water surface.

The EAARL system uses a "digitizer only" design, which eliminates all hardware-based high-speed front-end electronics, start/stop detectors, time-interval units, range gates, etc., typically found in LiDAR systems. The EAARL system instead uses an array of four high-speed waveform digitizers connected to an array of four sub-nanosecond photo-detectors. Real-time software is used to implement the system functions normally done in hardware. Each photo-detector receives a fraction of the returning laser backscattered photons. The most sensitive channel receives 90% of the photons, the least sensitive receives 0.9%, and the middle channel receives 9%. The fourth channel is available for either water Raman or 1064-nm infrared backscatter depending on the application. All four channels are digitized synchronously with digitization beginning a few nanoseconds before the laser is triggered and ending as long as 16,000 ns later. A small portion of the outgoing laser pulse is sampled by fiber optic and injected in front of one of the photo-detectors to capture the actual shape, timing, and amplitude of the laser pulse shortly after it is generated. The backscattered laser energy for each laser pulse is digitized into 65,536 samples, resulting in more than 150 million digital measurements being taken every second. The resulting waveforms are partially analyzed in real time to locate the key features such as the digitized transmit pulse, the first return, and the last return. The real-time waveform processor automatically adapts to each laser return waveform and retains only the relevant portions of the waveform for recording. Thus, the storage space required for returns from tall trees or deep water is more than the storage requirement for beach or shallow water backscatter. In addition to the LiDAR, the EAARL sensor suite includes a digital three-band color infrared camera, a red-green-blue (RGB) digital camera, a dynamically tuned Inertial Measurement Unit (IMU), and precision kinematic Global Positioning System (GPS) receivers that together provide for sub-meter geo-referencing of each laser and photographic pixel.

Post-processing of EAARL data is accomplished using a custom-built Airborne Lidar Processing System (ALPS) that combines laser return backscatter digitized at 1-ns intervals with aircraft positioning data derived from the IMU and GPS receivers. The ALPS software enables the exploration and processing of LiDAR waveforms and the creation of Digital Elevation Models (DEMs) for bare-Earth, canopy-top, submerged topography, and vegetation canopy structure. The EAARL system utilizes Earth-centered coordinate and reference systems, thereby eliminating the need for referencing submerged topography data to relative water level or tide gauges.

The EAARL has been operational since the summer of 2001, when it was used to survey the coral reef tract in the northern Florida Keys (Wright and Brock, 2002; Brock et al., 2004). Subsequent surveys in 2002, 2004, and 2006 along the Florida reef tract have enabled the creation of submerged topography products at Biscayne National Park (Brock et al., 2006a), Florida Keys National Marine Sanctuary (Brock et al., 2007), and Dry Tortugas National Park (Brock et al., 2006b). Several surveys have been conducted using the EAARL system in a variety of coastal communities, including barrier islands along the Atlantic coast (Nayegandhi et al., 2005) and around the margins of an urbanized Gulf of Mexico estuary (Brock et al., 2002; Nayegandhi et al., 2006). An EAARL survey also was conducted along the Platte River in central Nebraska in March 2002 (Kinzel and Wright, 2002). The Platte River is a braided sand-bedded river that presents technological and logistical challenges with regard to collecting topographic and bathymetric measurements. The vertical accuracy of the system when compared with Real-Time-Kinematic (RTK) GPS surveys was estimated to be 16–22 cm root mean square error (RMSE) in the Platte River (Kinzel and Wright, 2002). Subsequent shallow river surveys conducted in the Lower Boise River, Idaho, yielded vertical accuracies of 14–18 cm RMSE (unpublished data). Further studies have estimated the vertical accuracy of the EAARL system to range from 10 to 14 cm (RMSE) for submerged topography (0.1–2.5 m water depth) and 16–20 cm for sub-canopy topography under a variety of dense coastal vegetation communities along the margins of Tampa Bay, Florida (Nayegandhi et al., in press).

Specific design considerations for the EAARL system, which make it an ideal system for mapping the topography and morphologic habitat complexity of shallow reef substrates, include the high spatial (20-cm-surface footprint at nominal flying altitude of 300 m AGL) and sample (1-ns digitizing interval) resolution. The EAARL system also is designed to map substrates in shallow water (<5 m) where traditional hydroacoustic ship-borne instruments cannot operate efficiently, field surveys are time-consuming and cost-prohibitive, and traditional bathymetric LiDARs are not applicable. These design considerations also are uniquely well suited for the seamless and simultaneous mapping of shallow, clear channel-bed topography in rivers and streams, and for resolving the bare-Earth topography of the surrounding floodplain.

References

Brock, J.C., Wright, C.W., Clayton, T.D., and Nayegandhi, A., 2004, Optical rugosity of coral reefs in Biscayne National Park, Florida: Coral Reefs, v. 23, p. 48-59.

Brock, J.C., Wright, C.W., Nayegandhi, A., Clayton, T., Hansen, M., Longenecker, J., Gesch, D., and Crane, M., 2002, Initial results from a test of the NASA EAARL LiDAR in the Tampa Bay Region: Proceedings of the 2002 Gulf Coast Association of Geological Societies Conference (CD-ROM).

Brock, J.C., Wright, C.W., Patterson, M., Nayegandhi, A., Patterson, J., Harris, M.S., and Mosher, L., 2006a, USGS-NPS-NASA EAARL Submarine Topography – Biscayne National Park: U.S. Geological Survey Open-File Report 2006-1118 (DVD).

Brock, J.C., Wright, C.W., Patterson, M., Nayegandhi, A., and Patterson, J., 2006b, USGS-NPS-NASA EAARL Submarine Topography – Dry Tortugas National Park: U.S. Geological Survey Open-File Report 2006-1244 (DVD).

Brock, J.C., Wright, C.W., Nayegandhi, A., Woolard, J., Patterson, M., Wilson, I., and Travers, L., 2007, USGS-NPS-NASA EAARL Submarine Topography – Florida Keys National Marine Sanctuary: U.S. Geological Survey Open-File Report 2007-1395 (DVD).

Feygels, V.I., Wright, C.W., and Kopilevich, Y.I., 2003, Narrow field-of-view bathymetric LiDAR: theory and field test, *in* Frouin, R.J., Gilbert, G.D., and Pan, D. (eds), Ocean Remote Sensing and Imaging II, Proceedings of the SPIE, v. 5155, p. 1-11.

Kinzel, P.J., and Wright, C.W., 2002, Evaluation of EAARL, an experimental bathymetric and terrestrial LIDAR, for collecting river channel topography along the Platte River, Nebraska: Geological Society of America, Abstracts with Programs, v. 34, no. 6, p. 232.

Nayegandhi, A., Brock, J.C., and Wright, C.W., in press, Small-footprint, waveform-resolving LiDAR estimation of submerged and sub-canopy topography in coastal environments: International Journal of Remote Sensing.

Nayegandhi, A., Brock, J.C., Wright, C.W., and O'Connell, M.O., 2006, Evaluating a small-footprint, waveform-resolving LiDAR over coastal vegetation communities: Photogrammetric Engineering and Remote Sensing, v. 12, p. 1408-1417.

Nayegandhi, A., Brock J.C., and Wright, C.W., 2005, Classifying vegetation using NASA's Experimental Advanced Airborne Research LiDAR (EAARL) at Assateague Island National Seashore: Proceedings of the American Society of Photogrammetry and Remote Sensing Annual Conference, Baltimore, MD (CD-ROM).

Wehr, A., and Lohr, U., 1999, Airborne laser scanning – an introduction and overview: Journal of Photogrammetry and Remote Sensing, v. 54, p. 68-82.

Wright, C.W., and Brock, J.C., 2002, EAARL: A LiDAR for mapping shallow coral reefs and other coastal environments: Proceedings of the 7th International Conference on Remote Sensing for Marine and Coastal Environments, Miami, FL (CD-ROM).

This page left intentionally blank

Chapter 2.—Stream and Riparian Habitat Analysis and Monitoring with a High-Resolution Terrestrial-Aquatic LiDAR

Jim McKean[1], Dan Isaak[1], and Wayne Wright[2]

Abstract

Management of aquatic habitat in streams requires description of conditions and processes both inside the channels and in the adjacent riparian zones. Biological and physical processes in these environments operate over a range of spatial scales from microhabitat to whole river networks. Limitations of previous survey technologies have focused management and research activities on either ends of this spectrum. Environmental monitoring also is very challenging as habitat conditions and specie use can vary over a wide range of temporal scales. We used a narrow-beam airborne green LiDAR, the Experimental Advanced Airborne Research LiDAR (EAARL), to study channel and floodplain conditions and processes at length scales from several meters to tens of kilometers with a spatial resolution of about 1 meter. We also monitored channel change over a period of 3 years using repeated EAARL surveys. The EAARL mapped beds of channels correctly, but tended to smooth the edges of steep banks. In 10 kilometers of unconfined channel, there is a hierarchy of spatial scales of salmon spawning habitat controlled by a combination of post-glacial valley evolution and modern channel hydraulics. Wavelets are a powerful technique to analyze the continuous EAARL data and describe habitat distribution in the frequency domain. This terrestrial-aquatic LiDAR could catalyze rapid advances in understanding, managing, and monitoring aquatic ecosystems.

Introduction

Integrated management of stream and riparian habitat is hampered by a limited ability to define, analyze, and monitor the basic topographic template on which physical and biological processes operate, particularly inside active channels. Detailed stream studies have been of restricted spatial extent because of costs and logistics; consequently, it has been difficult to analyze process interactions and habitat among larger channel domains or to extrapolate to the scale of whole stream networks. Earlier remote sensing techniques have shown some capacity to map channel bathymetry over larger stream segments, but not with high resolution or without some local calibration (see review in Mertes, 2002).

We successfully used the Experimental Advanced Airborne Research LiDAR (EAARL) to map and monitor channels and floodplain topography in streams that provide spawning and rearing habitat of a federally listed (threatened) population of Chinook salmon (*Oncorhynchus tschawytscha*) in central Idaho. EAARL data allowed us to investigate and analyze spatial scales of habitat distribution ranging from meters to tens of kilometers, considering both bed topography in the mainstem channels and the location and extent of features in the adjacent floodplain such as “off-channel” aquatic habitat. We also observed local changes in stream physical habitat between LiDAR surveys done 3 years apart.

Field Area and Methods

Channel characteristics in our study area ranged from low-gradient, sand- and gravel-bed streams with meandering pool-riffle morphology, to steeper confined channels carrying gravel- and cobble-sized sediment. The median grain size in the bed ranged from about 50 mm in the low gradient streams to about 120 mm in the steeper confined channels. Channel size ranged from 10 to 30 m wide, 0.1 to about 4 m deep, and longitudinal gradients were 0.17–1.5%, calculated over 200 m reach lengths. Our analyses to date have concentrated on upper Bear Valley Creek and Elk Creek (fig. 1). Figure 2 shows the typical low gradient gravel-bed meandering channel with pool-riffle form in upper Bear Valley Creek.

[1]USDA, Forest Service, Rocky Mountain Research Station, Boise Aquatic Sciences Lab, 322 E. Front St., Suite 401, Boise ID, 83702

[2]U.S. Geological Survey, Center for Coastal and Watershed Studies, USGS FISC - St. Petersburg, 600 Fourth Street South, St. Petersburg, FL 33701

The technical specifications of the EAARL system are described in Wright and Brock (2002), Brock et al. (2004), Nayegandhi et al. (2006), and Nayegandhi et al. (this volume). EAARL data were acquired over about 150 km of streams during 5 hours of flight-time in October 2004 and about 75 km during 3 hours of flight-time in October 2007 (fig. 1). All flights were done in low-flow conditions with very good water clarity. The bathymetric data were gridded with a 3-m spacing to construct a digital representation of the channel topography. The digital topography was processed into basic visual displays for interpretation of channel and floodplain topographic characteristics. Typical products included shaded relief models, contour maps, and 3D wire mesh models. When the data are viewed at greater than reach scales, the valley topographic gradient can be distracting in standard shaded relief models. We used a lowess local regression procedure (R Project, 2008) to "detrend" the data and remove the valley gradient while still preserving the local morphology of the floodplain and channel.

EAARL data always include high resolution digital color-infrared photos and medium resolution color videography (Wright and Brock, 2002; Brock et al., 2004; Nayegandhi et al., 2006; Nayegandhi et al., this volume). Although not used extensively in this study, these data complement the LiDAR information and should be extremely valuable, for example, for defining riparian vegetation characteristics. An example of the photography is provided later.

Performance of the instrument was evaluated by comparison with intensive field surveys of channel morphology in six stream reaches, each about 150 m long. Each control site survey was done over about a 2-day period by a two-person crew using a combination of total station

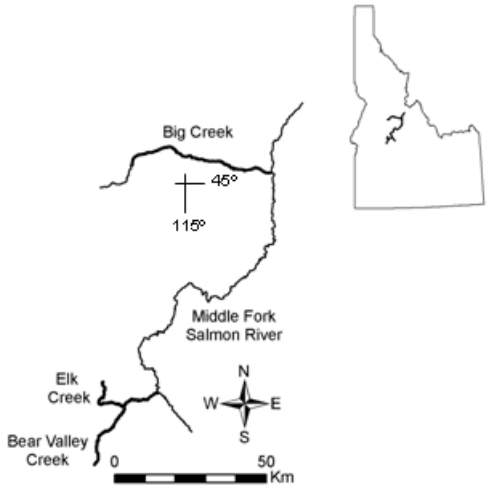

Figure 1. Locations of 2004 and 2007 EAARL data. Big Creek was only mapped in 2004. Elk and Bear Valley Creeks were mapped both years.

Figure 2. Typical meandering pool-riffle, gravel-bed channel mapped with the EAARL instrument in Bear Valley Creek, Middle Fork Salmon River, Idaho. Channel is 15 m wide and gradient is about 0.2%. Median grain size in bed is 50 mm. View is downstream.

and survey-grade GPS methods to measure point elevations of channel bed and bank topography. These site surveys were designed to have greater precision, accuracy, and overall data density than did the LiDAR data. Both the LiDAR and field survey data were then gridded and contoured in exactly the same manner. Assessment of accuracy of remote measurements of channel morphology is complex and appropriate metrics depend strongly on the intended use of the data. Accuracy can be measured at points, along lines of data, across areas or volumes, or using higher order derivatives such as slope or topographic curvature. Our principal concern has been mapping basic fish habitat units and here we report tests of EAARL accuracy for that purpose using surface areas and volumes of "pools," which are perhaps the primary morphologic feature of streams. Pools were defined as portions of the streambed lying below an arbitrary contour elevation and having a concave-upward form.

We quantitatively analyzed the spatial structure of channel physical habitat using 1D continuous wavelet transforms (McKean et al., 2008). The channel bed topography was described by the thalweg profile, hand digitized in the digital topography produced from the 2004 data. The wavelet technique analyzes spatial or temporal patterns in the frequency domain by comparing pieces of a continuous signal (the channel thalweg elevation profile) to a reference waveform and calculating transform coefficients that describe the similarity of any portion of the original signal to the reference wavelet (Mallat, 1989; Daubechies, 1992; Hubbard, 1998;Torrence and Compo, 1998). We used an 8th order Gaussian reference wavelet that has a smoothly varying form similar to channel bed profiles. When centered

on a channel profile convexity, the wavelet coefficients are positive; when the wavelet is out-of-phase and centered on a pool or concavity, the coefficients are negative. The magnitude of coefficients is proportional to the vertical amplitude of the bed elevation changes. Spatial scaling can be explored by recalculating the wavelet similarity coefficients while changing the length, or spatial scale, of the reference wavelet. The wavelet coefficients at any spatial scale can be squared to predict the distribution of spectral power at that spatial scale.

Monitoring of channel change between 2004 and 2007 has been done to date by simply constructing digital channel topography from each year, using identical gridding methods, and subtracting the 2007 topography from that of 2004.

Results

Figure 3 shows a typical result of a performance test of the EAARL sensor in a 150 m long reach of pool-riffle topography in upper Bear Valley Creek. The 3D surface area of pools was essentially identical in the data pair. However, the EAARL bathymetry predicted 17% greater pool volume than did the field survey. Later field checking revealed the field survey had missed a small (in surface area) deep pocket in the pool at coordinates 626890E, 4913265N, and thus in this case, the LiDAR data appear to be more accurate than the control field data.

Figure 3 also illustrates a bias in the bathymetric data. The instrumentation and geometry of airborne terrestrial and aquatic LiDARs dictates they measure elevations more accurately than horizontal position. Fewer LiDAR measurements also are taken from bank surfaces and the edges of banks than on the gentler channel bed and floodplain. As a result, EAARL mapping errors are larger along channel banks, particularly when the bank slope approaches vertical. The result is that steep banks in the LiDAR-mapped topography are gentler and the top and bottom edges of banks are more rounded than is correct. In figure 3, this bias is revealed by the wider-spaced LiDAR contours on the outside of meander bends where the flow has eroded near-vertical banks.

Figure 4 is an EAARL-derived DEM of 10 km of upper Bear Valley Creek with elevations classified by color. A distinctive change in valley and channel morphology occurs at a channel distance of 4 km. There is about a 3 m-tall step in the valley profile at this location, interpreted by McKean et al. (2008) as the headward extent of post-glacial valley erosion that has regraded the lower valley to the level of a base level control at the valley outlet at a channel distance of about 10 km. A similar, but smaller, step occurs at a channel distance of about 3 km. Downstream of 4 km, the channel is unconfined, meanders widely, and has very good pool-riffle morphology preferred by species like salmon. Upstream of that point, the channel is against a Pinedale-age glacial terrace (about 22,000 years old; Schmidt and Mackin, 1970) and has a straight, plane-bed morphology that is seldom used by spawning fish.

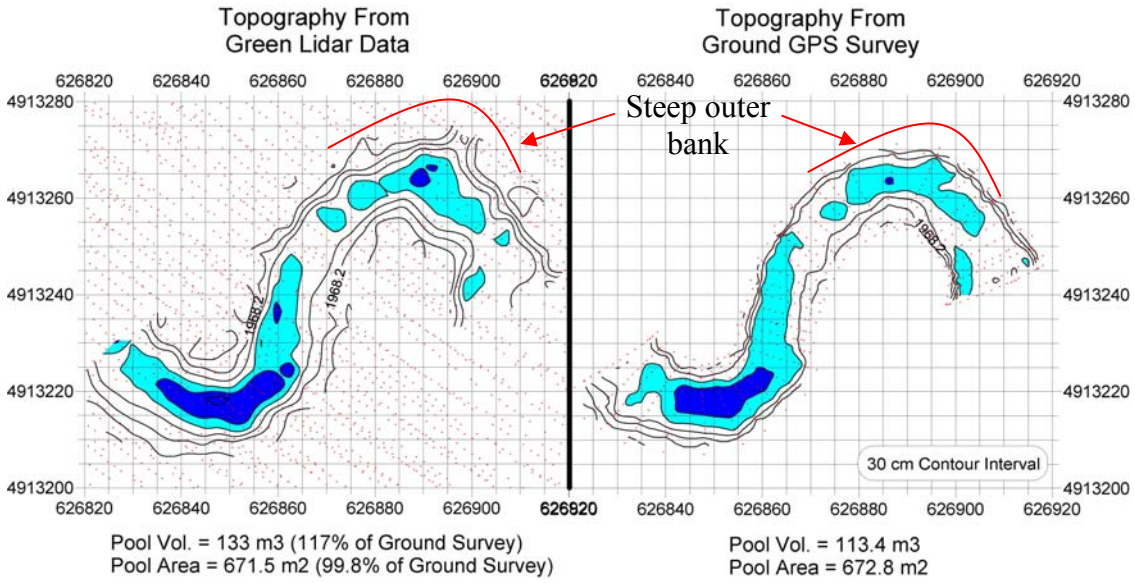

Figure 3. Comparison of topography mapped in the same pool-riffle channel reach with EAARL data (left panel) and survey-grade GPS (right panel). Red dots are points were elevation data were collected by each method. Notice the continuous EAARL data acquisition inside the channel and in the surrounding floodplain.

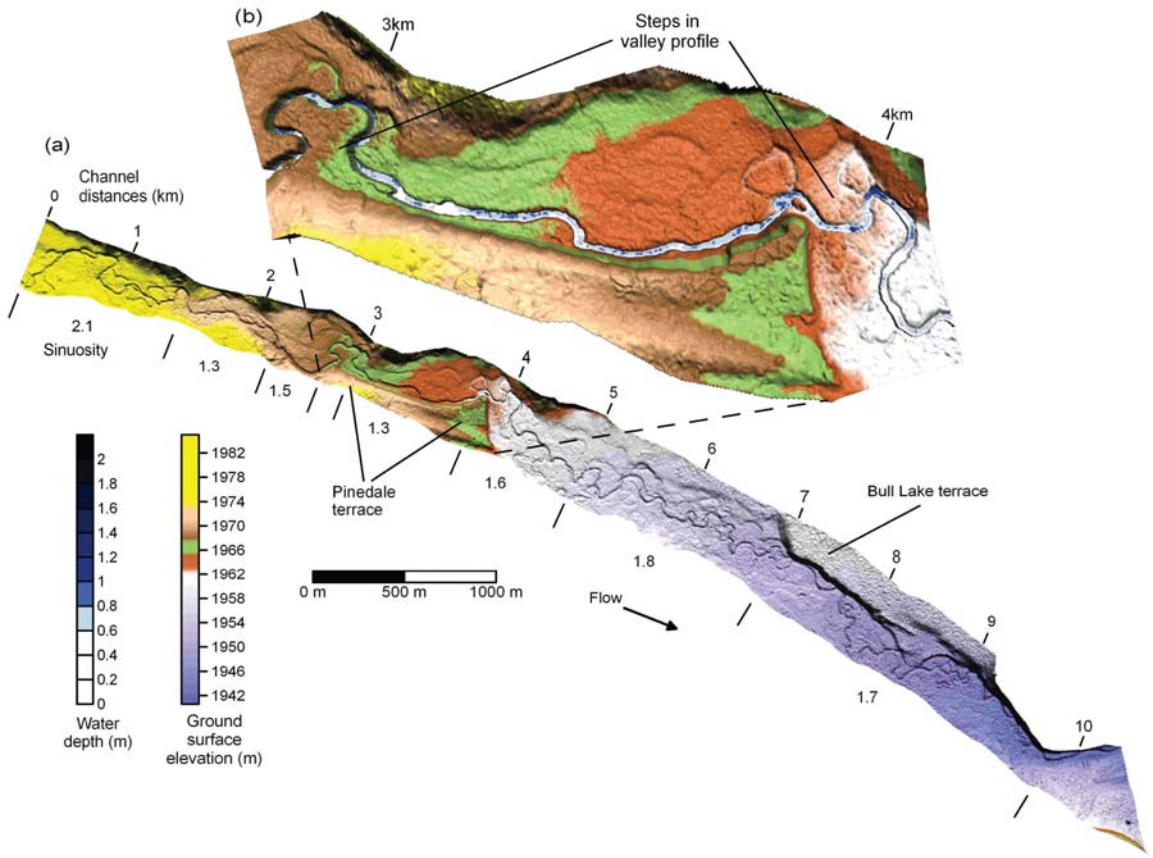

Figure 4. (a) Digital elevation model of upper Bear Valley Creek. Digital topography produced from EAARL data gridded to a 3 m interval. Reference distances are measured along the channel and sinuosity is calculated as channel length/straight-line valley distance over the indicated valley segments. (b) Inset showing degraded step in the valley profile at distance about 3,800 m and shorter valley step at about 2,800 m.

In figure 5, the EAARL data have been "detrended" to remove the valley gradient. Now the numerous inset erosion surfaces and abandoned channel positions are readily visible in the floodplain. Figures 5b and 5c show the bathymetric detail that can be mapped simultaneously with the floodplain topography. Much of the off-channel habitat used by small fish is in semi-abandoned channels that are still connected to the mainstem at higher flow stages. Several of these are noted in figure 5c.

Figure 6 illustrates the spatial distribution of spectral power in upper Bear Valley Creek at a scale of 100 m, i.e. the reference Gaussian wavelet was made 100 m long. Power is not evenly distributed along the channel but rather is concentrated at 0–2 and 8–10 km of channel distance with more isolated power spikes from 2 to 8 km. Over this 10 km stream segment, changes in power as a function of the spatial scale of the reference wavelet depend on a combination of geomorphic history and contemporary channel hydraulics (McKean et al., 2008). They also found that concentrations of fish spawning sites closely follow the bed topography spectral power over a wide range of spatial scales.

Repeated high-resolution EAARL surveys allow monitoring of changes in physical habitat conditions over large portions of channel networks. Figure 7 shows topographic change in a 400 m reach of Elk Creek between 2004 and 2007 mapped by the LiDAR. In this sand-gravel reach, the channel 3D geometry often changes significantly during the annual snowmelt peak runoff. Scour can be seen at several meander bends and a large pool near the downstream end of the reach also filled significantly over this period.

Figure 8 shows a combination of the CIR camera imagery of the floodplain and EAARL bathymetry within the channel in a portion of Elk Creek. Patterns of riparian vegetation and many abandoned channels are easily seen in the image.

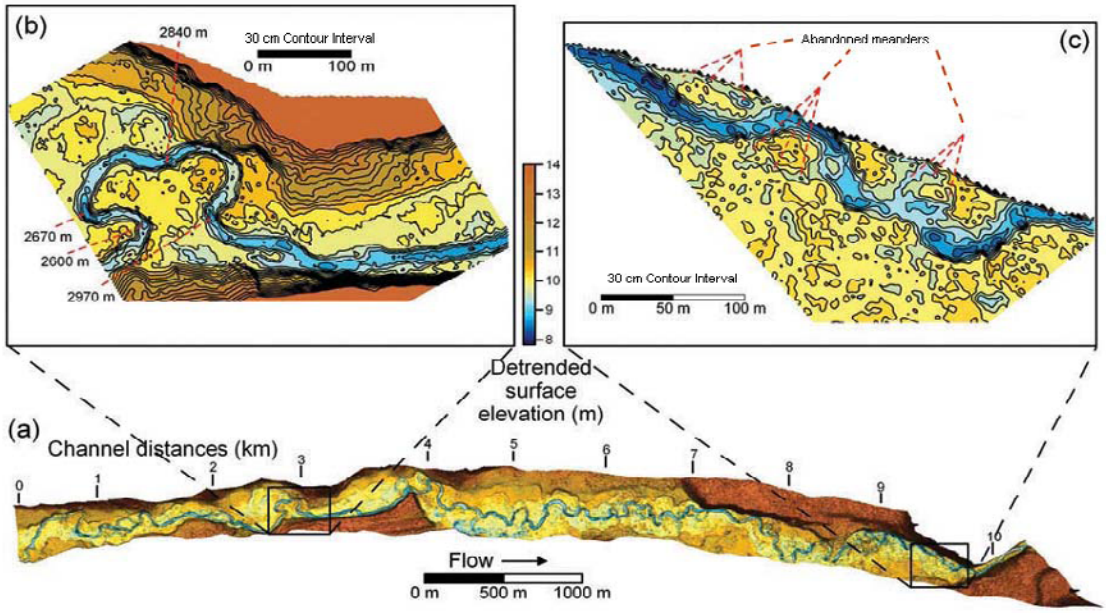

Figure 5. (a) Channel, floodplain, and terrace topography after the valley gradient has been removed. (b and c) Contour maps of selected channel reaches, showing the ability of EAARL to simultaneously resolve floodplain, terrace, and channel topography. All digital topography produced from EAARL data gridded to a 3-m interval.

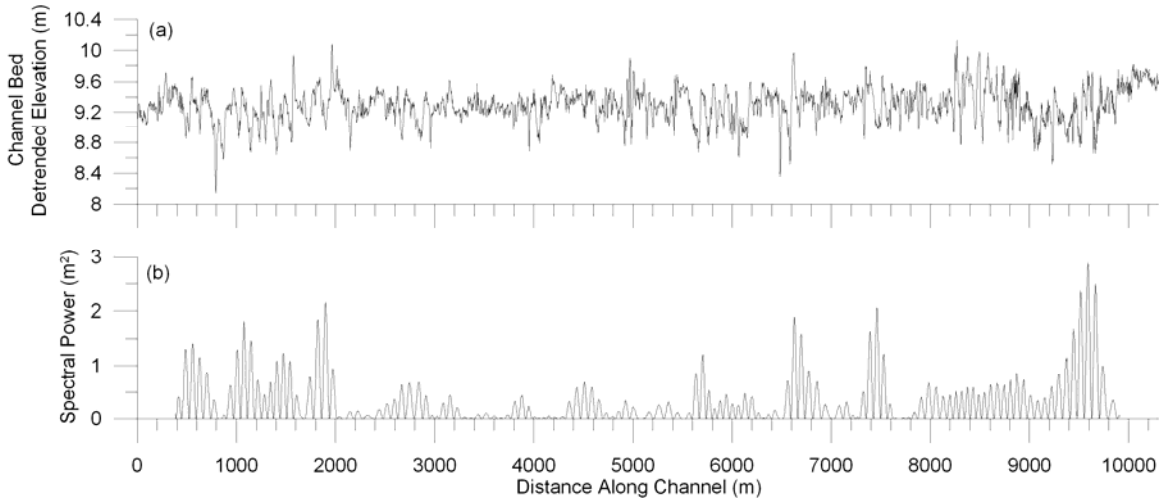

Figure 6. (a) Detrended thalweg profile of upper Bear Valley Creek mapped by EAARL in 2004. (b) Spatial variation in thalweg profile elevations described by 1D continuous wavelet analysis. The reference wavelet was a Gaussian 8th order wavelet with a length of 100 m. Larger spectral power peaks correspond to segments of the channel with higher amplitude bedforms having a wavelength of about 100 m. Wavelet analysis was done on undetrended thalweg profile; detrended profile shown for clarity of local bed elevations.

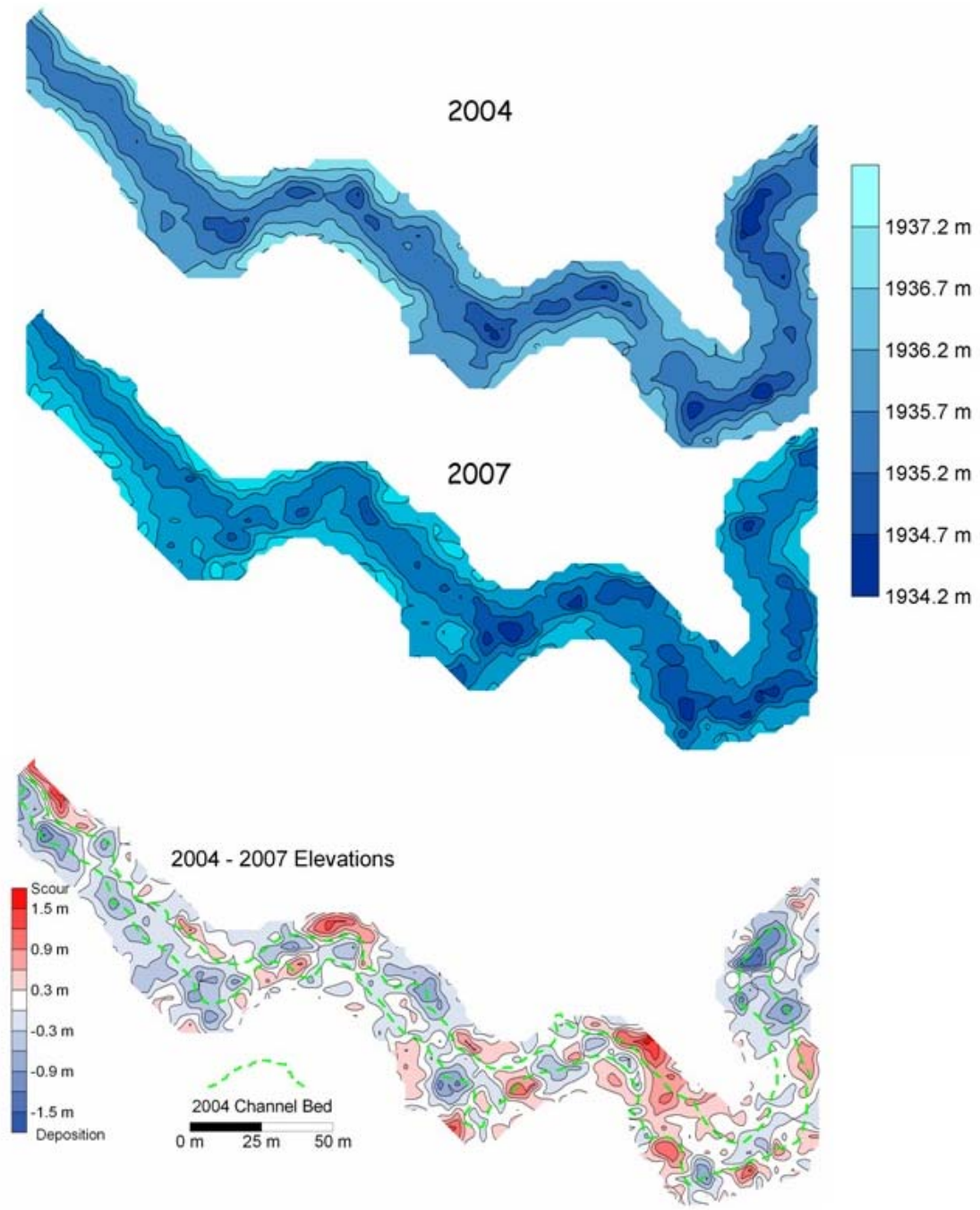

Figure 7. Change in Elk Creek between EAARL surveys in 2004 and 2007. Flow is left to right. The dashed green line shows the limits of the channel bed in 2004 for reference.

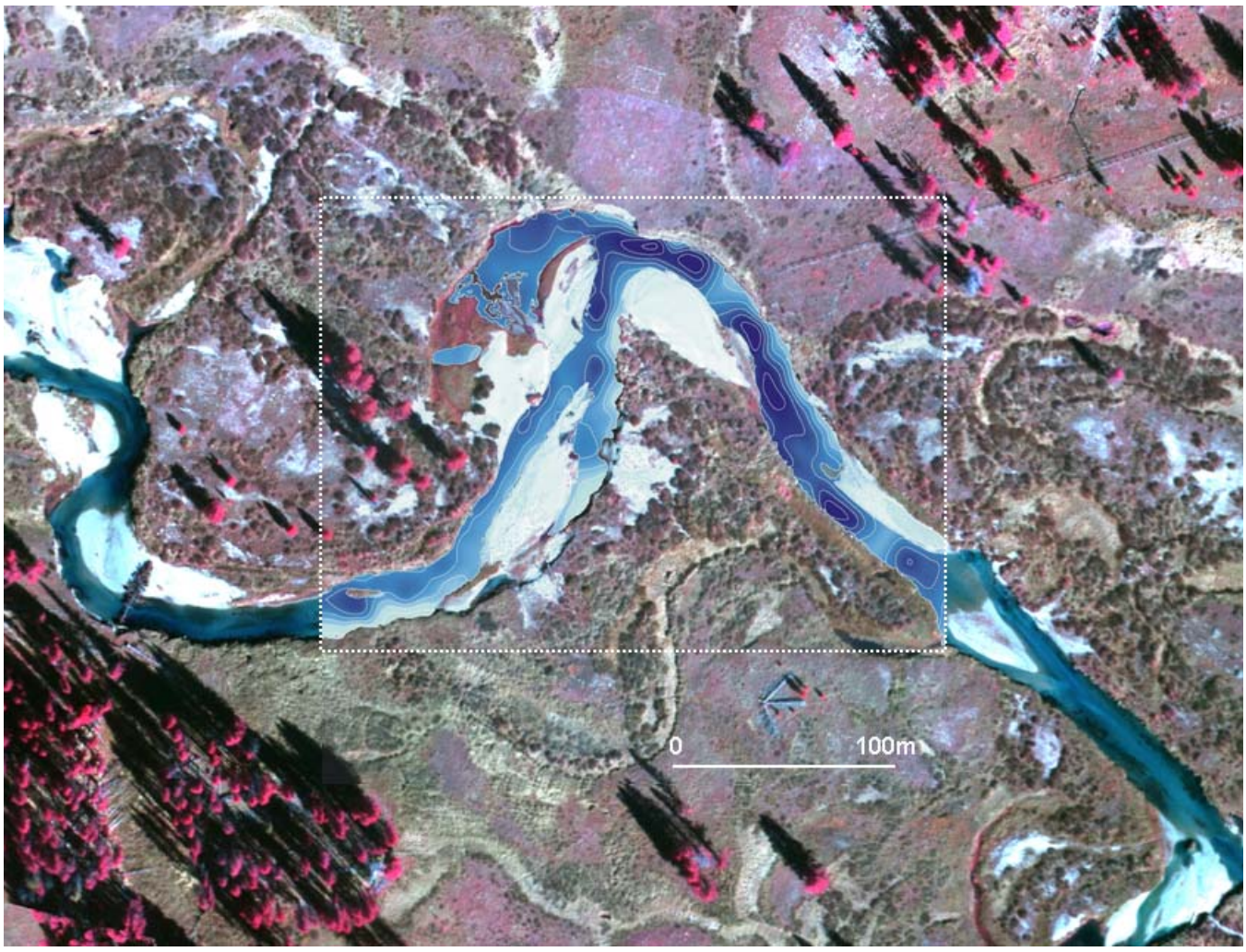

Figure 8. EAARL bathymetry of a portion of Elk Creek (bathymetry confined to area of channel within white box) overlaid on a mosaic of digital color-infrared imagery. The color-infrared imagery has not been rigorously ortho-rectified and co-registered to the bathymetry. The imagery and bathymetry were acquired simultaneously by the EAARL system. Bathymetric contours are at 50 cm intervals.

Discussion and Conclusions

The EAARL bathymetric LiDAR offers many advantages to aquatic ecologists and river managers. The ecological scope of the instrument (defined as the length of channel that can be surveyed divided by the finest scale resolvable in the data) is about 105–106. Thus, the data can be used to study channel and floodplain physical characteristics that range from meters to many kilometers in scale. The larger end of this spectrum has always been relatively inaccessible to high resolution analyses. For example, detailed field surveys are normally limited to less than perhaps a few hundred meters of channel length. The airborne bathymetric survey also resolves channel and floodplain access issues. Data describing the bare earth floodplain topography, channel bathymetry and the vegetation canopy can be collected in one integrated mission. The integrated bathymetry, terrestrial bare earth topography, vegetation DEM, and broad-band spectral data from the CIR camera are a particularly powerful combination of data to map and investigate riparian and channel habitat and process interactions.

The EAARL instrument is currently based in Virginia and operated by the USGS LiDAR survey costs are very site-specific and affected by mobilization, terrain flying conditions, length of channel surveyed, and the mapping width of channel plus floodplain. Estimates of data acquisition costs in 2008 projects in the western U.S. have ranged from $1,400 to $5,300 per kilometer. These costs do not include data processing, which can be contracted from the USGS or done by individual users with training and access to the processing software ALPS (Nayegandhi et al., this volume). Plans are underway to improve the system in 2009 with the goal of

increasing the density of data (number of point elevation measurements per area) by about six-fold and increasing the power of the laser for better water penetration. The synoptic spatially continuous EAARL data lends itself to analysis in the frequency domain. Techniques such as wavelets offer the possibility to depict and monitor aquatic and riparian habitat in powerful new ways. Wavelets rapidly describe habitat over a large range of spatial scales and identify nested scalar hierarchies of topography and habitat. Wavelet analyses are objective, quantitative and completely repeatable. It also is possible to quantify stream restoration measures by their wavelet characteristics.

The simplest applications of EAARL data include basic habitat mapping (subaqueous and subaerial topography as well as vegetation) and monitoring habitat change over time. Current channel monitoring protocols are based on labor-intensive field samples of small stream reaches. The limited size of each sample reach mandates great care in placement and number of sample sites. Federal land management agencies budget several millions of dollars per year for this work. The EAARL sensor can efficiently inventory and monitor much of the topography of large portions of channel networks and allow local field-based monitoring to focus on biological attributes and those geomorphic attributes that are inaccessible to the LiDAR (e.g., undercut banks and bank stability). Table 1 defines the physical habitat attributes mappable with the EAARL system.

The high resolution of EAARL data provides an opportunity for automated mapping of many aspects of channel geometry. We are constructing a web-based GIS tool that will interrogate EAARL data and extract commonly used at-a-station channel characteristics (see fig. 9 for a screen capture of the partially completed tool). Users will be able to define where they want channel and floodplain cross sections and the tool will compute metrics such as channel width/depth, point of maximum depth, longitudinal channel gradient, and amount of off-channel habitat connected to any channel reach at a given water stage. An option is included to incorporate field photos with any cross-section and data from groups of cross-sections can be copied for use, for example, in a 1D flow model. When completed, this tool will be made freely available on a website.

The data also describe the channel and floodplain boundary condition topography necessary to operate computational fluid dynamics models of channel flow and sediment transport and flood routing models. The topographic data could also be used to support individual-based and population-level biological models.

Although the EAARL system is clearly a major advancement in stream mapping technology, there are, of course, limits to its performance. In particular, shallow water (less than about 10–15 cm depth) and turbid conditions can be problematic. The instrument distinguishes water depth by the difference between the detected water surface and channel bed in each laser pulse. In very shallow flow conditions,

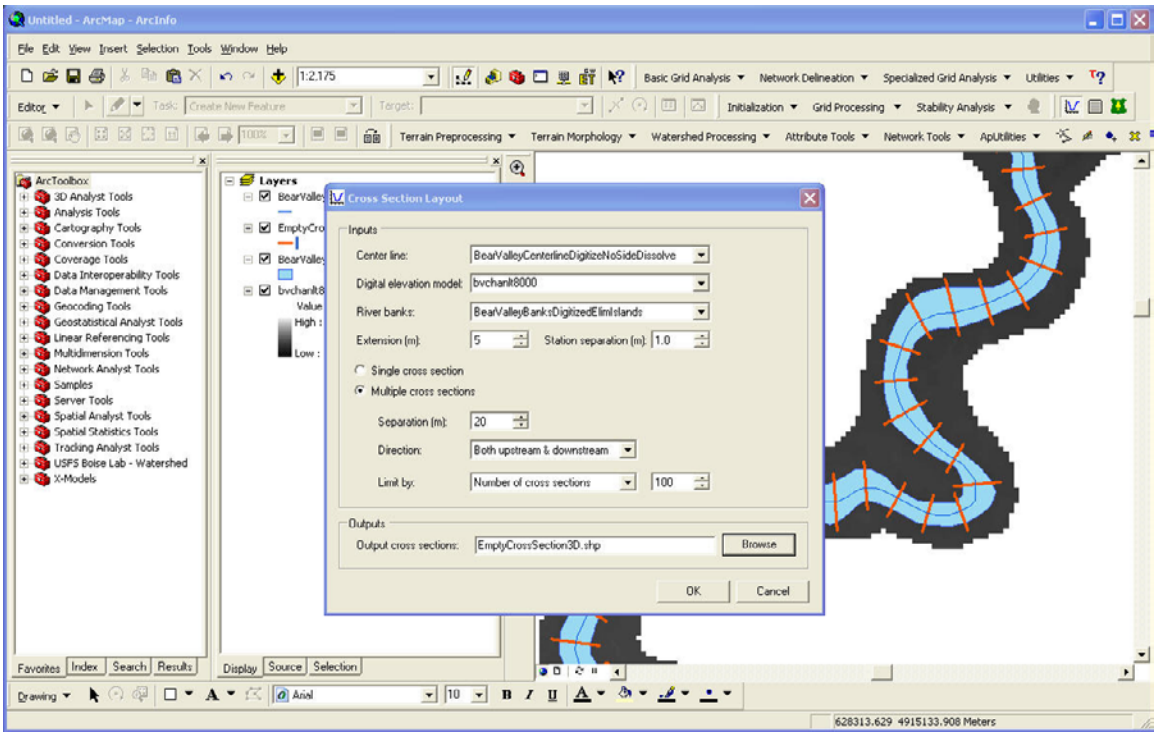

Figure 9. Screen capture of a web-based GIS tool being developed to automatically extract common channel and stream habitat metrics from EAARL data.

Table 1. Channel and floodplain topographic attributes (arranged by spatial scale) that can be mapped with the EAARL sensor.

Spatial extent	Stream feature	Comments
Microhabitat scale (10^0 m)	Water depth	
	Bed slope	Over user-defined channel length.
Channel unit scale (10^1–10^2 m)	Pools, riffles, runs, backwaters	Areal extent, volume, residual pool depth, bedform amplitude, etc.
	Channel cross-section	Bankfull width, depth, cross-sectional area, maximum depth, wetted perimeter, hydraulic radius, bank height and angle, channel entrenchment, symmetry, etc.
	Off-channel habitat	Length, area, volume, connection to mainstem, stage dependence.
Reach-to-network scale (10^2–10^4 m)	Planform geometry	Sinuosity, axial wavelength, arc wavelength, bend amplitude, arc height, radius of curvature, etc.
	Diversity/complexity	Spatial metrics characterizing composition, configuration, complementation, and connectivity of habitats.
	Off-channel habitat	Length, area, volume, connection to mainstem, stage dependence.

the signals from the surface and bed can sometimes become convolved. Suspended sediment and/or entrained air bubbles are point laser reflectors and if too dense, they can prevent the laser energy from reaching the bed. Research is currently ongoing to improve separation of the water surface and bed reflections in shallow water and to quantify the limitations posed by poor water quality and the range of field conditions within which acceptable bathymetric data can be expected.

The instrument resolves surface elevations better than horizontal positions, due to the geometry of the data acquisition and the GPS solutions of the aircraft position during flights. Consequently, points of sharp topographic curvature, such as the top and bottom edges of channel banks, are mapped less accurately than are the elevations of gentler surfaces such as floodplains, terraces, and the channel bed. This bias against correctly mapping high topographic curvature will be lessened, but not eliminated, by increasing the data density as a result of the 2009 system improvement mentioned above. A more inclusive accuracy assessment of the 2004 and 2007 Bear Valley and Elk Creek data is underway. A full assessment of the accuracy of EAARL measurement of point elevations inside a shallow sand-bed channel was reported by Kinzel et al. (2007).

The EAARL appears to be a new generation of technology that could revolutionize how we map, monitor, and investigate integrated aquatic and terrestrial habitat and physical and biological processes. In particular, it will allow high-resolution studies of habitat and processes over a much wider range of spatial scales than previously possible.

References

Brock, J.C., Wright, C.W., Clayton, T.D., and Nayegandhi, A., 2004, Optical rugosity of coral reefs in Biscayne National Park, Florida: Coral Reefs, v. 23, p. 48-59.

Daubechies, I., 1992, Ten lectures on wavelets: Philadelphia, PA, Society for Industrial and Applied Mathematics.

Hubbard, B.B., 1998, The World According to Wavelets, 2nd ed.: Natick, MA, A.K. Peters, Ltd.

Kinzel, P.J., Wright, C.W., Nelson, J.M., and Burman, A.R., 2007, Evaluation of an experimental LiDAR for surveying a shallow, braided, sand-bedded river: American Society of Civil Engineers, Journal of Hydraulic Engineering 133, p. 838-842.

Mallat, S.F., 1989, A theory for multiresolution signal decomposition: The wavelet representation: IEEE Transactions on Pattern Analysis and Machine Intelligence, v. 11, p. 674-693.

Mertes, L.A.K., 2002, Remote sensing of riverine landscapes: Freshwater Biology, v. 47, p. 799-816.

McKean, J.A., Isaak, D.J., and Wright, C.W., 2008, Geomorphic controls on salmon nesting patterns described by a new, narrow-beam terrestrial–aquatic lidar: Frontiers in Ecology and Environment, v. 6, no. 3, p. 125-130.

Nayegandhi, A., Brock, J.C., Wright, C.W., and O'Connell, M.O., 2006, Evaluating a small-footprint, waveform-resolving LiDAR over coastal vegetation communities: Photogrammetric Engineering and Remote Sensing, v. 12, p. 1408-1417.

R Project for Statistical Computing, 2008, http://www.r-project.org/

Schmidt, D.L., and Mackin, J.H., 1970, Quaternary geology of Long and Bear Valleys, west-central Idaho: U.S. Geological Survey Bulletin 311-A.

Torrence, C., and Compo, G.P., 1998, A practical guide to wavelet analysis: Bulletin of the American Meteorological Society, v. 79, p. 61-78.

Wright, C.W., and Brock, J.C., 2002, EAARL: A LiDAR for mapping shallow coral reefs and other coastal environments: Proceedings of the 7th International Conference on Remote Sensing for Marine and Coastal Environments, Miami, FL (CD-ROM).

Chapter 3.—Advanced Tools for River Science: EAARL and MD_SWMS

Paul J. Kinzel[1]

Abstract

Disruption of flow regimes and sediment supplies, induced by anthropogenic or climatic factors, can produce dramatic alterations in river form, vegetation patterns, and associated habitat conditions. To improve habitat in these fluvial systems, resource managers may choose from a variety of treatments including flow and/or sediment prescriptions, vegetation management, or engineered approaches. Monitoring protocols developed to assess the morphologic response of these treatments require techniques that can measure topographic changes above and below the water surface efficiently, accurately, and in a standardized, cost-effective manner. Similarly, modeling of flow, sediment transport, habitat, and channel evolution requires characterization of river morphology for model input and verification. Recent developments by the U.S. Geological Survey with regard to both remotely sensed methods (the Experimental Advanced Airborne Research LiDAR; EAARL) and computational modeling software (the Multi-Dimensional Surface-Water Modeling System; MD_SWMS) have produced advanced tools for spatially explicit monitoring and modeling in aquatic environments. In this paper, we present a pilot study conducted along the Platte River, Nebraska, that demonstrates the combined use of these river science tools.

Introduction

In many western rivers in the United States, changes in flow and sediment regime caused by water-resource development, landscape modification, or climatic factors have altered in-channel and riparian habitat conditions. As a consequence, recovery programs in these river basins for species with endangered or threatened designations have adopted adaptive management (Holling, 1978) as a strategy toward habitat enhancement and species recovery. To function effectively and iteratively, adaptive management in aquatic environments requires monitoring programs that include geomorphic, hydrologic, and biological components. Ground surveys have traditionally been used to collect these monitoring data at sampling points, often using statistical methods to determine the locations, spacing, or frequency of these measurements. Although discrete sampling has utility and practicality, it does not completely represent the aquatic ecosystem that is continuous with spatial gradients in habitat quality and quantity. These gradients are determined by a variety of physical and biological factors and include the degree of connectivity/isolation brought about by the presence of disturbance and topological features in the landscape.

Spatial monitoring in the form of remote sensing has been seen as an innovative alternative to conventional monitoring approaches (Walters, 1997). Remote sensing commonly is used to delineate landscape features for river studies, with aerial photography being the most ubiquitous acquisition. In addition to feature data, high-resolution and high-quality three-dimensional topographic datasets are being increasingly sought by river scientists seeking to understand and model the complex relationships between ecological processes, channel form, flow, and sediment supply. Desire for this level of topological characterization in rivers and the difficulties associated with using discrete conventional survey methods have motivated researchers to investigate photogrammetric, passive optical, and active remote-sensing techniques. Examples of these methods include those of Hicks et al. (2001) (airborne laser scanning, photogrammetry, and passive optical) and Westaway et al. (2003) (photogrammetry and passive optical). Despite these efforts, simultaneous and integrated measurement of both terrestrial and submerged topography, channel topography, in rivers using a single remote sensor and technique has been a challenging goal.

Airborne laser scanning or Light Detection and Ranging (LiDAR) technology has become readily available for detailed terrestrial surveys of large areas. However, the use of LiDAR in rivers typically has been confined to overbank areas (Bowen and Waltermire, 2002), because the near-infrared wavelength commonly used in these lasers is strongly absorbed and attenuated in water. Within the last decade, large-footprint, high-powered bathymetric LiDARs developed for coastal applications have been used in rivers (Tiffan et al., 2002; Hilldale and Raff, 2008). The tradeoff between laser power and eye safety in these LiDARs results in sampling footprints on the order of meters, a design suitable for surveying coastal areas but less optimal for narrow river channels.

[1]USGS Geomorphology and Sediment Transport Laboratory, Golden, CO.

Experimental Advanced Airborne Research LiDAR

Recently, the National Aeronautics and Space Administration (NASA) developed the Experimental Advanced Airborne Research LiDAR (EAARL) sensor (Wright and Brock, 2002). The instrument initially was designed for surveying coral reefs in relatively clear water. The relatively low-power, small-footprint laser (about 20 cm), which operates in the blue-green spectral region with a short (about 1 nanosecond) pulse width at a high sampling rate with temporal waveform capture, has demonstrated considerable promise for simultaneous acquisition of in-channel and adjacent floodplain topography (Kinzel et al., 2006; McKean et al., 2008). The system is operated from a Cessna 310 platform at a nominal altitude of 300 m and uses a kinematic global positioning system (GPS) and an inertial measurement unit to geolocate each laser spot. The EAARL instrument suite also has two cameras to facilitate the interpretation of the digital topographic data. Digital images acquired with a high resolution (about 20 cm per pixel at 300-m flying height) color infrared (CIR) camera are co-registered with the laser-derived topographic data. It also has a lower resolution red, green, and blue (RGB) camera (about 80 cm per pixel), which is tightly coupled to a digital image player within its processing software, Airborne Lidar Processing System (ALPS), allowing instant access to any photograph by clicking on an image of the flight track (fig. 1). ALPS is an open-source software written in the Yorick and TCL/TK programming languages and runs on a Linux operating system (Nayegandhi et al., 2006). Processing algorithms in ALPS are used to detect peaks and inflections in the time history of the backscattered laser intensity (waveforms). The algorithms enable measurement of the range of the aircraft to the first-surface encountered, the bare-earth surface, and surfaces below the water. These data can be exported from ALPS for use in mapping, statistical, or modeling software.

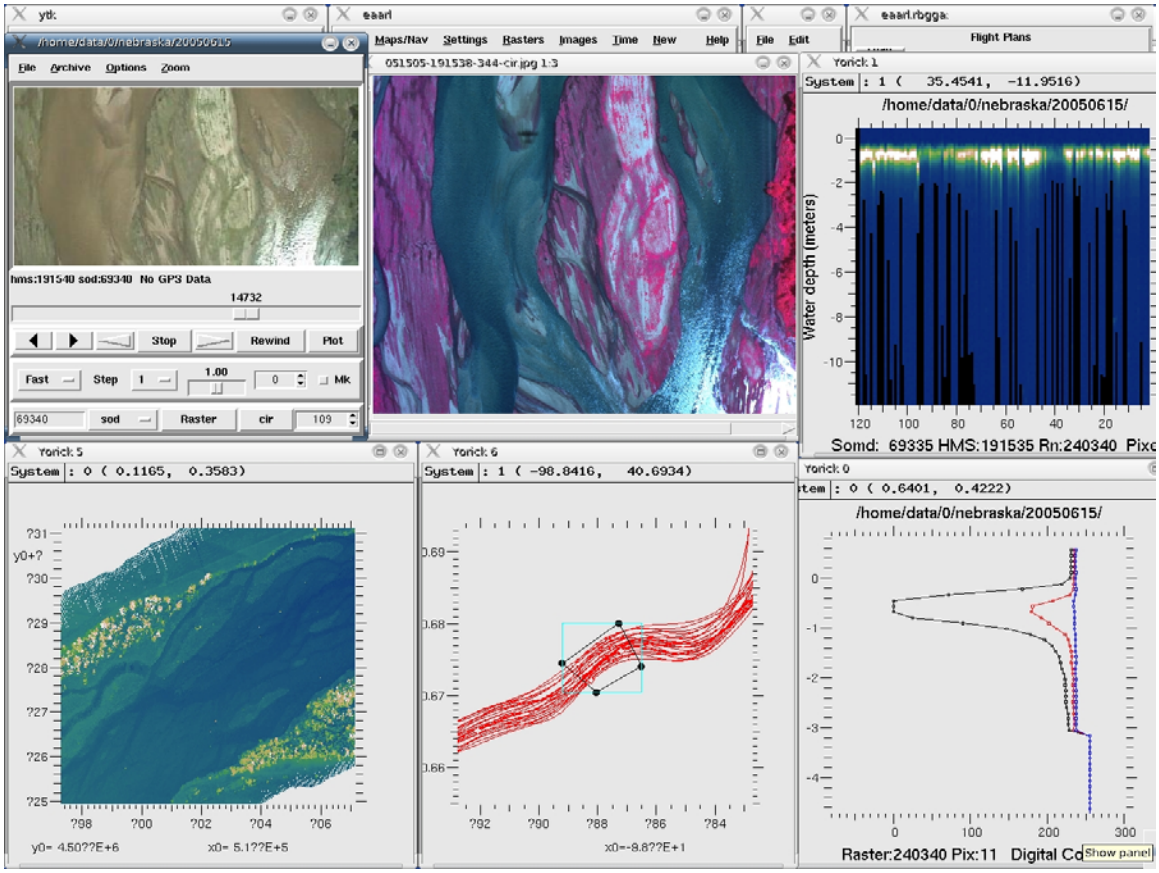

Figure 1. Screen capture of the ALPS software. Clockwise from upper left: RGB imagery, color-infrared imagery, laser raster, waveforms, flight line map, and first-surface elevation map.

Multi-Dimensional Surface-Water Modeling System

Over the last 10 years, the U.S. Geological Survey (USGS) has developed the Multi-Dimensional Surface-Water Modeling System, MD_SWMS, a graphical user interface for computational models of surface-water hydraulics and sediment transport in rivers (McDonald et al., 2001; McDonald et al., 2005). MD_SWMS runs on a PC operating system, is available at no cost to the user, and can be downloaded from: http://wwwbrr.cr.usgs.gov/gstl/2D-Download.php. The MD_SWMS software provides a framework for distributing surface-water models, developed by the USGS's National Research Program and other researchers, to scientists within the USGS, other government agencies, and the private sector. MD_SWMS is not a model but a software tool allowing users to interact with input data (channel topography) and generate numerical grids used by the surface-water models that are executed within it. Additionally MD_SWMS gives the user the means to visualize the output from the models and compare model predictions to verification data (water-surface elevations, velocities, and aerial images). In its preprocessing tools, MD_SWMS has the capability to filter raw input topography, useful for large LiDAR data sets, and the ability to delete data points, add data points, or interpolate between them.

Currently (2009), two hydraulic models can be run from MD_SWMS. Flow and Sediment Transport with Morphologic Evolution of CHannels (FaSTMECH) (Nelson et al., 2003) is a depth-averaged, quasi-three-dimensional flow model using a structured, curvilinear orthogonal coordinate system. A sediment-transport module in FaSTMECH allows users to examine sediment mobility in the channel for different grain sizes. The flow and sediment-transport routines can be used together in an iterative manner to predict spatial patterns of erosion and deposition (channel evolution). System for Transport and River Modeling (SToRM) is a two-dimensional flow model that uses an unstructured grid composed of irregular-triangular elements (Simões and McDonald, 2004).

Projects that have used MD_SWMS include: modeling hydraulics near bridges in cooperation with the Alaska Department of Transportation (Conaway and Moran, 2004), analysis of hazards due to radioactive mine tailings along the floodplain of the Colorado River in cooperation with the Utah Department of Environmental Quality (Kenney, 2005), and restoration of endangered white sturgeon habitat in the Kootenai River in cooperation with the Kootenai Tribe of Idaho (Barton et al., 2005). Each of these studies used MD_SWMS to answer a complex and spatially explicit problem. A critical component in each of these investigations was the detailed measurement of channel topography. The rivers in these investigations were of sufficient depth that conventional boat measurements with acoustic technology (echo sounding) could be used in submerged areas and combined with terrestrial topography to create maps of river channel topography used for hydraulic modeling.

Pilot Study – Platte River, Nebraska

The Platte River in central Nebraska is a shallow, braided river channel. In 2006, a recovery program was signed by the States of Colorado, Nebraska, and Wyoming, and the U.S. Department of Interior to improve habitat for the four endangered and threatened species in the Platte River basin (Governance Committee, 2006). Over the first increment of the Platte River Recovery Implementation Program (13 years), monitoring will be conducted to evaluate program actions (flow and habitat enhancements) and guide the adaptive management process. The collection of topographic data will be an important component of monitoring for the recovery effort. Conventional ground surveys with total stations or real-time kinematic global positioning systems (RTK-GPS) have been used to collect elevations along channel cross sections in the Platte. However, the application of these technologies to collect topographic information over long reaches is neither practical nor efficient. Similarly, acoustic techniques used in the above-mentioned examples are not feasible because of the shallow depths. These difficulties prompted the USGS in 2001 to research the state of the art with regard to remote-sensing techniques. This research resulted in a formal proposal and eventual support from the USGS Venture Capital Fund to conduct field tests of the EAARL in a shallow river.

In 2002 and 2005, the EAARL was flown over the Platte River to evaluate the vertical accuracy of the system. Topographic measurements made on the ground with RTK-GPS equipment were compared with nearby topographic points collected with the EAARL sensor (Kinzel et al., 2007). In 2005, the vertical accuracy of topography collected with the EAARL system using a first-surface algorithm was determined to be ±18 cm in subaerial areas and ±24 cm for measurements in submerged areas. A bathymetric processing algorithm in ALPS was found to improve the ranging accuracy to the river bottom in submerged areas where convolved backscatter from the water column and bottom was encountered. However, EAARL measurements made in submerged areas were less precise than those made in areas above the water surface. Further, in deep (about >50 cm) and turbid areas, it was difficult to distinguish a weak bottom return, if present at all, from the stronger water-column backscatter.

The application of the EAARL data in a hydraulic modeling context was explored by using the MD_SWMS interface and the FaSTMECH model to compute a flow solution through the EAARL channel topography collected in 2005 (fig. 2). Although a LiDAR-derived topographic data point is less precise than a point obtained from a ground survey, LiDAR point densities (number of points per square meter) have the advantage of being much greater than point densities that could be gathered from a ground survey. To avoid introducing bias in hydraulic model computations made from LiDAR-derived channel topography, the vertical errors in the LiDAR data need to be normally distributed about zero. This condition was met to a greater degree above the water surface than below it with the Platte River EAARL data. It should be noted that the process of creating a structured hydraulic modeling grid is itself an abstraction of the raw survey data. In models using structured grids, the raw topography is mapped to a regularly spaced series of grid nodes. The FaSTMECH model can determine the topographic elevation of each node by locating a point or points within a specified search radius of the node. If one point is located in the search radius, the node is given that elevation value. If more than one point is located, the node is assigned an elevation value that is the inverse distance weighted average of those points. If no point is located, the search radius is expanded until a point or points are found. It follows that if the search template is large relative to the density of the LiDAR data it could be equally likely for the elevation of a node to be mapped higher or lower than its true elevation, assuming the errors are randomly distributed through the reach.

The procedure for running a hydraulic model in MD_SWMS is relatively straightforward. The first step is to import the raw survey data and define a numerical grid. In figure 2*A*, a curvilinear numerical grid is overlain on the EAARL data. The grid was generated by digitizing the centerline of the channel and specifying the width of the grid across the centerline and the grid cell dimensions, in this case approximately 5×5 m. The raw topography was then mapped to the numerical grid (fig. 2*B*). The FaSTMECH model was run in MD_SWMS using the downstream water-surface elevation corresponding to a flow rate of 19 m^3/s). These boundary conditions were used to simulate the water-surface elevation and distribution of inundated area at the time of the EAARL survey. The predicted depths and velocities in the channel for this flow rate are shown in figures 2*C* and 2*D*. Water-surface elevation points determined by conventional survey were used as verification data in MD_SWMS (fig. 2*E*). A correspondence plot shows good agreement between predicted and measured values with a root mean square error of approximately 3 cm. Similarly, predictions of inundated and exposed area in the study reach compared favorably with manually registered color infrared imagery collected with the EAARL platform (figs. 2*F*–2*G*). Closer inspection of figure 2*F* indicates that the model, even with the relatively coarse grid resolution and the challenge of predicting wetting and drying of nodes in very shallow water (fig. 2*C*), reproduces the complex flow pattern around the vegetated sandbars in the study reach. In the future, automated georeferencing of EAARL imagery in ALPS will provide a raster data layer that could be used within MD_SWMS for model verification.

Previous hydraulic modeling with channel topography obtained from ground-survey data has shown the use of depth and velocity fields computed by FaSTMECH in MD_SWMS for habitat characterization (Kinzel et al., 2005). Additionally, EAARL topography acquired over multiple time periods has also been used to infer changes in riparian and in-channel areas (Kinzel et al., 2006). The example in this paper illustrates the use of both MD_SWMS and EAARL to make predictions of depth, velocity, and water-surface elevation. These predictions could be used to infer habitat quantity and quality in the reach for a range of hypothetical or real streamflows. Similarly, predictions of shear stress in the channel (not shown) could be used to compute sediment transport and movement of barforms in the reach during these flow events.

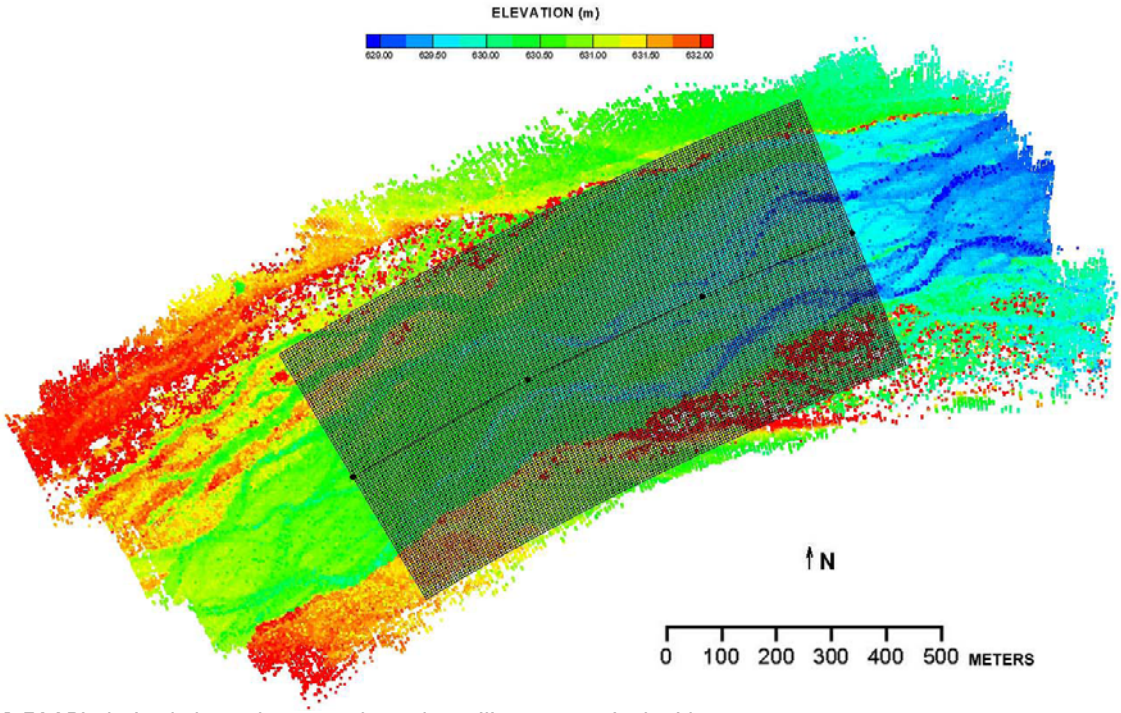

A. EAARL-derived channel topography and curvilinear numerical grid.

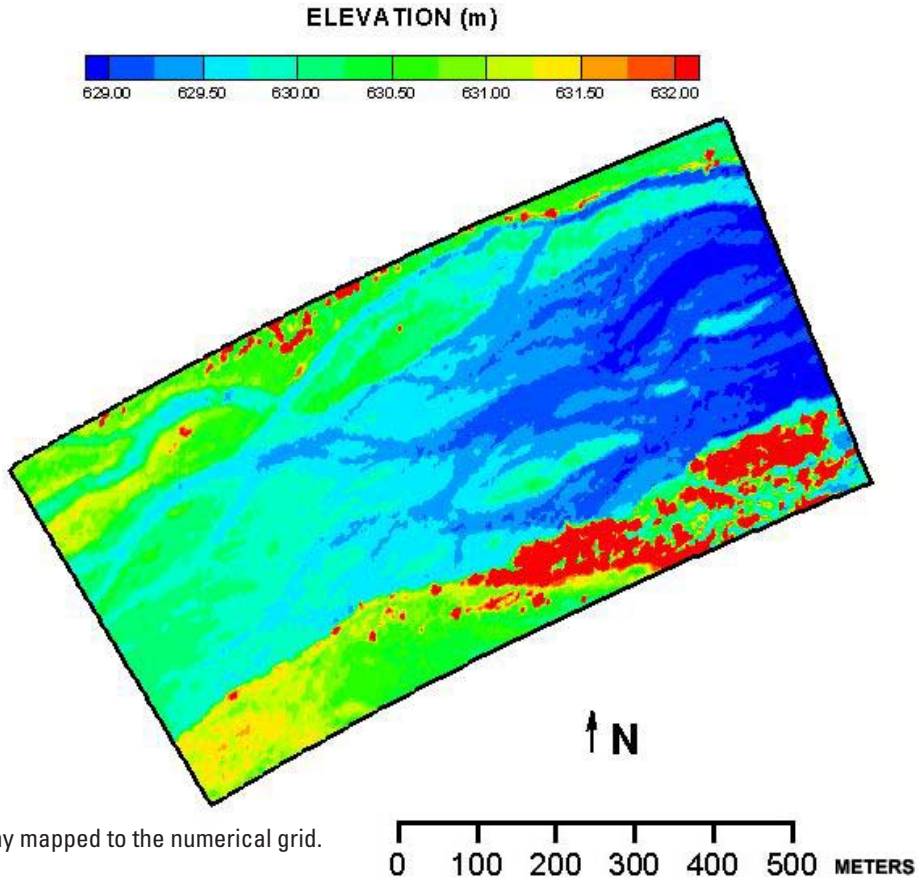

B. EAARL topography mapped to the numerical grid.

Figure 2. Output from MD_SWMS showing the use of EAARL data collected along a reach of the Platte River.

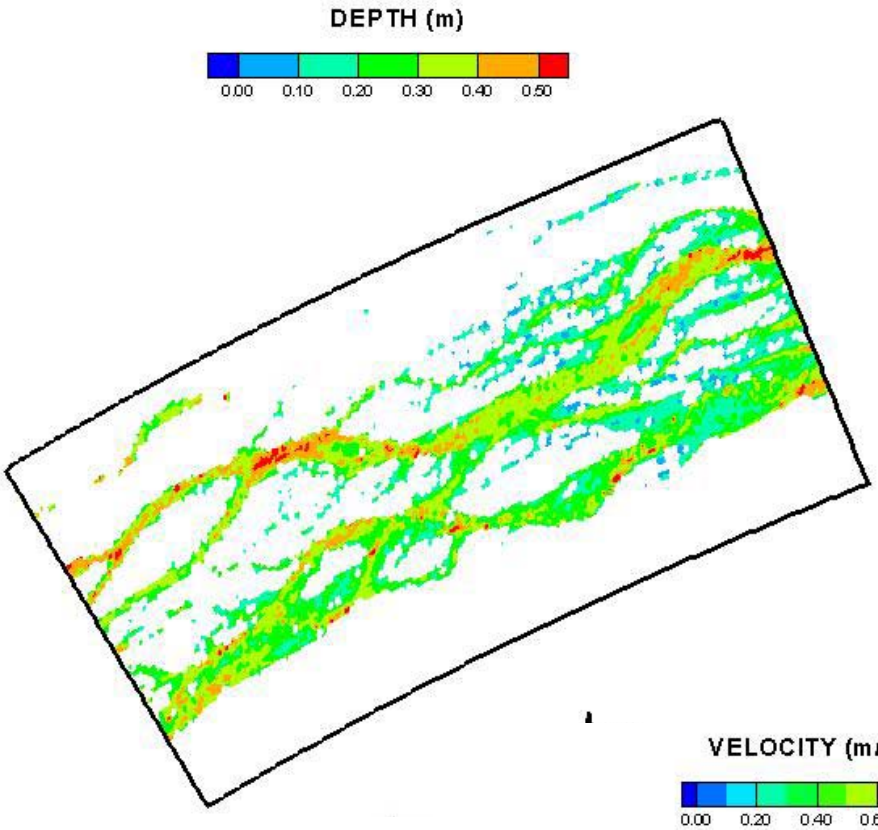

C. Predicted depth distribution using the FaSTMECH model.

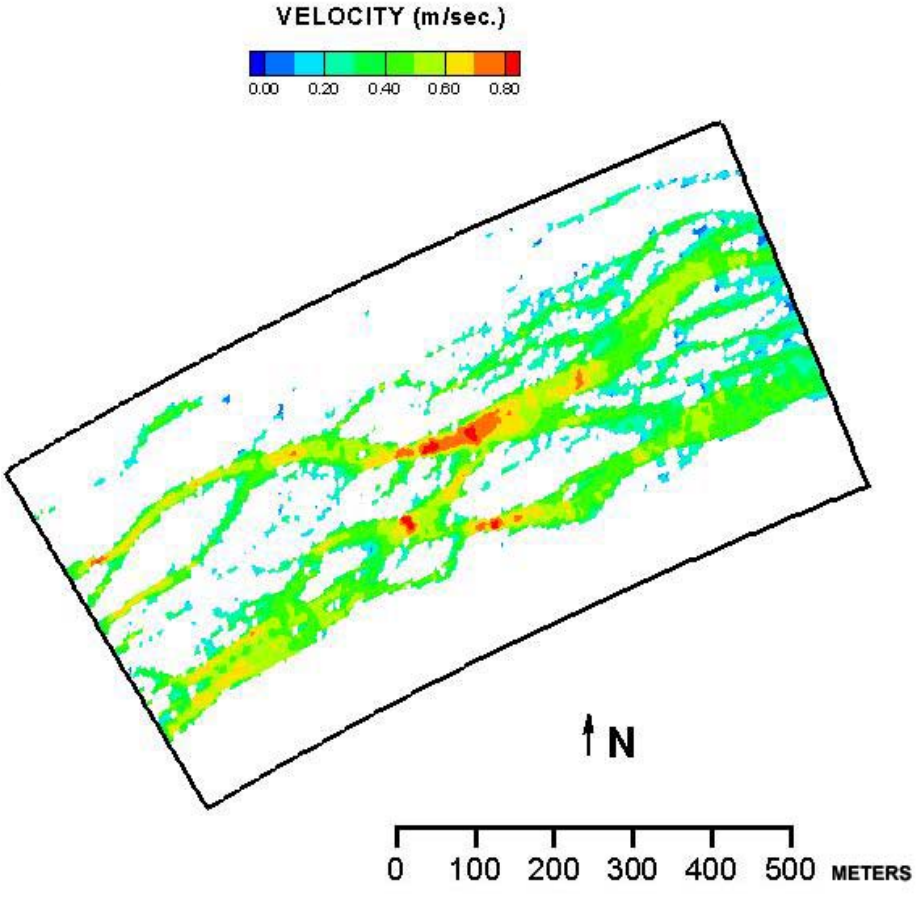

D. Predicted velocity distribution using the FaSTMECH model

Figure 2. Output from MD_SWMS showing the use of EAARL data collected along a reach of the Platte River.—Continued

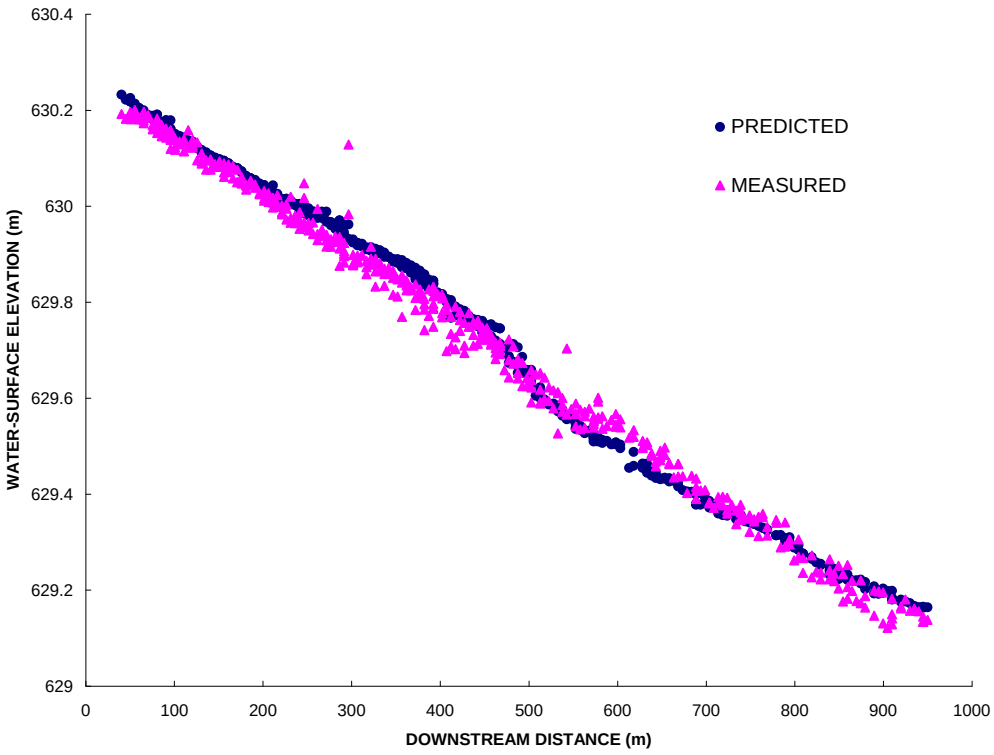

E. Comparison of measured water surface elevations with those predicted using the FaSTMECH model and EAARL collected topography.

Figure 2. Output from MD_SWMS showing the use of EAARL data collected along a reach of the Platte River.—Continued

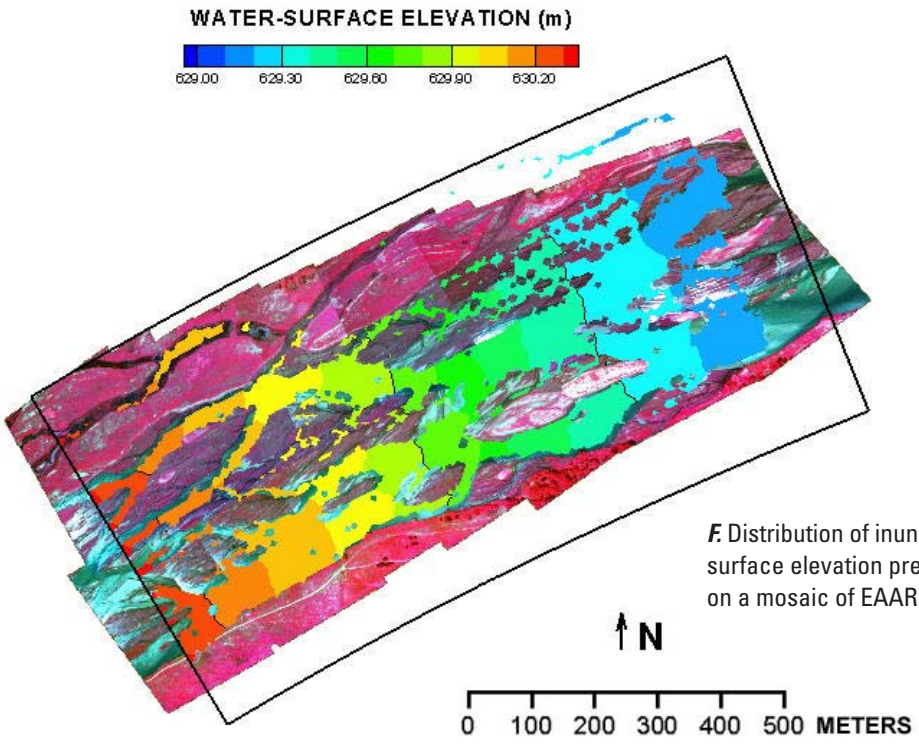

F. Distribution of inundated area, as indicated by the water-surface elevation predicted by the FaSTMECH model, overlain on a mosaic of EAARL collected color-infrared imagery.

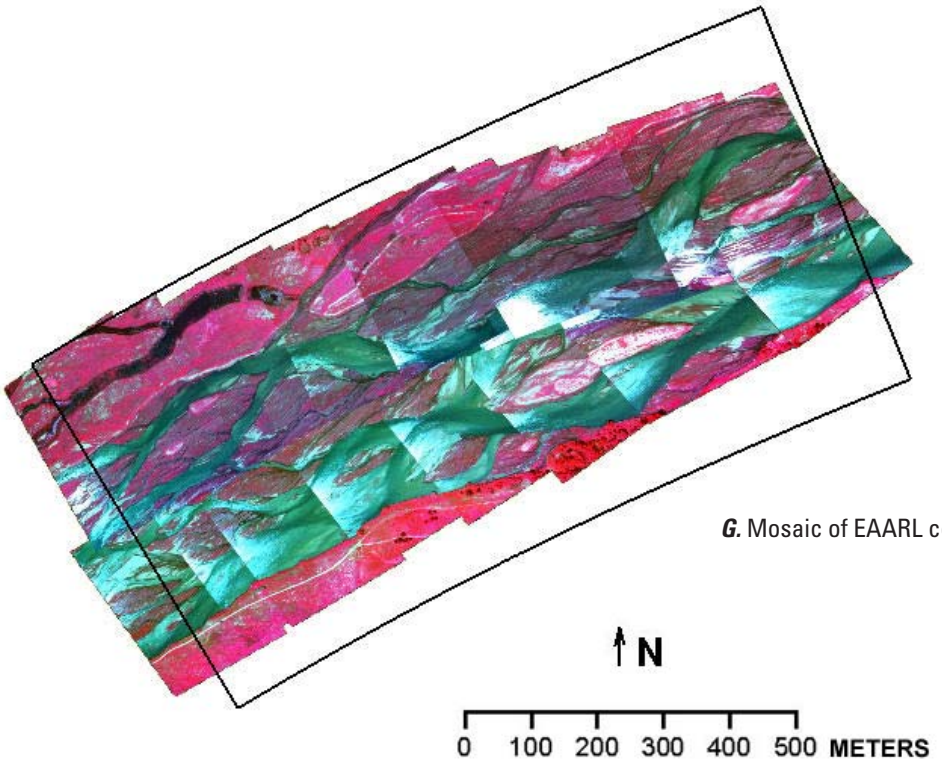

G. Mosaic of EAARL collected color-infrared imagery.

Figure 2. Output from MD_SWMS showing the use of EAARL data collected along a reach of the Platte River.—Continued

Conclusions

Advances in remote-sensing technology are improving the quality and quantity of topographic data gathered in and along rivers enabling unprecedented use in hydrodynamic modeling applications. In this paper, Experimental Advanced Airborne Research LiDAR (EAARL) data were used within the Multi-Dimensional Surface-Water Modeling System (MD_SWMS) to simulate flow in a reach of the Platte River. Water-surface elevations and inundated areas predicted by the model were similar to those measured and delineated with conventional ground surveys and aerial imagery. However, we plan on conducting a more detailed comparison of model results using channel topography collected with the EAARL to model results using channel topography collected from ground surveys. This will help quantify the effect of using EAARL surveys over ground surveys for flow computations. Hardware improvements in the EAARL platform are anticipated to occur that have the potential to improve its performance in shallow rivers. These improvements include increased laser power and point density in each laser swath or raster. Software improvements including processing algorithms able to accommodate the complex convolved waveforms returned from shallow areas also are envisioned. As additional EAARL surveys are conducted in rivers, ground-truth evaluations such as those conducted along the Platte River will be necessary to evaluate system performance in rivers with varying depths, turbidities, and substrates.

Future MD_SWMS enhancements include addition of an eddy-resolving, two-dimensional, structured, non-orthogonal, finite-difference model (H2KE), and a habitat suitability module. Continued collaboration between the USGS Geomorphology and Sediment Transport Laboratory and the USGS Center for Coastal and Watershed Studies is planned to further integrate the use of MD_SWMS and EAARL in river studies.

References

Barton, G.J., McDonald, R.R., Nelson, J.M., and Dinehart, R.L., 2005, Simulation of flow and sediment mobility using a multidimensional flow model for the white sturgeon critical-habitat reach, Kootenai River near Bonners Ferry, Idaho: U.S. Geological Survey Scientific Investigations Report 2005-5230, 64 p.

Bowen, Z.H., and Waltermire, R.G., 2002. Evaluation of Light Distancing and Ranging (LiDAR) for measuring river corridor topography: Journal of the American Water Resources Association, v. 38, no. 1, p. 33-41.

Conaway, J.S., and Moran, E.H., 2004, Development and calibration of a two-dimensional hydrodynamic model of the Tanana River near Tok, Alaska: U.S. Geological Survey Open-File Report 2004-1225, 22 p.

Governance Committee, 2006, Platte River Recovery Implementation Program Cooperative Agreement: http://platteriverprogram.org/Documents/PRRIP%20Program%20Agreement%20Final.pdf

Hicks, D.M., Duncan, M.J., Walsh, J.M., Westaway, R.M., and Lane, S.N., 2001, New views of the morphodynamics of large braided rivers from high-resolution topographic surveys and time-lapse video in Dyer, F.J., Thoms, M.C., and Olley, J.M., eds., The structure, function and management implications of fluvial sedimentary systems: International Association of Hydrological Sciences Publication No. 276, p. 373-380.

Hilldale, R.C., and Raff, D., 2008, Assessing the ability of airborne LiDAR to map river bathymetry: Earth Surface Processes and Landforms, v. 33, p. 773-783.

Holling, C.S., 1978, Adaptive environmental assessment and management: New York, John Wiley.

Kenney, T., 2005, Initial-phase investigation of multi-dimensional streamflow simulations in the Colorado River, Moab Valley, Grand County, Utah, 2004: U.S. Geological Survey Scientific Investigations Report 2005-5022, 69 p.

Kinzel, P.J., Nelson, J.M., and Parker, R.S., 2005, Assessing sandhill crane roosting habitat along the Platte River, Nebraska: U.S. Geological Survey Fact Sheet 2005-3029, 2 p., accessed March 6, 2009, at http://pubs.usgs.gov/fs/2005/3029/.

Kinzel, P.J., Nelson, J.M., and Wright, C.W., 2006, Monitoring changes in the Platte River riparian corridor with serial LiDAR surveys: U.S. Geological Survey Fact Sheet 2006-3063, 4 p., accessed March 6, 2009, at URL: http://pubs.usgs.gov/fs/2006/3063/.

Kinzel, P.J., C.W. Wright, C.W., J.M. Nelson, J.M., and A.R. Burman, A.R., 2007, Evaluation of an experimental LiDAR for surveying a shallow, braided, sand-bedded river: Journal of Hydraulic Engineering, v. 133, no. 7, p. 838-842.

McDonald, R.R., Bennett, J.P., and Nelson, J.M., 2001, The USGS multi-dimensional surface water modeling system: Proceedings of the 7th Interagency Sedimentation Conference, March 25–29, 2001, Reno, Nevada, v. 1, p. I161-167.

McDonald, R.R., Nelson, J.M., and Bennett, J.P., 2005, Multi-dimensional surface-water modeling system user's guide: U.S. Geological Survey Techniques and Methods 6-B2, 136 p.

McKean, J.A., Isaak, D.J., and Wright, C.W., 2008, Geomorphic controls on salmon nesting patterns described by a new, narrow-beam terrestrial–aquatic LiDAR: Frontiers in Ecology and the Environment, v. 6, no. 3, p. 125-130.

Nayegandhi A., Brock, J.C., Wright, C.W., and O'Connell, M.J., 2006, Evaluating a small-footprint waveform resolving LiDAR over coastal vegetation communities: Photogrammetric Engineering and Remote Sensing, v. 72, no. 12, p. 1407-1417.

Nelson, J.M., Bennett, J.P., and Wiele, S.M., 2003, Flow and sediment transport modeling in Kondolph, M., and Piegay, H., eds., Tools in Geomorphology: Wiley and Sons, Chichester, p. 539-576.

Simões, F.J., and McDonald, R.R., 2004, A modeling system for 2D flow in surface waters: Proceedings of the 6th International Conference on Hydroscience and Hydroengineering, Brisbane, Austrailia, May 31–June 3, 2004, CD-ROM.

Tiffan, K.F., Garland, R.D., and Rondorf, D.W., 2002, Quantifying flow-dependent changes in subyearling fall chinook rearing habitat and stranding area using two-dimensional spatially-explicit modeling: North American Journal of Fisheries Management, v. 22, p. 713-726.

Walters, C., 1997, Challenges in adaptive management of riparian and coastal ecosystems: Conservation Ecology, v. 1, no. 2, p. 1. URL: http://www.consecol.org/vol1/iss2/art1

Westaway, R.M., Lane, S.N., and Hicks, D.M., 2003, Remote survey of large-scale braided, gravel bed rivers using digital photogrammetry and image analysis: International Journal of Remote Sensing, v. 24, p. 795-816.

Wright, C.W., and Brock, J.C., 2002, EAARL: A LIDAR for mapping coral reefs and other coastal environments: 7th International Conference on Remote Sensing for Marine and Coastal Environments, National Oceanic and Atmospheric Administration, Miami, Florida, 8 p.

Chapter 4.—Using Bathymetric and Bare Earth LiDAR in Riparian Corridors: Applications and Challenges[1]

Robert C. Hilldale[2], Jennifer A. Bountry[2], and Lucille A. Piety[3]

Abstract

LiDAR products have greatly advanced the technological capabilities in river and floodplain assessments, however, depending on application and data-quality needs certain challenges remain. The focus of this paper is to describe (1) how bare earth and bathymetric LiDAR is currently being applied in multi-disciplined river and riparian restoration assessments in the Pacific Northwest, and (2) how LiDAR products might be improved to expand future capabilities in these studies. Examples applications will be provided from several river studies. This paper is expected to benefit both users and data providers of airborne LiDAR.

There is a growing need to precisely and accurately represent river bathymetry with high resolution to study fluvial environments for flow hydraulics, flood routing, sediment transport, aquatic habitat, and monitoring of geomorphic change. This is especially true for long study reaches at watershed scales where field survey methods can be time consuming and costly. Hydraulic modeling and geomorphic studies require well represented terrain, above and below water, in order to decrease uncertainty in conclusions resulting from such studies. To date, the Bureau of Reclamation has acquired airborne LiDAR bathymetry (ALB) on rivers in Washington, California, and Idaho and has made use of ALB flown in Nebraska. Future bathymetric LiDAR flights are currently being considered and more will likely be needed. This paper highlights some of the areas in which improvements to ALB would benefit those interested in riverine studies. These include improved definition in high relief areas, improved resolution, decreased error and standard deviation, improved water surface detection, and improved guidelines related to water clarity requirements. Some of these issues might be realized through a decrease in output power, processing multiple returns, and improved understanding of variation in data quality.

Bare earth LiDAR has been utilized in Pacific Northwest restoration assessments to delineate geologic controls and surface breaks (e.g., terraces, alluvial fans) along the river system, determine channel slopes, identify historical channel paths, determine connectivity of present channels, locate human features, and map vegetation. Bare earth LiDAR has been particularly advantageous in densely vegetated areas where access is difficult for distinguishing historical channels and surfaces underneath a vegetation canopy. The resolution of LiDAR needed for these applications typically is 1 meter spot spacing for both first return and bare earth. When utilizing LiDAR in vegetated, steep, and wetted areas, data quality is often difficult to ascertain. LiDAR tends to represent most terrain well, but checks with ground survey data can reveal significant differences in critical areas. For example, quality-control checks generally are not located in areas of poor GPS coverage with dense vegetation and high relief, leaving questions related to data quality in these areas that typically are of greatest interest. Improvements in post¬processing and quality-control checks could greatly increase utilization and confidence when using LiDAR as a monitoring tool, for numerical modeling, and tracking temporal changes to topography.

Introduction

Airborne LiDAR products have greatly improved the ability to map various terrain types in a multitude of environments applied over a broad spectrum of disciplines (e.g., Woolard and Colby, 2002; Popescu et al., 2003; Haneberg et al., 2005; Downing et al., 2007). This paper focuses on airborne LiDAR data collected in river corridors and applied to geomorphic investigations and numerical modeling. Filtered and unfiltered terrestrial LiDAR is used for geomorphic investigations while a combination of bare earth and bathymetric LiDAR is used for hydraulic modeling for sediment transport, flood evaluation, and aquatic habitat. In order to provide context, sample applications of LiDAR usage in river corridors are included in this paper. In the course of using various airborne LiDAR products, some challenges or shortcomings have been noted and are discussed in such a way as to benefit users and provide feedback to the industry for possible future improvement. These observations are derived from the perspective of an end-product user, and thus may be limited in technical rigor with respect to specific details related to hardware and software improvements. Nonetheless, the authors believe the suggested improvements to be within reasonable limits of current capabilities.

---

[1]This paper was originally published in the International LiDAR Mapping Forum (ILMF) 2008 conference proceedings (Denver, Colorado) and is reprinted with permission by ILMF.

[2]Hydraulic Engineer, Sedimentation and River Hydraulics Group, Bureau of Reclamation, Denver, CO

[3]Geologist, Seismotectonics and Geophysics Group, Bureau of Reclamation, Denver, CO

The most noticeable advantages of airborne terrestrial LiDAR over traditional ground survey techniques for geomorphic assessments are: the significant increase in point density, the availability of additional products (e.g., first return data, intensity images), and the tremendous efficiency of data collection allowing for coverage of larger areas (Jones et al., 2007). The advantage of airborne LiDAR over photogrammetry is the ability to acquire elevation data in densely vegetated areas that may be otherwise difficult to access and collect data. Quantitative comparison by Jones et al. (2007) of geomorphic maps produced using either LiDAR data or aerial photographs with field mapping showed that nearly 90% of the mapped geomorphic features were recognized by both techniques. A similar comparison, although qualitative, by Reclamation for the heavily vegetated Quinault and Methow riparian corridors in Washington found that paleochannels, which are used to define channel migration areas and floodplain boundaries, were more easily recognized and mapped using LiDAR than aerial photographs, even when historical photographs were incorporated (Bountry et al., 2005). Jones et al. (2007) also reported that paleochannels were more likely to be recognized on the LiDAR and reported about a 10% greater length of mapped paleochannels from the LiDAR than from the aerial photographs.

If complete survey coverage of a river bed is required, Airborne LiDAR Bathymetry (ALB) provides three key advantages over traditional surveys using boat-mounted acoustic in conjunction with total station or Real Time Kinematic Global Positioning Satellite (RTK GPS) surveying equipment: (1) greater point densities, (2) more efficient data collection at a watershed scale, and (3) more complete coverage of wetted areas to be surveyed. A traditional survey using boat mounted acoustics generally provides an incomplete survey of a river channel due to time constraints, limited access in shallow water, minimum depth requirements of acoustic devices, and possible motor restrictions on rivers that may limit access through regulation (fig. 1). Inconsistent satellite and radio reception near dense riparian vegetation or in areas where nearby terrain relief increases the horizon angle, such as in a canyon-like setting, also create difficulties for traditional acoustic surveys using GPS equipment. Recent adaptations in post-processing bed elevation data from an Acoustic Doppler Current Profiler (ADCP) using AdMap software (David S. Mueller, USGS, written commun.; Dinehart and Burau, 2005) allows for the detection of up to four elevations from a single ping. In spite of this improvement in acoustic surveys, complete coverage is often unattainable without a very labor intensive effort usually involving topographic surveys on foot. This is especially true when side channels are numerous and too shallow for boat access (fig. 1).

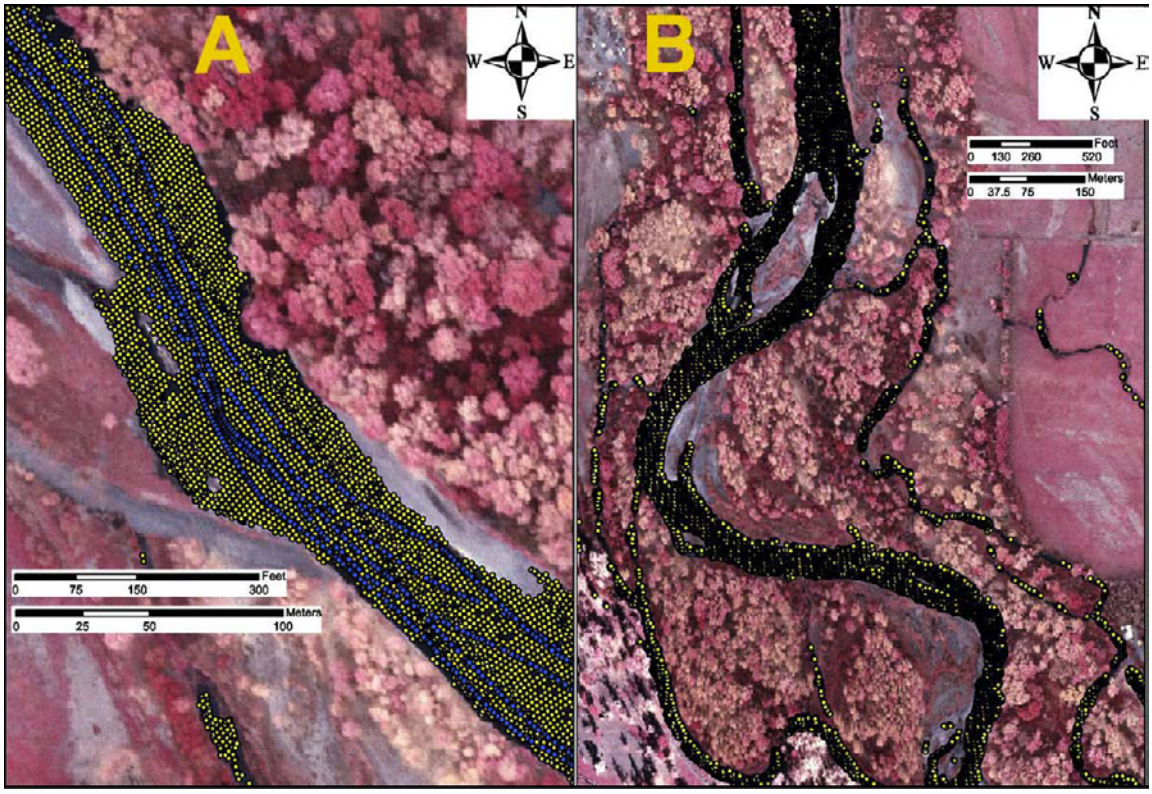

Figure 1. Aerial photographs showing (**A**) survey coverage using ALB (yellow) and boat-mounted acoustics (blue) and (**B**) ability of ALB to obtain coverage in wetted side channels, Yakima River, Washington.

Sample Applications of Airborne LiDAR in River Corridors

In assessing geomorphic processes and hydraulic conditions in river corridors, Reclamation uses airborne terrestrial LiDAR data primarily in two ways: (1) to create a geomorphic map of the floodplain, including channels and paleochannels, geomorphic surfaces that define the boundaries of the floodplain and channel migration zone, vegetation, and infrastructure (e.g., bridges, levees), and (2) to collect the floodplain elevation data needed for one-dimensional (1-D) and two-dimensional (2-D) hydraulic models for flood inundation, sediment transport and aquatic habitat assessments. The terrain surface in a 1-D model is based on data from discrete cross sections only, which can be generated by either LiDAR data or ground surveys. The terrain surface in 2-D model uses elevation data from the entire floodplain and channel, which are difficult to obtain by ground surveys, but can be easily generated from LiDAR data.

To address the inability of terrestrial LiDAR to map underwater portions of a floodplain, Reclamation has combined ALB with above water elevation data provided by either bare earth LiDAR or photogrammetric methods to construct the continuous terrain surface needed for 2-D modeling. Through examples from Reclamation's work, the uses and challenges of both types of LiDAR data will be discussed in the following sections.

Terrestrial LiDAR

With terrestrial LiDAR, a geomorphic map can be made for large areas of the floodplain, and then validated through field checking by a multi-disciplined team of scientists. In watersheds with large areas being considered for restoration actions, airborne terrestrial LiDAR mapping helps determine where more refined analyses, such as hydraulic modeling, should be focused to better meet the needs of the project. Airborne LiDAR mapping on the Quinault River (Washington) was utilized to interpret floodplain boundaries and the extent of historical channel migration zones (fig. 2). In addition to flood hazards, channel migration can represent a significant risk to property and infrastructure. Although significant field work is required to define such parameters, airborne LiDAR greatly aids this process.

Terrestrial LiDAR also can be used to create the elevation terrain needed for 2-D hydraulic models. 2-D models constructed with LiDAR are an efficient way to provide visual tools to end users that are easy to understand and interpret. Additional survey data, analysis and modeling typically will be needed for smaller areas, where projects are actually implemented.

The 2-D models can be used to better understand existing hydraulic conditions, which in many river systems include human features that have impacted physical river processes and disrupted channel and floodplain connectivity at overbank flows. An example is Reclamation's assessment for Nason Creek, where LiDAR was used to develop a

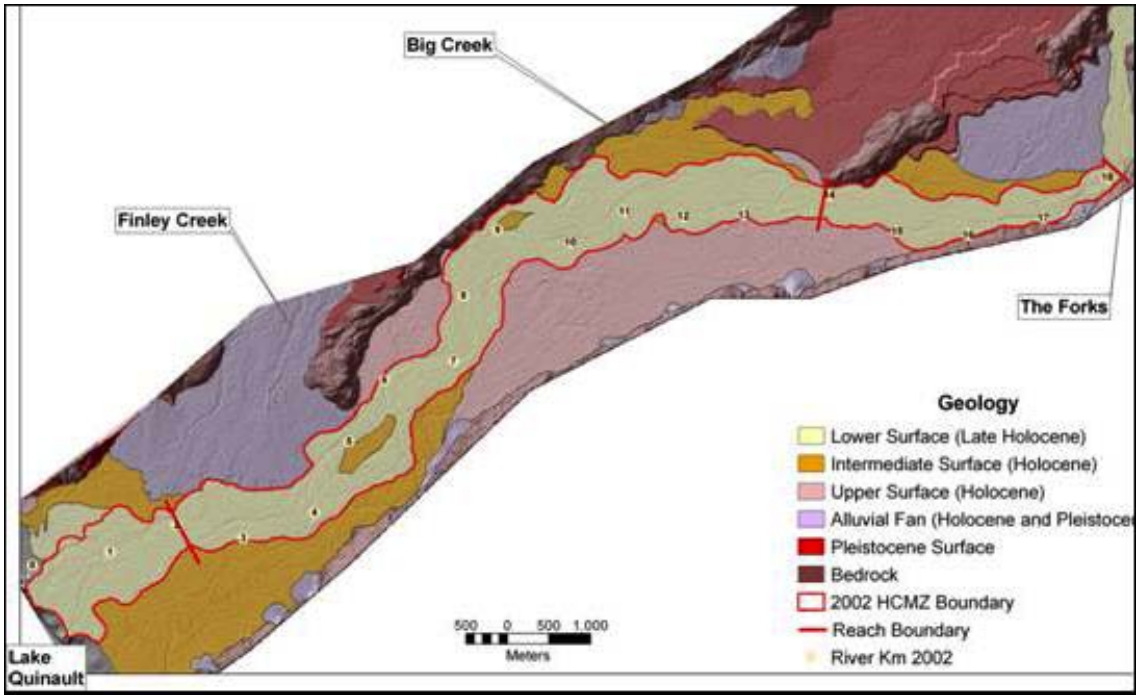

Figure 2. Example of LiDAR mapping in the Quinault watershed in northwest Washington in a heavily vegetated area to map surficial features. Significant field mapping also is required for this level of analysis.

DEM (digital elevation model) to identify limiting factors in current fisheries habitat. In addition to showing existing hydraulic conditions, elevation adjustments were made to the DEM that represented the removal of a berm upon which railroad tracks were constructed. The hydraulic model was run again without the impediments to flow and then shared with biologists, landowners, and stakeholders to demonstrate what improvements could be realized if actions were taken to restore natural connectivity between the channel and floodplain (fig. 3).

In addition to the uses for bare earth LiDAR, data obtained using the first return from airborne terrestrial LiDAR data can be used to generate a difference DEM indicating canopy height. This information can be used to estimate roughness, a parameter that incorporates resistance to flow (from vegetation or other features), in the hydraulic model. Features that influence roughness in the floodplain are easier to identify and delineate with LiDAR data, especially when used in conjunction with aerial photography. For Nason Creek (Washington), first return data were utilized to distinguish various vegetation types (tall, dense trees; low growing shrubs, etc.). Polygons were drawn around the different types, delineating areas with varying roughness.

Numerical representations of river hydraulics depend on well defined channel banks and the surrounding floodplain. Improperly mapped channel banks can result in depth and velocity values that do not represent the true condition. Misrepresentation of these features can result from inaccurate or nonexistent elevation data in these areas.

Bathymetric LiDAR

To date, ALB, in combination with elevation data generated from terrestrial LiDAR data or photogrammetric methods, has been used by Reclamation for both one-dimensional (1-D) and two-dimensional (2-D) hydraulic models for sediment transport and habitat assessment.

Because using ALB to create channel bed elevation data is relatively new, data quality was investigated for ALB flown on the Yakima River in Washington (Hilldale and Raff, 2007). Mean vertical error (systematic error) fell between 0.10 and 0.27 m across various reaches in both rivers while standard deviation (random error) ranged from 0.12 to 0.31 m. When all sources of error are considered, including error in the ground check surveys, overall measurement error of the ALB fell within the manufacturer's specifications.

In the Yakima River, aquatic habitat was evaluated with a 2-D hydraulic model, taking advantage of both bare earth LiDAR and ALB. Among the habitat features evaluated with 2-D modeling were mesohabitat (pools, riffles, and glides), side channels, and spawning habitat. Similar modeling analyses have been performed with bathymetric data collected using an acoustic survey (e.g., Reuter et al., 2003). Habitat analysis also can be accomplished using multi-spectral digital imagery and pixel color to map water depth (e.g., Marcus, 2002); however, the effect of discharge on habitat quality and quantity is important to many applications, which would require multiple flights using this method. The primary advantage of using a hydraulic model is the ability to evaluate a wide range of discharges without repeated data-collection flights. The locations of pools, riffles, and glides (fig. 4) and spawning locations (fig. 5) were successfully predicted with the 2-D model and were verified with field observations (Hilldale, 2007). The habitat mapping method uses the Froude number, a dimensionless ratio of inertial forces to gravitational forces used to define free surface flows.

Future applications of 2-D hydraulic modeling for salmonid habitat by Reclamation include a more rigorous evaluation than mentioned above. Habitat polygons will be constructed with hydraulic modeling results using depth, velocity and distance to edge of water. Significant field data will be gathered on this project for rigorous verification of modeling results.

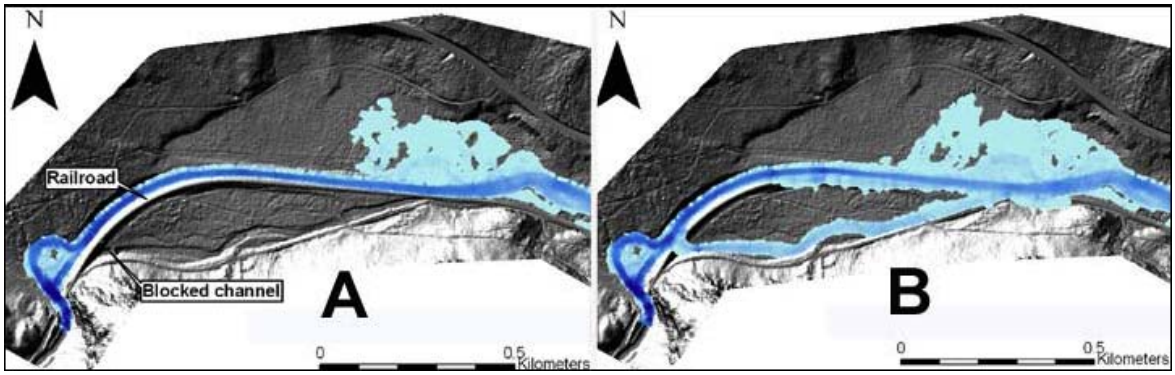

Figure 3. Application of LiDAR providing surface representation for input to a 2-D hydraulic model on Nason Creek in eastern Washington. The above figures show the results of hydraulic modeling displayed on a hillshade for the same discharge. Velocity and inundation area are indicated, with velocity increasing as the shade darkens (**A**) Existing conditions where a railroad grade has blocked off a historical channel (visible on the hillshade). (**B**) Proposed configuration based on removing all human features that block floodplain access (flow is left to right).

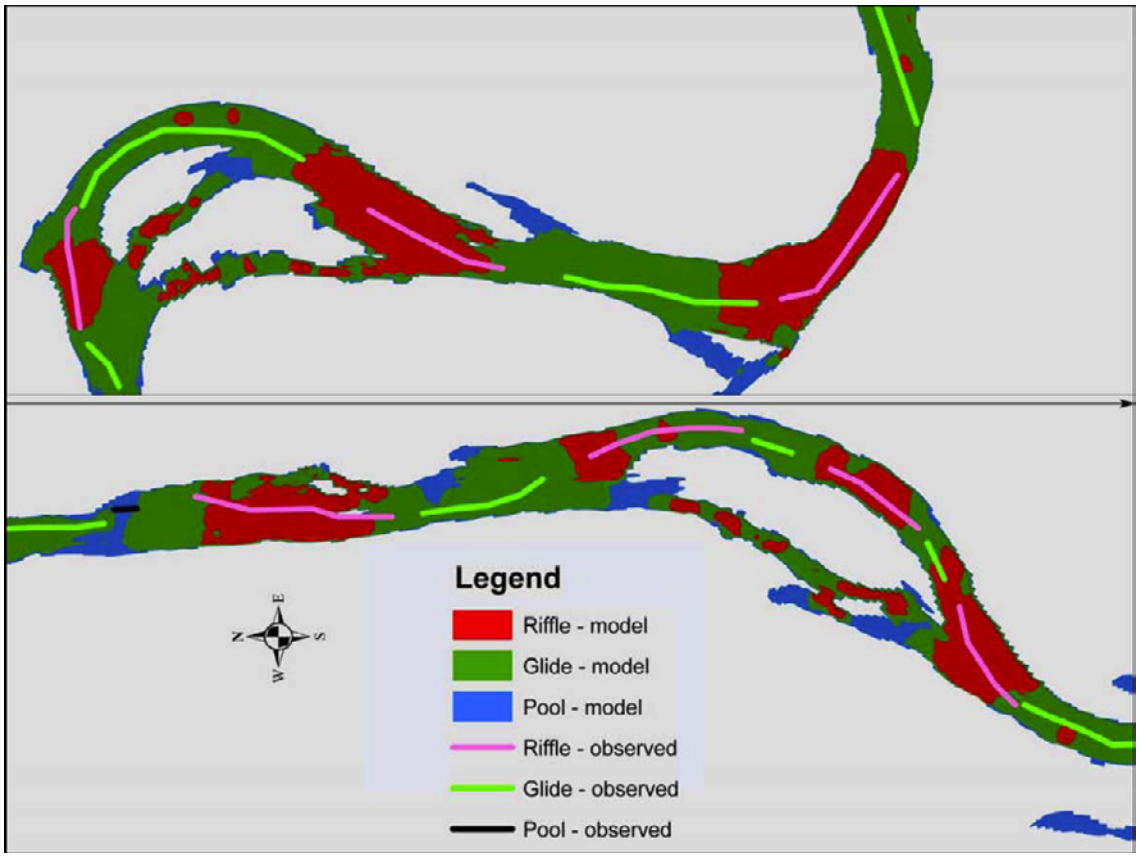

Figure 4. Example of hydraulic modeling results that map the location of pools, glides and riffles. The bathymetry for the model was acquired using ALB.

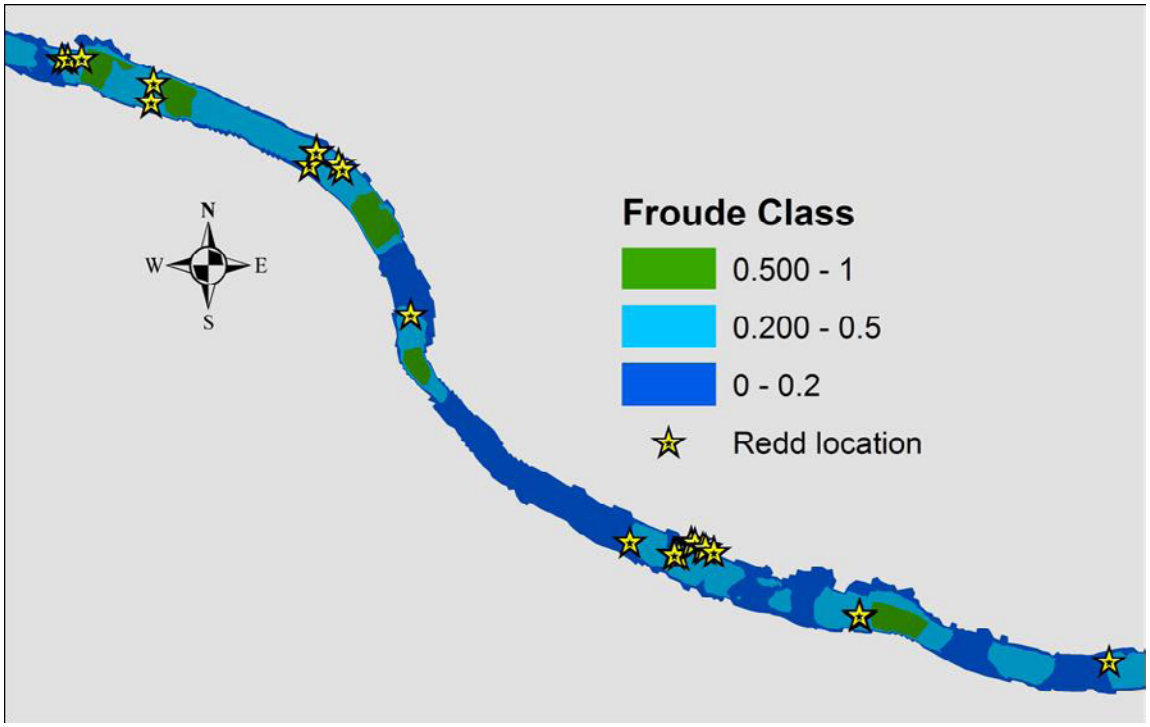

Figure 5. Example of hydraulically suitable spawning locations (0.2<Fr<0.5) determined with a hydraulic model. The bathymetry for the hydraulic model was acquired using ALB.

Critical to evaluating habitat with a 2-D model is well represented channel bathymetry and proper identification of physical features. Without proper representation of these features, specific habitat types may go unnoticed or improperly represented. Moderately sized features and abrupt changes in a channel bed can represent significant habitat value and thus must be included in the terrain representation.

Existing Challenges for Airborne LiDAR

Airborne Terrestrial LiDAR

Collecting airborne LiDAR in river corridors poses certain challenges currently known to the industry, primarily dense vegetation cover and steep slopes. These conditions are often spatially coincident in river corridors, where steep, vegetated river banks are encountered more often than not. For example, Bowen and Waltermire (2002) compared LiDAR surveys to ground surveys in a river corridor covering various terrain types. These authors report that vertical root mean square error ($RMSE_z$) was greatest in a sloped terrain (>45°) and in cross sectional profiles near the active channel, where high slopes on channel banks are vegetated. These errors were often outside the stated precision of the survey. Although the industry has taken measures to address these challenges, such as improvements in multi-return post processing to obtain bare earth and improvements in positional accuracy to reduce error for steep slope measurements, challenges remain. Difficulties often arise for data users when overall data quality (accuracy and precision) is reported only for gently sloping terrain devoid of vegetation. Measurements of data quality on this type of terrain generally are not applicable to steep, vegetated river banks, often leaving users uncertain of data quality in areas of greatest interest.

One of the more time-consuming challenges in applying terrestrial LiDAR to geomorphic assessments and 2-D modeling is manipulating the large amount of data. Point data are particularly cumbersome when the project area covers a large area, and broad, flat floodplains need to be evaluated for overbank flooding. When evaluating river channel and floodplain areas, in many cases more resolution is needed within the active portion of the river channel and/or channel migration zone, and less resolution is needed on valley floors and terraces that contain minimal elevation relief (e.g., agricultural lands). Tools and methods are being developed for software commonly used by Reclamation to filter the data and provide varying resolutions based on general boundaries of valley floor (less resolution) versus riparian areas (more resolution). More sophisticated methods often available to data providers are sometimes difficult to utilize, as terrain relief is often known only after the delivery of the data.

Airborne LiDAR Bathymetry

One of the primary drawbacks of commercially available bathymetric LASERS is the large spot size. The minimum limit for spot size is due to the requirement for eye-safe conditions, whereby the high energy required for a LASER pulse to penetrate the water column is diffused over a large area, reducing potential danger to the human eye. Bathymetric LASER units are currently configured for coastal applications, where penetration to 50 m or more is claimed by the manufacturer, however, this penetration depth is not needed for river applications. By reducing the output power of the LASER, eye-safe conditions could be met with a significantly reduced spot size. This would tremendously improve the ability to detect features on the bed such as sharp drop-offs and large roughness elements such as boulders or large woody debris (fig. 6). Additionally, positional accuracy is likely to improve with a smaller spot. For river applications, water penetration to more than approximately 10 m is not necessary, as rivers with a large portion of their depth greater than 10 m will not likely have sufficient water clarity for successful bottom detection using ALB.

Another drawback of current commercial bathymeters is the coarse spot spacing relative to terrestrial airborne LiDAR units. Reduced spot spacing will obviously improve resolution, also leading to better detection of critical features on the riverbed.

Another potential improvement for ALB is processing of multiple returns. Terrestrial airborne LiDAR post processing is currently capable of evaluating multiple returns to detect bare earth under vegetation. Similar processing techniques may be applied to ALB to improve the ability to penetrate some aquatic vegetation and overhanging vegetation. Processing multiple returns also may improve the ability to detect abrupt changes in the riverbed and other moderately sized features such as sand dunes.

The final limitation to ALB is the cost, which may be the greatest limitation mentioned in this paper. As the reach of interest becomes larger, ALB becomes more feasible for two reasons; (1) optimization of unit costs, and (2) more intense labor requirements for data collection with boat-mounted acoustics, possibly supplemented with a topographical survey in areas inaccessible by boat such as shallow areas and side channels. In spite of the benefits mentioned, the large cost of ALB generally is prohibitive to all but a few projects with very large budgets. Considering current pricing and maximizing the economy of scale for the ALB, a traditional boat-mounted acoustic survey may cost approximately one-fifth or less of an ALB survey that delivers 2×2 m spot spacing. Significant cost reduction will allow this capability to be used by a much broader spectrum of scientists and engineers.

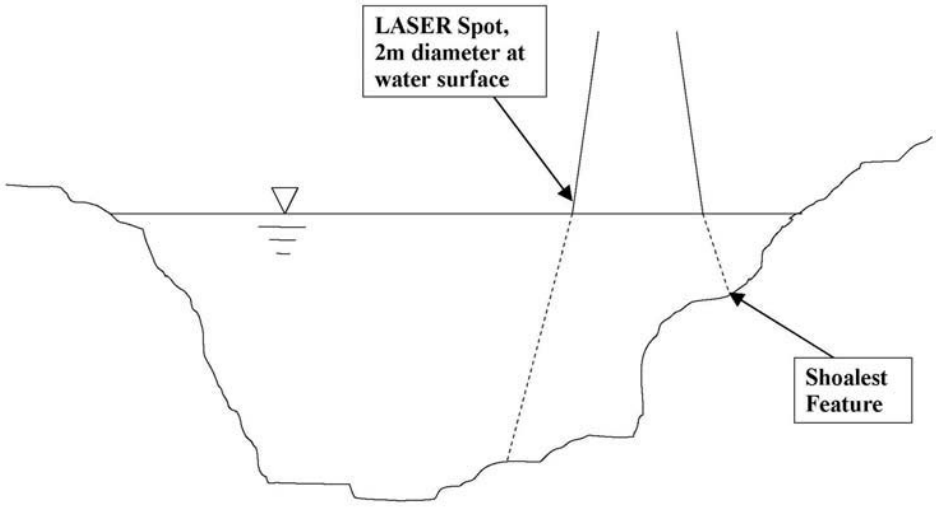

Figure 6. Sample cross section showing an abrupt change in bed elevation that can bias the bottom elevation measurement, particularly under conditions of a large spot size.

Discussion

Some of the issues or challenges mentioned regarding terrestrial airborne LiDAR surveys can be addressed with negotiations prior to the survey. It is the responsibility of the customer to insure proper collection and delivery of desired data and also to understand the limitations of the measurement technique. It is assumed here that agreements have been reached regarding such things as spatial resolution and extent of coverage. However, some issues often overlooked by the customer are measurement and definition of data quality, limitations of airborne LiDAR, and the applicability of secondary products such as intensity plots. Guidelines for ground check points of elevation in areas obscured by vegetation or on steep slopes can and should be negotiated in a contract prior to data collection if these areas are of interest. Definitions of data quality may be more useful if defined for separate terrain types, such as gentle or steep slopes and vegetated or unvegetated areas. This can be defined according to the needs of the customer and terrain encountered in the study area.

The customer also needs to be aware of national and international standards of aerial data collection (e.g., International Hydrographic Organization, National Map Standards, etc.). Applicable mapping standards are most always met by data providers; however, these standards may need to be exceeded to meet the specific needs of the customer. For example, a data provider may claim national map standards have been met by an airborne survey ‘with the exception of obscured areas’. The U.S. Army Corps of Engineers’ hydrographic surveying manual (2002) chapter on river engineering focuses primarily on very large rivers and engineering structures with no mention of habitat modeling. It is up to the customer to understand applicable standards, whether or not these standards are sufficient for the use of the data, and to determine ahead of time what data quality will be required to meet project goals.

The authors believe that with decreased costs for ALB, this technology will be in increasing demand. Improvement in those areas mentioned in this paper also will attract more users. Concerns about and awareness of our aquatic resources are growing rapidly. Projects related to aquatic riverine habitat are increasingly in need of broader scale studies, involving multi-disciplined teams to tackle such issues as dam decommissioning, listing of endangered species, and continuing decline of habitat due to adverse human constructs. ALB could play a significant role in providing the data necessary for addressing such issues.

References

Bountry, J.A., Piety, L.A., Randle, T., Lyon, Jr., E.W., Abbe, T., Barton, C., Ward, G., Fetherston, K., Armstrong, B., and Gilbertson, L., 2005, Geomorphic investigation of Quinault River, 18 km reach of Quinault River upstream of Quinault Lake: Unpublished, developed by Bureau of Reclamation, Herrera Environmental Consultants, and Quinault Indian Nation Fisheries Department.

Bowen Z.H., and Waltermire R.G., 2002, Evaluation of Light Detection and Ranging (LiDAR) for measuring river corridor topography: Journal of the American Water Resources Association, v. 38, no. 1, February, p. 33-41.

Dinehart, R.L., and Burau, J.R., 2005, Repeated surveys by acoustic Doppler current profiler for flow and sediment dynamics: Journal of Hydrology, v. 314, p. 1-21.

Downing J.B., Konsoer, K.M., and Kite, J.S., 2007, LiDAR based surficial geology mapping in comparison to more traditional methods in the heavily vegetated Appalachian Mountains: Paper No. 58-2, Geological Society of America annual meeting, Denver, CO, Oct. 28-31.

Haneberg W.C., Creighton, A.L., Medley, E.W., and Jonas, D.A., 2005, Use of LiDAR to assess slope hazards at the Lihir gold mine, Papua New Guinea, *in* Hungr, O., Fell, R., Couture, R., and Ebert, E., eds., Landslide risk management: Proceedings of the International Conference on Landslide Risk Management, Vancouver, Canada, May 31–June 3.

Hilldale, R.C., 2007, Using bathymetric LiDAR and a 2-D hydraulic model to identify aquatic river habitat: Proceedings, World Environmental and Water Resources Congress, ASCE, Tampa, FL, May 15-19.

Hilldale R.C., and Raff, D., 2008, Assessing the ability of airborne LiDAR to map river bathymetry: Earth Surface Processes and Landforms, v. 33, p. 773-783.

Jones, A.F., Brewer, P.A., Johnstone, A., and Macklin, M.G., 2007, High resolution interpretive geomorphological mapping of river valley environments using airborne LiDAR data: Earth Surface Processes and Landforms, v. 32, p. 1574-1592.

Marcus, W.A., 2002, Mapping of stream microhabitats with high spatial resolution hyperspectral imagery: Journal of Geographic Systems, v. 4, 113-126.

Popescu, S.C., Wynn, R.H., and Nelson, R.F., 2003, Measuring individual tree crown diameter with lidar and assessing its influence on estimating forest volume and biomass: Canadian Journal of Remote Sensing, v. 29, no. 5, p. 564-577.

Reuter, J.M., Jacobson, R.B., and Elliot, C.M., 2003, Physical stream habitat dynamics in lower Bear Creek, northern Arkansas: Biological Sciences Report USGS/BRD/BSR-2003—002, Columbia Environmental Research Center, Columbia, MO.

Woolard, J.W., and Colby, J.D., 2002, Spatial characterization, resolution, and volumetric change of coastal dunes using airborne LiDAR: Cape Hatteras, North Carolina: Geomorphology, v. 48, no. 1-3, November, p. 269-287.

U.S. Army Corps of Engineers, 2002, Engineering and Design – Hydrographic Surveying, Publication Number: EM 1110-2-1003, January, accessed June 2007, at http://www.usace.army.mil/inet/usace-docs/eng-manuals/em1110-2-1003/toc.htm.

Chapter 5.—Application of the SHOALS Survey System to Fisheries Investigations in the Columbia River

By Kenneth F. Tiffan[1], Paul G. Wagner[2], Keith S. Wolf[2], and Paul A. Hoffarth[3]

Abstract

We used a Scanning Hydrographic Operational Airborne LiDAR (Light Detection and Ranging) Survey (SHOALS) system to collect high-resolution bathymetry for 33 km of the Hanford Reach. Data were used in conjunction with hydrodynamic and predictive habitat models within a GIS (Geographical Information System) framework to evaluate the effects of a varying hydrograph on juvenile fall Chinook salmon rearing habitat and risk from stranding and entrapment. Furthermore, we were able to estimate the number of juvenile fish that were stranded and entrapped in pools when operations at Priest Rapids Dam caused rapid decreases in river flows. Our findings were ultimately used to estimate impacts of power generation operations at Priest Rapids Dam and develop long-term policy and operational guidelines to protect juvenile fall Chinook salmon during the spring rearing period.

Introduction

The Hanford Reach is the only unimpounded section of the Columbia River between Bonneville Dam and the Canadian border (fig. 1). Because the Hanford Reach retains many of the riverine processes that no longer exist in the impounded Columbia River, it supports the largest population of fall Chinook salmon *Oncorhynchus tshawytscha* in the Columbia River Basin (Huntington et al., 1996; Dauble and Watson, 1997). These fish are part of the "Upriver Bright" fall Chinook stock and are a primary contributor to ocean and freshwater sport, commercial, and in-river tribal fisheries. They also are a component of the international Pacific Salmon Treaty between the United States and Canada and their status affects management decisions throughout the West Coast (Wolf and Wagner, 1998; Wolf, 1999). Fall Chinook salmon are unique in that they spawn and rear in mainstem habitats rather than in tributaries like many other anadromous salmonids. Each year the Hanford Reach produces an estimated 13–39 million juvenile salmon (Paul Hoffarth, Washington Department of Fish and Wildlife (WDFW), unpublished data), which rear along shallow mainstem shorelines for 2–4 months before migrating seaward during the summer.

Flows through the Hanford Reach are regulated by upstream hydroelectric dams of which Priest Rapids Dam at the head of the Reach exerts the greatest local influence. Changes in discharge at Priest Rapids Dam to meet power demand, termed power peaking, can cause tail-water elevations to fluctuate more than 3 vertical meters in 6 h. These fluctuations can potentially change the amount of rearing habitat available to juvenile fall Chinook salmon on a daily and hourly basis. Sharp decreases in flow also strand fall Chinook salmon in substrate and in disconnected pools when water rapidly recedes from low-gradient shoreline habitats, causing significant mortality of young salmon (Wagner et al., 1999).

In 1998, we initiated a study to examine the effects of flow fluctuations on juvenile fall Chinook salmon rearing habitat and susceptibility to stranding, entrapment, and level of survival. However, to make inferences ranging from the scale of the individual fish to the scale of the reach presented a unique challenge that required high-resolution data over a broad spatial area. To address this challenge, we collected LiDAR (Light Detection and Ranging) data from 33 km of river using a Scanning Hydrographic Operational Airborne LiDAR Survey (SHOALS) system (Guenther et al., 1996; Lillycrop et al., 1996; Parson et al., 1996). The resulting detailed riverbed bathymetry was used in conjunction with one- and two-dimensional hydrodynamic modeling, predictive statistical models, and a spatially explicit analysis to predict the effects of flow changes on rearing habitat. Furthermore, we were able to quantify the effects of a variable hydrograph from Priest Rapids Dam on juvenile fall Chinook salmon stranding and entrapment to ultimately derive estimates of mortality over the course of an entire rearing season. The use of remote sensing coupled with direct monitoring provided information to support policy discussions and decisions leading to broad agreements and decreased impacts to this principal salmon population.

[1]U.S. Geological Survey, Western Fisheries Research Center, 5501A Cook-Underwood Rd., Cook, Washington 98605

[2]KWA Ecological Sciences, Inc., P.O. Box 73, Plymouth, Washington 99346

[3]Washington Department of Fish and Wildlife, 2620 N. Commercial Ave., Pasco, Washington 99301

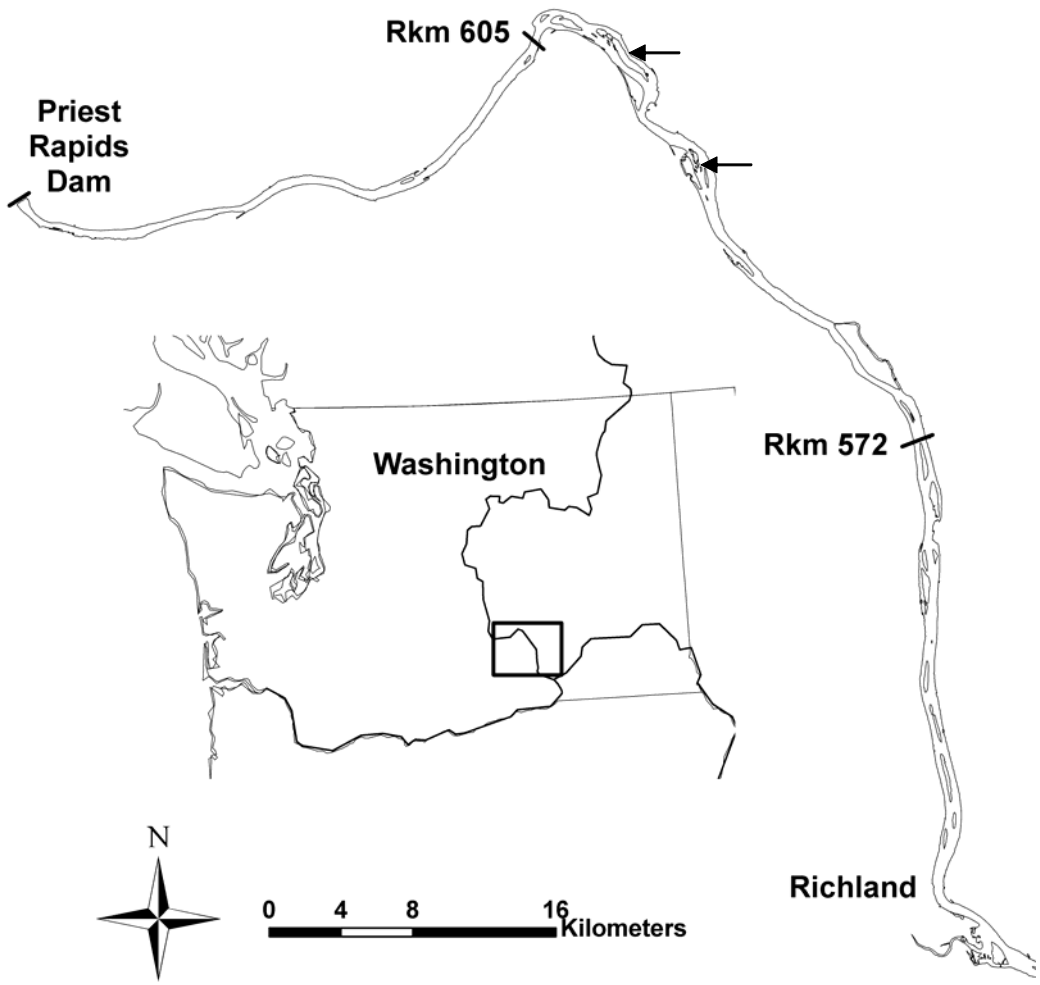

Figure 1. The Hanford Reach of the Columbia River in Washington showing the river kilometers (Rkm) that delineated our study area.

Study Area

The Hanford Reach extends 90 km from Richland, Washington, upstream to Priest Rapids Dam (fig. 1). We restricted our study to a 33-km area between river kilometers (kilometers from the mouth, Rkm) 572 and 605 because this area supports large numbers of rearing juvenile fall Chinook salmon and contains a range of geomorphic and hydraulic features. Steep bluffs bound the northern and northeastern side of the river in the upper half of the study area, and there are numerous alluvial islands. The average channel width is about 0.7 km, depths typically are less than 10 m, and the longitudinal elevation change along the channel is less than 1 m/km. The bed is composed primarily of gravel and cobble size sediment (Dauble and Geist, 2000). The riparian community is relatively sparse and is composed predominantly of forbs, grasses, and a few shrubs and trees (Fickeisen et al., 1980).

Methods

SHOALS Survey

We required a high-resolution, digital elevation model of the study area for two-dimensional hydrodynamic modeling and a geographic information system (GIS)-based analysis of juvenile fall Chinook salmon rearing, stranding, and entrapment areas. For this reason, we contracted with the U.S. Army Corps of Engineers to conduct a SHOALS survey of 33 km of the Hanford Reach between Rkm 572 and 605 during the first week of August 1998. The SHOALS system we used was able to rapidly collect highly accurate elevation data over a large area both above and below the water surface (Guenther et al., 1996; Lillycrop et al., 1996; Parson et al., 1996). A LiDAR surveying unit was attached to the bottom of a helicopter whose position and altitude were determined using

a kinematic global positioning system (GPS). Kinematic GPS base stations were established at three locations over National Geodetic Survey benchmarks to reference all data to known elevations and geographic positions. Surveys were flown at an altitude of 200 m above the river to obtain a density of one sample point for every 16 m^2 (4×4 m cell). Horizontal accuracy of positions was <±1 m, and vertical accuracy was <±12 cm (Lillycrop et al., 1996).

We limited our SHOALS survey to shoreline areas because they contain important rearing habitats for juvenile fall Chinook salmon (Becker, 1973; Dauble et al., 1989). We surveyed the area between shorelines created at flows of 50 and 400 kcfs, which encompass the range of flows typical during the fall Chinook salmon rearing period. The survey area bounded by these flows was determined from a one-dimensional flow model (MASS1) developed for the Hanford Reach (Richmond and Perkins, 1998). MASS1 is a steady-state model that estimates water-surface elevations and mean cross-sectional velocities for a given input flow. We had hydrosystem operators reduce Columbia River flows to 50 kcfs in the Hanford Reach during our SHOALS survey to dewater as much of the river channel as possible to avoid problems associated with measuring elevations in water less than 1 m deep.

The SHOALS survey collected more than 2.2 million riverbed points, which were incorporated in GIS to create a bathymetric coverage of the study area. Because dense vegetation such as bushes and trees caused false elevations in our data, we manually removed these from the dataset and interpolated ground elevations for those areas. Video records collected during the survey confirmed the locations of dense vegetation. Because our survey did not cover the center of the river channel, we completed our bathymetric coverage using riverbed elevations collected every 27 m along cross sections spaced every 0.4 km throughout the study area (U.S. Army Corps of Engineers, unpublished data).

Rearing Habitat

The amount of rearing habitat available to juvenile fall Chinook salmon was estimated for a range of flows from Priest Rapids Dam. We defined suitable rearing habitat as having lateral bed slopes <40% and water velocities <0.4 m/s. These variables were the best predictors of fish presence in our spatially explicit analysis. We used a logistic regression model to predict the probability that fall Chinook salmon would occupy habitat cells (4×4 m created in GIS) that contained lateral bed slopes ranging from 0 to 40% (in 10% increments) and with water velocities ranging from 0 to 0.4 m/s (in 0.1 m/s increments; Tiffan et al., 2002). Cells with probabilities >0.5 were deemed to contain suitable rearing habitat. The lateral bed slope of each cell was calculated in GIS as a grid-based two-dimensional slope and was expressed as a percent (Burrough, 1986; Environmental Systems Research Institute, Inc., 1998). Depth-averaged water velocities were estimated for each cell under a range of flows likely to be encountered by rearing fall Chinook salmon. We modeled water velocities at 36 steady-state flows ranging from 50 to 400 kcfs in 10-kcfs increments using a two-dimensional hydrodynamic model (RIVER_2D; Ghanem et al., 1996; Tiffan et al., 2002). The hydrodynamic model also enabled us to identify topographic depressions in rearing areas that could potentially entrap fish when these depressions became disconnected from the main river channel. We calculated the total area of disconnected pools that were created in the study area when flows were decreased by 20 and 30 kcfs increments from each flow modeled. These are the daily-flow-reduction increments currently allowed by fishery managers to minimize the stranding and entrapment of juvenile fall Chinook salmon when mean daily discharge is less than 110 kcfs.

Stranding and Entrapment

SHOALS bathymetry data were used in conjunction with the MASS1 unsteady flow model to estimate shoreline locations for flows ranging from 40 to 400 kcfs in 10-kcfs increments. These were used to estimate the area of the riverbed dewatered by each 10-kcfs reduction in flow to guide the sampling and analysis of the juvenile fall Chinook salmon stranding and entrapment (Nugent et al., 2002a). Following flow reduction events, circular plots (344.4 m^2) were randomly selected and sampled within the wetted area of a 40-kcfs flow band that bounded the affected area (Nugent et al., 2002a). Within each sample plot, field crews counted the number of alive and dead juvenile fall Chinook salmon that were stranded or entrapped in pools. Other data recorded at the sites included bird activity (i.e., tracks), entrapment water temperatures, dominant and subdominant substrate size and embeddedness (Platts et al., 1983), and vegetation density (absent, sparse, medium, or dense; Nugent et al., 2002a and 2002b).

The total number of juvenile fall Chinook salmon mortalities due to stranding/entrapment was estimated for the study area. We enumerated the number of dead fish in each sample plot and accounted for the number of plots in each flow band, the area of the flow band, the number of flow reductions that occurred during the study period, and the attenuation of the amplitude of the fluctuations in river flows as the flows move down through the Hanford Reach. A statistical analysis of these data was performed to estimate mortality and associated confidence intervals for the 1999 and 2000 sampling years (Nugent et al., 2002a and 2002b).

Results

Rearing Habitat

Our approach enabled us to make the first quantitative estimates of the amount of juvenile fall Chinook salmon rearing that exists at different flows in the Hanford Reach. We found the amount of juvenile fall Chinook salmon rearing habitat generally decreased as flows increased (fig. 2). Habitat area ranged from a high of 275 ha at a flow of 50 kcfs to a low of 125 ha at a flow of 400 kcfs. We summed the lengths of shoreline that contained suitable rearing habitat cells to determine what percent of the total shoreline was available to rearing fall Chinook salmon. The percentage of suitable shorelines also decreased as flow increased. For the entire study area, the percent of suitable shoreline ranged from 77 to 97% over the range of flows we modeled.

Our spatially explicit analysis also allowed us to identify how rearing habitat was distributed throughout the study area and how habitat area changed with flow fluctuations. Figure 3 provides a graphical example of available rearing area at Rkm 587. The steeper shoreline on the right side of the river contains less suitable area than the islands on the left side of the river where the velocities and lateral slopes are lower. Fish abundance generally was higher in habitats with high suitability than in lower quality habitats. Our evaluation showed that habitat area can change up to 8% daily under flow fluctuations currently allowed at Priest Rapids Dam.

Stranding and Entrapment

The area of disconnected pools that could potentially strand juvenile fall Chinook salmon in the Hanford Reach also varies with river flow. We were able to identify specific flows from which additional reductions caused the formation of a significant amount of entrapment pool area. We also were able to identify the areas that pose the greatest risk of entrapment to juvenile fall Chinook salmon both in terms of the size and number of entrapments created by different flow reductions. Figure 2 shows the amount of area potentially dewatered within each 10 kcfs-flow fluctuation zone for our study area. The area of shoreline exposed by flow fluctuations at lower river elevations (50–120 kcfs) is much larger than at higher fluctuation zones. However, the amount of shoreline exposed at some flow levels actually increases with increasing river elevations (i.e., 170–180 kcfs) suggesting steep banks may give way to flats or flood terraces. The extent of steep banks and flood terraces vary with river kilometer.

For the first time, we were able to estimate the stranding/entrapment-related mortality of juvenile fall Chinook salmon due to flow fluctuations over 36 km of river. We estimated 126,695 (95% CI = 50,724 – 200,666) fish were lost to stranding and entrapment in 1999, and an additional 381,897 (95% CI = 1,026 – 764,141) fish were placed at risk of mortality. In 2000, we estimated 72,362 (95% CI = 34,270 – 110,454) juvenile fall Chinook salmon mortalities were caused by stranding and entrapment with an additional 255,222 (95% CI = 17,743 – 492,701) fish placed at risk of mortality (Nugent et al., 2002a and 2002b).

Discussion

The SHOALS system enabled us to collect high-resolution bathymetry over a broad, complex geographic area in the Hanford Reach that supported the development of hydrodynamic models to estimate fish habitat attributes such as water velocity, depth, flow direction and turbulence, and meso-habitat features. These in turn were used to assess the amount and suitability of habitat under different flow scenarios. The approach we describe will enable fishery scientists to predict the effects of different river operations and management actions on fish habitat use and survival.

Our use of the SHOALS system represents the first use of this technology in the Columbia River Basin. Since that time, the remainder of the Hanford Reach was surveyed with the “next generation” SHOALS technology (Compact Hydrographic Airborne Rapid Total Survey (CHARTS); Heslin and Lillycrop, 2003), and about 160 km of Hells Canyon on the Snake River was surveyed with a LiDAR system (Idaho Power Company, 2002). A number of factors contributed to the success of the SHOALS survey of the Hanford Reach and should be considered in other applications. First, we were able to have river flows reduced to their minimum levels for the survey. This ensured that all shoreline rearing areas were dewatered, which improved the quality of our data. Second, terrestrial vegetation is relatively sparse so the false elevations these produced were removed without too much effort. However, vegetation density may be of greater concern in other applications, in which the advantages of vegetation-penetrating LiDAR may need to be weighed against those of water-penetrating LiDAR. Finally, a number of geographic and elevation benchmarks existed along the river that facilitated accurate geo-referencing of our data.

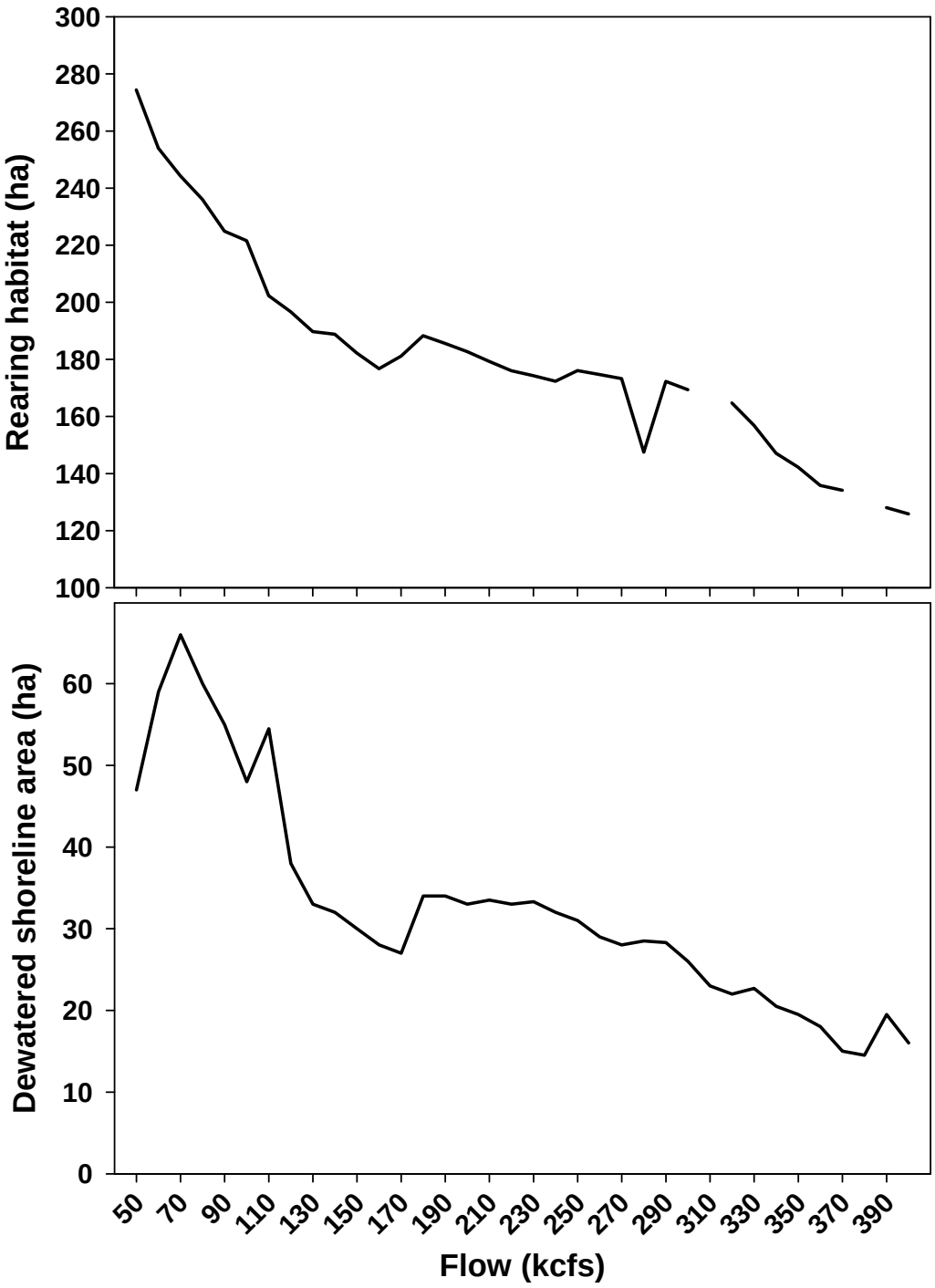

Figure 2. The amount of juvenile fall Chinook salmon rearing habitat (top panel) estimated at various flows in the Hanford Reach of the Columbia River. The bottom panel shows the amount of shoreline area that is dewatered by reducing flows in 10-kcfs increments from the flows shown on the *X* axis. Data are presented for that portion of the Hanford Reach between river kilometers 572 to 605 that was surveyed with the SHOALS system.

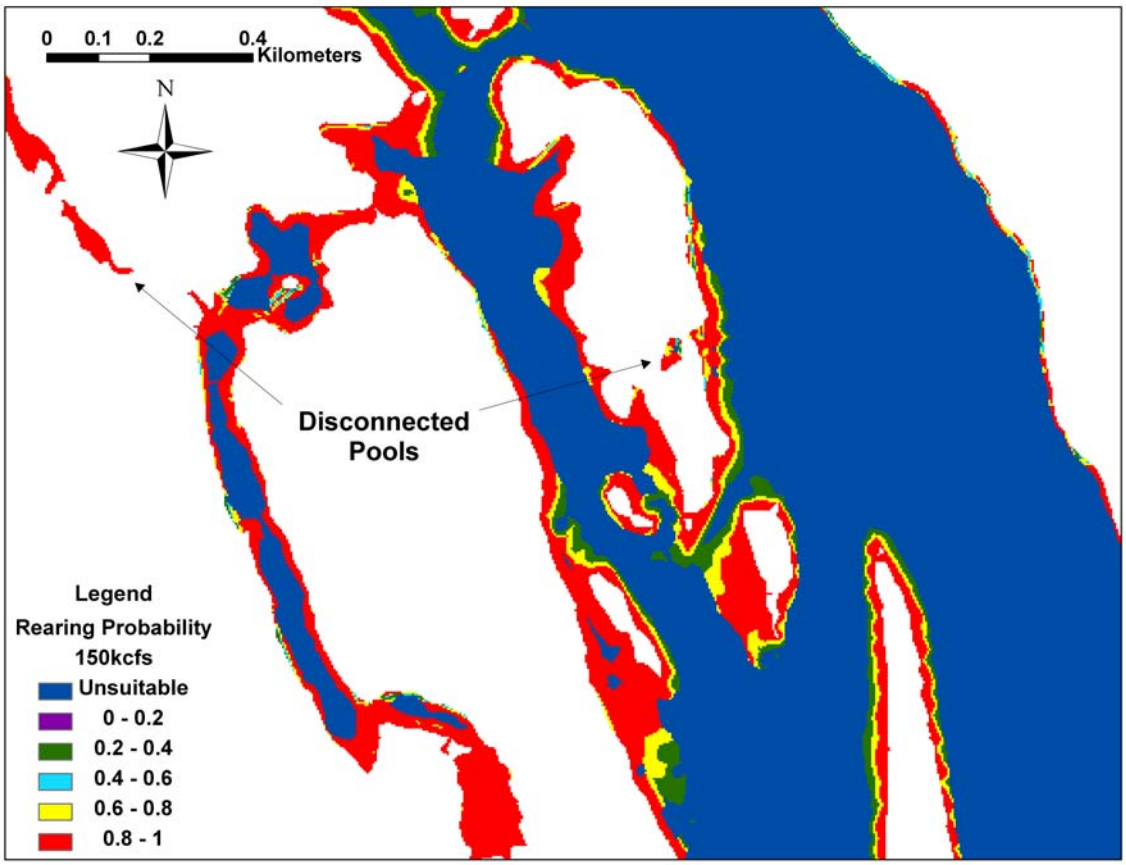

Figure 3. A GIS display of subyearling fall Chinook rearing area and entrapment pools at Rkm 587 in the Hanford Reach study area at a modeled flow of 150 kcfs. High probability areas (red and yellow) represent suitable rearing habitat. The dark blue represents unsuitable habitat where the water was too deep or fast for rearing.

Our analysis of juvenile fall Chinook salmon rearing habitat demonstrates the utility of combining remotely sensed bathymetry data with hydrodynamic modeling and a predictive statistical model to quantify habitat over at a large spatial scale. A GIS-based analysis enabled us to use our logistic regression model (developed at the scale of the individual fish) to make inferences at the landscape scale. This made it possible to quantify suitable habitat beyond the local field sampling unit and identify important rearing areas such as at 100F and Locke islands (fig. 1) by virtue of the greater distribution of suitable habitat found there compared to other areas. This type of analysis also enables one to quantify the distribution and connectivity of habitats in situations where actual field assessments of habitat are not possible. For example, Tiffan et al. (2006a) quantified changes in juvenile fall Chinook salmon rearing and migratory habitat in John Day Reservoir of the Columbia River under two different drawdown scenarios. This would not have been possible without the modeling approach we describe here. Being able to take a landscape level view of habitat changes due to natural or anthropogenic causes is critically important for fishes, particularly migratory species such salmon that move over great distances.

The geographic bathymetry data we collected with the SHOALS system facilitated a spatially explicit analysis using GIS. However, we were only able to consider important rearing habitat variables that could be incorporated into GIS, which limited our ability to fully characterize juvenile fall Chinook salmon rearing habitat. Incorporating lateral bed slope and water velocity in GIS was relatively easy because these variables could be estimated for the entire study area. In contrast, the transient nature of temperature and other time-varying determinants of habitat use by juvenile fall Chinook salmon (Tiffan et al., 2006b) could not easily be included in GIS-based analyses. Another variable that was not included was submerged terrestrial and aquatic vegetation. This multi-dimensional variable (e.g., height, density, area) also would be difficult to include in a spatially explicit analysis of a study area the size of ours. The compatibility habitat variables with GIS should be considered in future assessments using similar methodologies.

One of the consequences to juvenile fall Chinook salmon of changing habitat conditions caused by fluctuating flows in the Hanford Reach is stranding or entrapment in disconnected pools (Wagner et al., 1999). Consequently, mortality of stranded and entrapped fish is often high depending on pool size, drainage rate, exposure to lethal temperatures due to solar warming, exposure to predators, and time to reflooding and liberation. Our collection of high-resolution bathymetry data allowed us for the first time to evaluate the impacts of daily flow fluctuations from Priest Rapids Dam and generate seasonal mortality estimates. Using a one-dimensional hydrodynamic model to estimate shoreline locations at any given flow, we were able to calculate the area dewatered by incremental decreases in flow. Deploying field crews was necessary to collect field samples in order to extrapolate mortality estimates. GIS coverages of dewatered areas caused by flow drops were invaluable in refining search areas for field crews and creating randomized sampling strategies. However, a significant challenge we encountered was effectively sampling 36 km of river with a small number of field crews. This is likely to be a recurring problem in other broad-scale habitat assessments where limited effort is available for field verification of fish habitat use or operational effects. In such instances, a random stratified sampling approach would be beneficial.

Our data collection and analyses ultimately led to the implementation of a long-term protection plan for juvenile fall Chinook salmon in the Hanford Reach. In 1999, the first "Interim Agreement for the Hanford Reach Fall Chinook Population" was negotiated (Wolf, 1999) with the Grant County Public Utility District which operates the Priest River Dam. A Policy Team consisting of the "Joint Fisheries Managers" worked for over a year-and-a-half with the SHOALS data and study results to develop a plan to reduce stranding and the mortality associated with rapid flow fluctuations. These discussions consisted of a system-wide operations review due to the constraint on specific actions Grant County and the Priest Rapids Dam operations could implement. Subsequently, annual interim plans were updated based on new information. Ultimately, a long-term plan was derived and associated with the Vernita Bar Agreement—an agreement to protect pre-emergent juveniles. This combined plan now provides a single management framework for protecting spawning adults, pre-emergent, rearing, and outmigrating juveniles (Hoffarth, 2004). This plan specifies the operational constraints that operators of Priest Rapids Dam must abide by to limit fluctuations that would minimize stranding and entrapment events. Specific monitoring protocols are defined with integrated feedback mechanisms that inform hydro and fishery managers of the efficacy of the protection program. This adaptive management approach facilitates in-season operational corrections and policy decisions when field monitoring finds that juvenile fall Chinook salmon are adversely affected. This study provides a model of how remote sensing technology can be used to lay the foundation for an effective monitoring program. Such monitoring programs form a critical link between the status of natural resources and the policy makers tasked with protecting those resources.

References

Becker, C.D., 1973, Food and growth parameters of juvenile Chinook salmon, Oncorhynchus tshawytscha, in central Columbia River: U.S. National Marine Fisheries Service Fishery Bulletin 71, p. 387-400.

Burrough, P.A., 1986, Principles of geographical information systems for land resources assessment: Oxford University Press, New York.

Dauble, D.D., Page, T.L., and Hanf, Jr., R.W., 1989, Spatial distribution of juvenile salmonids in the Hanford Reach, Columbia River: U.S. National Marine Fisheries Service Fishery Bulletin 87, p. 775-790.

Dauble, D.D., and Watson, D.G., 1997, Status of fall Chinook salmon populations in the mid-Columbia River, 1948-1992: North American Journal of Fisheries Management 17, p. 283-300.

Dauble, D.D., and Geist, D.R. 2000, Comparison of mainstem spawning habitats for two populations of fall Chinook salmon in the Columbia River Basin: Regulated Rivers Research and Management 16, p. 345–361.

Environmental Systems Research Institute, Inc., 1998, ArcView version 3.2: Redlands, California.

Fickeisen, D.H., Dauble, D.D., Neitzel, D.A., Rickard, W.H., Skaggs, R.L., and Warren, J.L., 1980, Aquatic and riparian resource study of the Hanford Reach, Columbia River, Washington: Report to the U.S. Army Corps of Engineers, contract DACW67-79-C-0155, Seattle, Washington.

Ghanem, A., Steffler, P., Hicks, F., and Katopodis, C., 1996, Two-dimensional hydraulic simulation of physical habitat conditions in flowing streams: Regulated Rivers: Research and Management 12, p. 185-200.

Guenther, G.C., Thomas, R.W.L., and LaRoacque, P.E., 1996, Design considerations for achieving high accuracy with the SHOALS bathymetric LiDAR survey system: SPIE: Laser Remote Sensing of Natural Waters – From Theory to Practice.

Heslin, B.J., and Lillycrop, W.J., 2003, Charts: An evolution in airborne LiDAR hydrography:Joint Airborne LiDAR Bathymetry Technical Center of Expertise (JALBTCX).

Hoffarth, P.A., 2004, 2004 Washington Department of Fish and Wildlife evaluation of juvenile fall Chinook salmon entrapment in the Hanford Reach of the Columbia River: Report to signatory agencies to the Hanford Reach Fall Chinook Protection Program Agreement.

Huntington, C., Nehlsen, W., and Bowers, J., 1996, A survey of healthy native stocks of anadromous salmonids in the Pacific Northwest and California: Fisheries, v. 21, no. 3, p. 6-14.

Idaho Power Company, 2002, License Application to the Federal Energy Regulatory Commission, FERC Project 1971.

Lillycrop, W.J., Parson, L.E., and Irish, J.L., 1996, Development and operation of the SHOALS airborne LiDAR hydrographic system: SPIE: Laser Remote Sensing of Natural Waters – From Theory to Practice 2964, p. 26-37.

Nugent, J., Newsome, T., Nugent, M., Brock, W., Wagner, P., and Hoffarth, P., 2002a, 1999 Evaluation of Juvenile Fall Chinook Salmon stranding on the Hanford Reach of the Columbia River: Report to Bonneville Power Administration, Contract No. 00004294, Project No. 199701400, 215 electronic pages (BPA Report DOE/BP-00004294-1).

Nugent, J., Newsome, T., Nugent, M., Brock, W., Hoffarth, P., and Wagner, P., 2002b, 2000 Evaluation of Juvenile Fall Chinook Salmon stranding on the Hanford Reach of the Columbia River: Report to Bonneville Power Administration, Contract No. 00004294, Project No. 199701400, 92 electronic pages (BPA Report DOE/BP-00004294-2)

Parson, L.E., Lillycrop, W.J., Klein, C.J., Ives, R.C., and Orlando, S.P., 1996, Use of LiDAR technology for collecting shallow bathymetry of Florida Bay: Journal of Coastal Research 13, p. 1173-1180.

Platts, W.S., Megaham, W.F., and Minshall, H.W., 1983, Methods for evaluating stream, riparian, and biotic conditions: U.S. Forest Service, General Technical Report INT-138, Intermountain Forest and Range Experimental Station, Ogden, Utah.

Richmond, M.C., and Perkins, W.A., 1998, MASS1 (Modular Aquatic Simulation System 1D): A one-dimensional hydrodynamic and water quality model for river systems: Pacific Northwest National Laboratory Draft Report. Battelle – Hydrology Group. Richland, Washington, 29 p.

Tiffan, K.F., Garland, R.D., and Rondorf, D.W., 2002, Quantifying flow-dependent changes in subyearling fall Chinook salmon rearing habitat using two-dimensional spatially explicit modeling: North American Journal of Fisheries Management, v. 22, p. 713-726.

Tiffan, K.F., Garland, R.D., and Rondorf, D.W., 2006a, Predicted changes in subyearling fall Chinook salmon rearing and migratory habitat under two drawdown scenarios for John Day Reservoir, Columbia River: North American Journal of Fisheries Management, v. 26, p. 894-907.

Tiffan, K.F., Clark, L.O., Garland, R.D., and Rondorf, D.W., 2006b, Variables influencing the presence of subyearling fall Chinook salmon in shoreline habitats of the Hanford Reach, Columbia River: North American Journal of Fisheries Management, v. 26, p. 351-360.

Wagner, P.G., Nugent, J., Price, W., Tudor, R., and Hoffarth, P., 1999, 1997-99 evaluation of juvenile fall Chinook stranding on the Hanford Reach: Annual Report to the Bonneville Power Administration, Contract 97BI30417, Portland, Oregon.

Wolf, K.S., and Wagner, P.G., 1998, Hanford Reach juvenile fall Chinook stranding, entrapment and mortality: WDFW Fact Sheet, January 7, 1998.

Wolf, K.S., 1999, Proposed 1999 Interim Protection Plan for Hanford Reach Fall Chinook: Report to the Joint Fishery Managers from the Grant County Public Utility District and WDFW Hanford Reach Policy Development Team, March 1, 1999.

Chapter 6.—Use of Airborne Near-Infrared LiDAR for Determining Channel Cross-Section Characteristics and Monitoring Aquatic Habitat in Pacific Northwest Rivers: A Preliminary Analysis

Russell N. Faux[1], John M. Buffington[2], M. German Whitley[1], Steve H. Lanigan[3], Brett B. Roper[4]

Abstract

Aquatic habitat monitoring is being conducted by numerous organizations in many parts of the Pacific Northwest to document physical and biological conditions of stream reaches as part of legal- and policy-mandated environmental assessments. Remote sensing using discrete-return, near-infrared, airborne LiDAR (Light Detection and Ranging) and high-resolution digital imagery may provide an alternative basis for measuring physical stream attributes that are traditionally recorded by field crews in these monitoring efforts. Here, we compare physical channel characteristics determined from airborne LiDAR versus those measured from field surveys using a total station. Study sites representing three different channel types (plane-bed, pool-riffle, and step-pool) with bankfull widths ranging from 2.5 to 18.6 m were examined in the upper John Day River basin, Oregon. LiDAR was flown on each study reach at a native pulse density of about 4 pulses/m^2, with up to four returns per pulse. Channel cross sections and stream gradient were determined from LiDAR-derived digital elevation models (DEMs) and directly compared to total station measurements. The ability to remotely sense bankfull elevations and associated channel geometry was of particular interest in this study. Because bankfull mapping from LiDAR depends on topographic indicators (breaks in streambank slope), bankfull elevation was determined objectively from plots of hydraulic depth (flow area divided by width) as a function of flow height at each cross section, with bankfull defined as the maximum value of this function, or as the first plateau in the hydraulic depth function in channels with multiple terraces. The latter definition allows a blind test of remote sensing capabilities for cases where no field observations of bankfull elevation are available.

Preliminary results show that, with the exception of one outlier, the first-terrace elevations determined from LiDAR DEMs differed from those of the total station by 0–40 cm (15 cm RMSE), corresponding channel widths differed by 0.23–5.23 m, and reach-average water-surface slopes differed by 0.0–0.0018 m/m. Furthermore, the LiDAR-derived cross-sectional profiles generally corresponded with those of the total station measurements above the water-surface elevation. However, first-terrace elevations frequently differed from field observations of bankfull stage, indicating that successful remote sensing of bankfull geometry using airborne LiDAR requires field observations to train identification of bankfull topography in LiDAR DEMs. When properly applied, remote sensing using airborne LiDAR has the potential to extend the spatial coverage, speed, consistency, and precision of physical stream measurements compared to existing field based techniques, and can be used to quantify higher-order topographic metrics (e.g., areas, volumes, curvature, and topology) beyond the point and line metrics currently measured by channel monitoring programs.

Introduction

Each year hundreds of personnel are fielded by monitoring programs to collect data on aquatic and riparian conditions of streams in the western United States. The organizations participating in these programs are tasked with determining the status and trend of aquatic ecosystems across large areas. For example, the Aquatic Riparian Effectiveness Monitoring Program (Reeves et al., 2004) is an interagency group organized to evaluate the success of the Northwest Forest Plan (U.S. Department of Agriculture, Forest Service; U.S. Department of Interior, Bureau of Land Management, 1994) and is responsible for monitoring aquatic and riparian

[1]Watershed Sciences, Inc., 257B SW Madison Ave, Corvallis, OR 97333

[2]U.S. Forest Service, Rocky Mountain Research Station, Idaho Water Center, 322 E. Front St., Boise, Idaho 83702

[3]U.S. Forest Service/Bureau of Land Management, Aquatic Riparian Effectiveness Monitoring Program, 333 SW First Ave., Portland, OR 97208

[4]U.S. Forest Service, Fish and Aquatic Ecology Unit, Utah State University, 860 N. 1200 E., Logan, Utah 84321

conditions across three States and 57 million acres (Reeves et al., 2004). Similarly, the PACFISH/INFISH Biological Opinion Program is focused on monitoring federal lands in the Upper Columbia River Basin, a region that covers subwatersheds in six States (Kershner et al., 2004). In many cases, these monitoring programs do not directly measure biological parameters, but infer habitat and ecosystem condition from physical surrogates. For example, channel characteristics (e.g., width, depth, residual pool depth) are used to assess availability and quality of habitat for aquatic organisms.

As one might expect, there are challenges associated with long-term monitoring over large areas, given typically limited resources. The number of sites sampled per year is relatively low, hindering spatial and temporal detection of differences in ecosystem condition and trends (Roper et al., 2002). In addition, while observer consistency and repeatability is critical for successful monitoring of watershed trends, recent studies show that observer variability in these monitoring efforts can be problematic (Whitacre et al., 2007; Roper et al., 2008; Roper et al., in prep). One potential solution to these problems is the use of remote sensing, as it can provide objective, repeatable measurements over broad spatial scales.

Airborne LiDAR (light detection and ranging) is a remote sensing technology that is currently being used to develop high-resolution topographic and vegetation models. Several recent studies show the potential for using LiDAR to map many of the physical parameters commonly quantified in aquatic and riparian monitoring efforts. For example, Jones (2006) used a LiDAR-derived digital elevation model (DEM) to map side channels and to identify potential sites for restoration of salmon habitat in the Dosewallips River, western Oregon. In other applications, James et al. (2007) documented the potential for using LiDAR to map headwater streams under canopy in Sumter National Forest, North Carolina, and Cavalli et al. (2007) used LiDAR to detect the spatial extent of different stream types in the Italian Alps.

Two LiDAR instruments provide a variety of applications for aquatic habitat monitoring: near-infrared and green-wavelength LiDAR. Near-infrared LiDAR can not penetrate water and is therefore used to map topography above the wetted channel. Green-wavelength devices can penetrate water to determine channel depth and provide seamless maps of both the aquatic and terrestrial environments (Wright et al., 2006; Kinzel et al., 2007; McKean et al., 2008). Although green-wavelength LiDAR can map many of the physical channel characteristics used in aquatic monitoring in a continuous and spatially extensive manner, near-infrared LiDAR instruments are currently capable of significantly higher pulse rates and, therefore, can map terrestrial environments at higher topographic resolutions. Although small-footprint green-wavelength LiDAR (Wright et al., 2006) has the potential to significantly change how aquatic monitoring is conducted, its commercial availability is limited and the widespread application of this technology is still several years in the future.

Near-infrared LiDAR data and derived products (topographic and vegetation models) are becoming increasingly available to resource managers in the Pacific Northwest. Several regional initiatives for the acquisition and distribution of high-resolution LiDAR data are underway in the Pacific Northwest (fig. 1). In Washington, the Puget Sound LiDAR Consortium (PSLC) has acquired 4.9 million acres of LiDAR coverage since 2001. In addition to specific projects led by agencies and private entities, the recently formed Oregon LiDAR Consortium (OLC) has initially contracted to acquire 1.3 million acres in western Oregon, with an additional 3.5 million acres anticipated over the next 3 years. These data are now available to resource managers and are now enhancing our ability to assess habitat condition over multiple spatial scales.

During the summer of 2005, the Pacific Northwest Monitoring Partnership (PNAMP) conducted a study in the John Day basin, northeastern Oregon, to examine the performance and compatibility of field protocols used by different aquatic habitat monitoring programs (Lanigan et al., 2006; Roper et al., in prep.). As part of this project, intensive total station surveys were conducted to better describe the channel characteristics of each study site (Roper et al., in prep.). Airborne near-infrared LiDAR and digital color imagery also were collected to analyze the ability of these data to characterize the physical habitat and riparian characteristics of the study sites. This paper focuses on the accuracy of channel characteristics determined from LiDAR-derived DEMs and, in particular, the ability to remotely sense bankfull elevations and associated channel geometry. Preliminary results are presented, comparing remotely sensed channel characteristics to those obtained from total station field surveys.

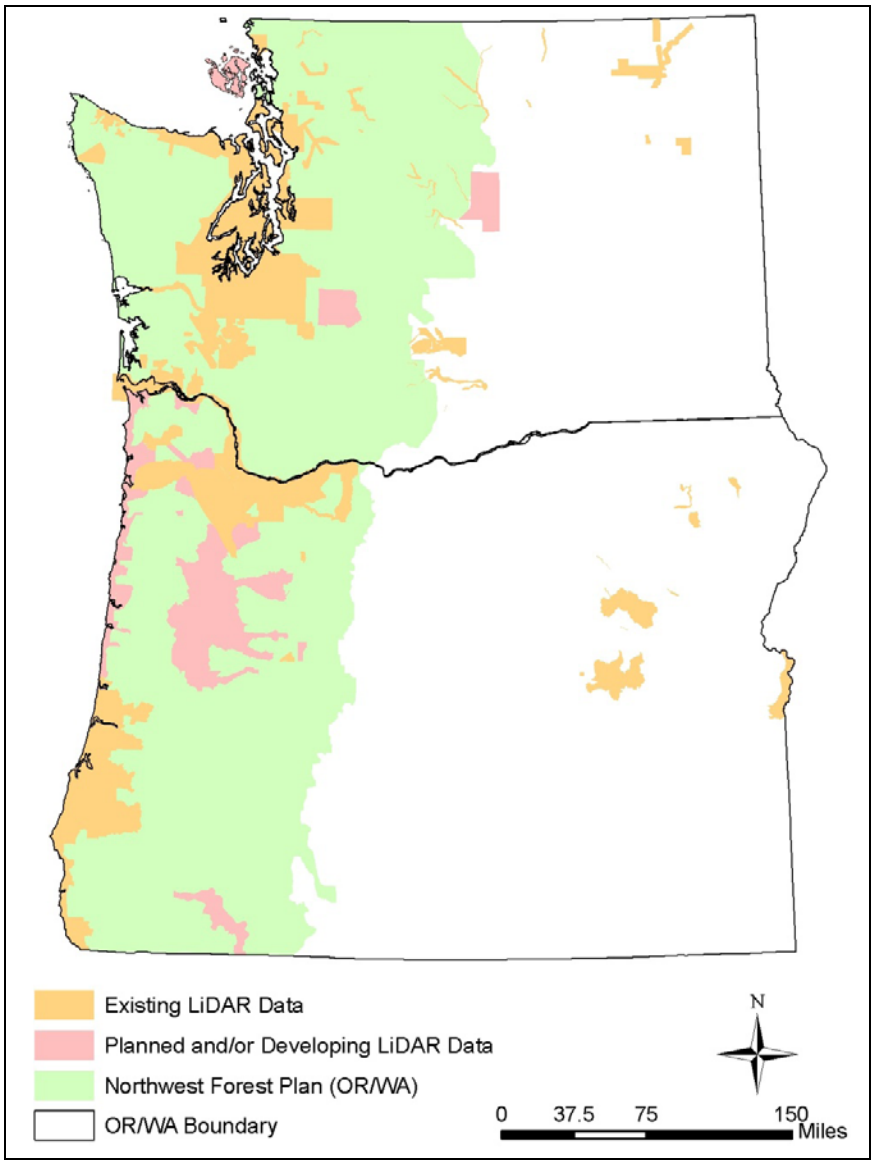

Figure 1. Monitoring region for the Aquatic and Riparian Effectiveness Monitoring Program (Reeves et al., 2004) in Oregon and Washington (part of the Northwest Forest Plan area) relative to spatial coverages of high-resolution LiDAR data that are either currently available or planned in 2009 for Oregon and Washington.

Study Area and Methods

Study Area

Eight mountain stream reaches were examined in the upper John Day River basin in northeastern Oregon (fig. 2). All streams were wadable, with bankfull widths ranging from 3.1 to 14.7 m, reach-average slopes from 0.94 to 9.7%, and median grain sizes (D_{50}) of 11.8–121.3 mm (table 1). The sampled reaches were 40 bankfull widths in length and selected to include three channel types (pool-riffle, plane-bed, and step-pool) (fig. 3).

Table 1. Channel characteristics determined from ground-based surveys

Stream	Stream type	Bed slope (%)	Bankfull width (m)	D_{50} (mm)
Crane	pool-riffle	0.94	8.01	11.8
Trail	pool-riffle	1.63	9.86	52.7
Bridge	plane-bed	1.03	8.12	37.4
Camas[1]	plane-bed	0.96	14.71	104.0
Tinker	plane-bed	2.86	3.14	33.7
Crawfish	step-pool	5.07	6.38	121.3
Myrtle	step-pool	9.70	3.96	27.7
Whiskey	step-pool	6.67	4.10	72.7

[1]Values based on limited sampling; 5 permanent cross sections only.

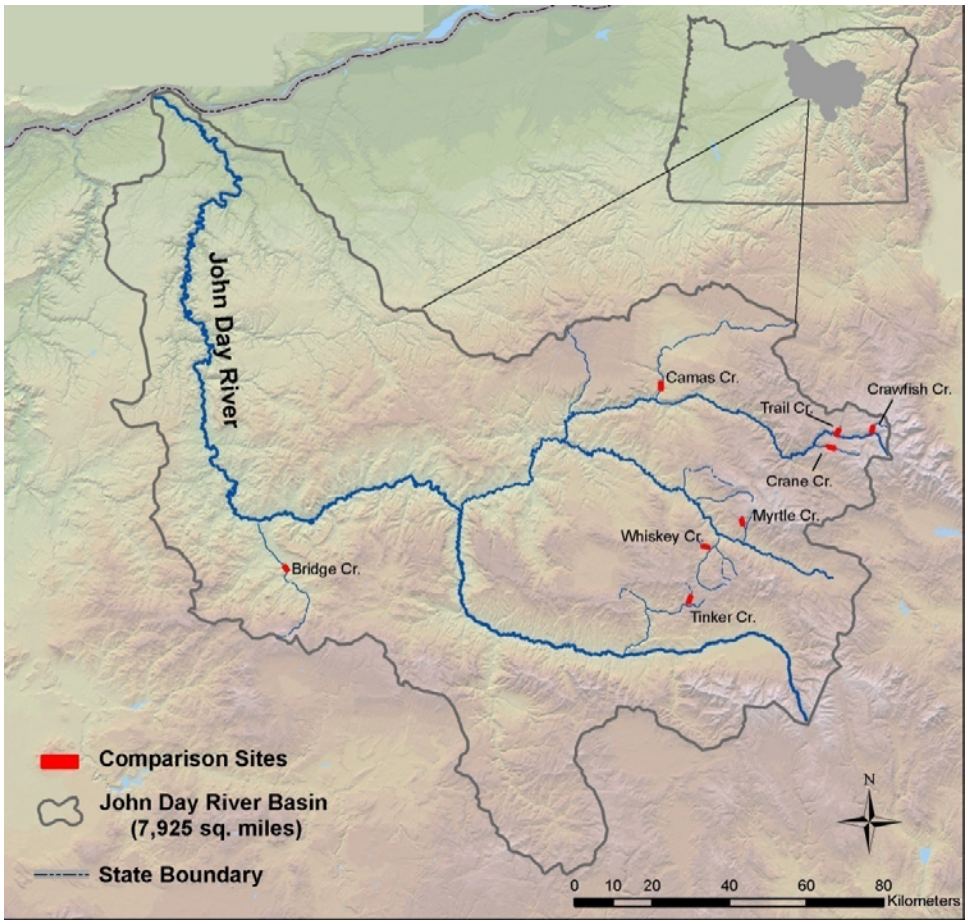

Figure 2. Study site locations within the John Day River basin, Oregon, USA.

Figure 3. Channel types examined in this study: (a) pool-riffle (Crane Cr.), (b) plane-bed (Camas Cr.) and (c) step-pool (Crawfish Cr.). See Montgomery and Buffington (1997) for further discussion of these channel types.

LiDAR Data

High-density LiDAR data were acquired for all eight sites from a fixed-wing platform, using an Optech 3100 ALTM system on September 28, 2005. The acquisition date was scheduled to correspond with late summer base-flow conditions in the study area, and early enough in the fall to avoid the possibility of early season snows that would interfere with LiDAR measurements. The settings consisted of a relatively narrow scan angle (±15°) and 50% overlap between opposing flight lines to increase laser pulse penetration through the canopy and to minimize shadowing by the vegetation (table 2). The vertical accuracy of the LiDAR data was assessed using 613 ground check points collected on hard, bare-earth surfaces (i.e., roads), and was found to have a root mean square error (RMSE) of 6.1 cm.

The raw LiDAR data were processed to produce geo-corrected coordinates for each laser return. Ground returns were classified from the raw point data using the TerraSolid processing software (TerraScan/TerraModeler from TerraSolid.fi) by implementing a series of filtering algorithms which defined the initial ground plane. The ground classification was then manually reviewed to remove any "clutter" or obvious misclassifications in the model. Across all sites, the average LiDAR pulse density was 3.1 pulses/m^2 with ground classified points having an average density of 1.2 returns/m^2 (table 2). The final ground-classified points were used to generate a 0.5 m DEM for each study reach, which took advantage of areas where the ground classified point density supported this resolution (fig. 4).

True color digital imagery was acquired coincidently with the LiDAR data using an Applanix Digital Sensor System 16 mega-pixel camera. The digital camera was integrated with a global positioning system (GPS) and inertial measurement unit, allowing direct geo-referencing of each pixel. The imagery was then orthorectified to the LiDAR DEM at a 15 cm (about 6 in.) ground sample distance, and was used to augment the interpretation of the LiDAR data.

Table 2. LiDAR system parameters.

System/acquisition parameter	Specification
Scan Angle	±15° from Nadir (30° total)
Number of Returns Collected Per Laser Pulse	4
Average Multi-Swath Pulse Density	3.1 pulses/m^2
Average Ground Return Density	1.2 returns/m^2
Adjacent Swath Overlap (Side-Lap)	≥ 50%
Assessed Vertical RMSE of LiDAR Survey	0.061 m

Total Station Data

Detailed topographic and geomorphic surveys of the study reaches were conducted from July 16 to September 12, 2005, using a Leica TPS1200 total station. Eighty cross sections were surveyed per reach, with cross sections placed at intervals of one-half the average bankfull width (fig. 5). Cross-sectional surveys recorded major topographic breaks, as well as water elevations, vegetation limits, bankfull elevations, floodplain topography, and hillslope margins in confined reaches. Because bankfull is defined as the elevation at which flow spills onto the floodplain (Leopold et al., 1964), it is relevant only to floodplain rivers. However, bankfull-equivalent indicators are commonly used in confined channels where floodplains are absent or poorly defined, as was the case for some of the plane-bed and step-pool channels examined in this study. Bankfull locations were identified based on the following standard field indicators (Dunne and Leopold, 1978; Harrelson et al., 1994), given in their order of reliance: break in bank slope corresponding with the active floodplain surface, high-flow markers (i.e., limit of bank scour, rock staining, sand/silt deposits, debris lines), vegetation limits, and bar tops. There is less confidence in perennial vegetation as a bankfull indicator because of its seasonal variability and interannual dependence on flow, scour and deposition. Similarly, bar tops typically indicate a lower-limit of bankfull flood stage because some additional depth of flow must occur over the tops of the bars for them to form through processes of sediment transport and deposition.

Five of the cross sections were monumented as reference sites for the PNAMP comparison of field monitoring protocols (Lanigan et al., 2006; Roper et al., in prep.). These cross sections were placed every 10 bankfull widths along the length of the channel and are referred to as "permanent cross sections" in this study (fig. 5).

The number of points sampled within the bankfull extent of each cross section ranged from 9 to 21 across the study sites, representing a point spacing of 5–13% of the bankfull width. In addition to cross sections, a longitudinal profile of the channel center-line was surveyed, as well as locations of all pool bottoms and downstream riffle crests. The overall data density within the bankfull channel typically was 0.4–3.7 points/m^2.

Although the survey points are accurate relative to each other, the coordinates for the benchmarks used in the total station surveys were recorded using a non-survey grade GPS and therefore the geographic precision of the benchmarks is unknown. The total station surveys were designed to compare to the other ground-based measurements being made as part of the comparison of monitoring protocols (Lanigan et al., 2006; Roper et al., in prep.), with the acquisition of airborne LiDAR data added late in the program. Therefore, precise geospatial references (i.e., surveyed benchmarks and/or air targets) were not included in the total station surveys.

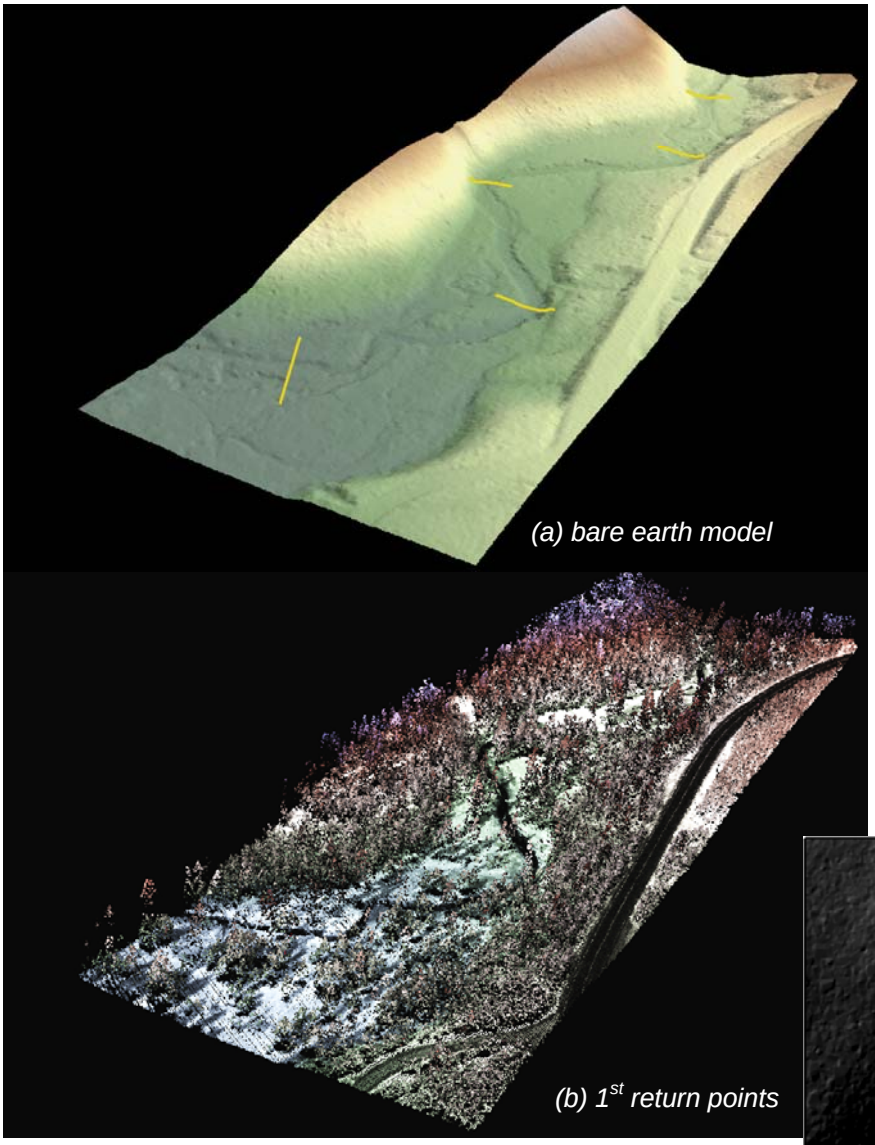

Figure 4. LiDAR-derived bare earth model (a) and LiDAR 1st return points (b) for Trail Creek. Yellow transects on the bare-earth model are the five monumented cross sections placed by the total station field crews.

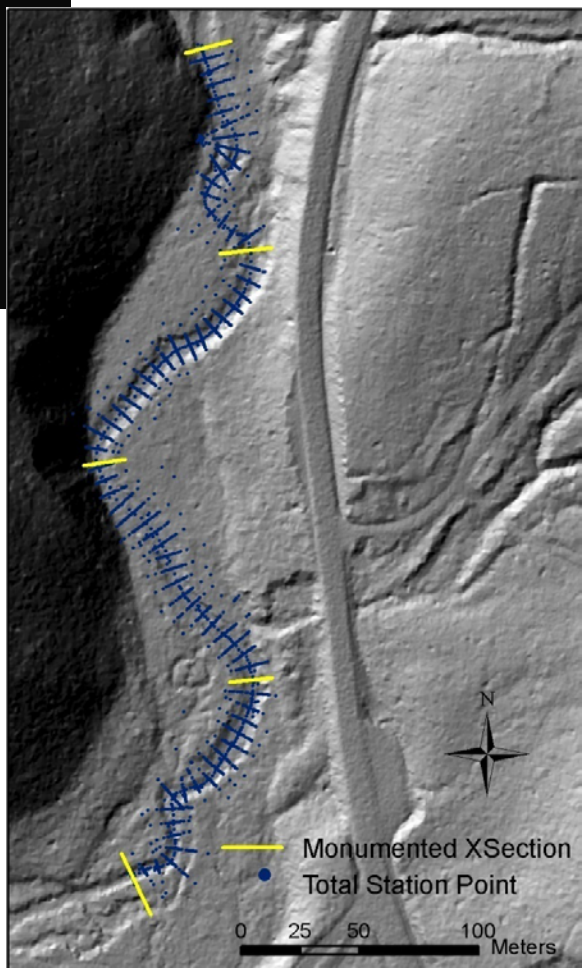

Figure 5. Locations of total station survey points ("ground points") and monumented cross sections on Trail Creek overlain on hillshade of the LiDAR 0.5-m DEM.

The lack of a good geographic reference was a potential source of error for comparing the geographically precise LiDAR points to the total station data.

For this analysis, we used a small subset of the available cross sections (two per site) for comparing channel characteristics determined from airborne LiDAR to those of the total station surveys. Our intent was to provide a preliminary comparison of the two approaches. Comparisons were conducted for monumented (or permanent) cross sections 2 and 4 (PXS2 and 4), located at longitudinal distances of 10 and 30 bankfull widths, respectively, in each study reach (fig. 5).

Analysis

Transect Placement

As a consequence of not having a precise geographic reference, some shifting in the horizontal (X, Y) plane was necessary to line-up the total station points with their true geographic coordinates. The X, Y shift was computed as a best-fit between the water-surface center line derived from the LiDAR DEM and the center-line profile measured by the total station crew. The five monumented cross sections in each reach were used as an additional reference, because hand-held GPS coordinates were available for the end-points of these cross sections. The shift maintained the integrity of the original data with no changes to the points relative to each other.

To accurately place the field data in the vertical dimension (Z), the relative elevations of the field measurements had to be given a true elevation datum. The water-surface elevation was used as a common datum for vertical alignment of the two data sets, and ortho-imagery was used to confirm the water-surface location in the LiDAR DEM. Although the datasets were collected at different times, both were collected during 2005 base-flow conditions, and differences in water-surface elevations between the two datasets were considered minimal (within a few cm) for these streams.

Channel Geometry

Once the total station transects were relocated relative to the LiDAR data, point elevations defining the channel cross sections were extracted along a corresponding transect in the LiDAR data. The ArcGIS extension EZ Profiler 9.1 (freeware) was used to generate the transect line and collect elevations from the LiDAR DEM at 0.5-m intervals.

The ability to remotely sense bankfull elevations and associated channel geometry is a key focus of this study. Bankfull elevation is a primary metric for fluvial studies (Leopold et al.. 1964) and commonly is used to scale and standardize channel characteristics relevant to aquatic habitat (e.g., Woodsmith and Buffington, 1996; Buffington et al., 2002). In the field, bankfull elevation is identified by a number of indicators, as discussed above (section, “Total Station Data”). In contrast, bankfull mapping from LiDAR depends almost entirely on topographic indictors (breaks in the streambank slope) identified from the LiDAR-derived DEM. In order to objectively compare bankfull elevations between the field- and LiDAR-based measurements, we plotted the hydraulic depth (flow area divided by width) as a function of flow height (elevation) at each cross section, where the maximum value of this function indicates a sudden increase in flow width at the elevation where water spills across the floodplain (i.e., bankfull) (fig. 6). This approach was suggested by McKean et al. (2005) and is a variant of the bankfull approaches discussed by Williams (1978).

We recognized that the above method for identifying bankfull elevation would work best in floodplain rivers and would be limited in confined channels that lack floodplains. The method is less definitive in channels with inset/multiple terraces, where one is faced with deciding which terrace and which plateau in the hydraulic depth function is the current bankfull elevation (i.e., the active floodplain) (fig. 7). Many of our study sites exhibited both characteristics confined channels and multiple terraces. Field observations can be used to guide selection of the correct overflow surface corresponding with the active floodplain (Williams, 1978), but we wished to conduct a blind test of the remote sensing capabilities of LiDAR (i.e., without recourse to field observations of bankfull). Consequently, where multiple terraces were present, we determined the elevation and channel width for the first terrace (i.e., lowest elevation terrace), which may or may not be equivalent to the actual bankfull elevation, depending on the local conditions and geomorphic history of a site. The hydraulic depth calculations were performed using the WinXSPRO program (Hardy et al., 2005) and were plotted versus elevation for the examined cross sections.

Stream Gradient

Water-surface elevations were measured from the LiDAR data by sampling directly from the DEM at 1-m intervals along the stream centerline. The stream centerline was generated using the flow accumulation function in ArcGIS Spatial Analyst and then manually edited within the GIS environment with the digital orthophotos as a visual reference. The extent of the study area was small enough that manual editing of the stream center was preferred for correcting for culverts and other features in the ground model that may create errors in the stream network. The custom ArcGIS extension TTools (Boyd and Kasper, 2005) was used to create equal-interval nodes along the centerline and to sample elevations directly from the DEM. LiDAR-derived water-surface slopes were compared to those determined from total station measurements at each site.

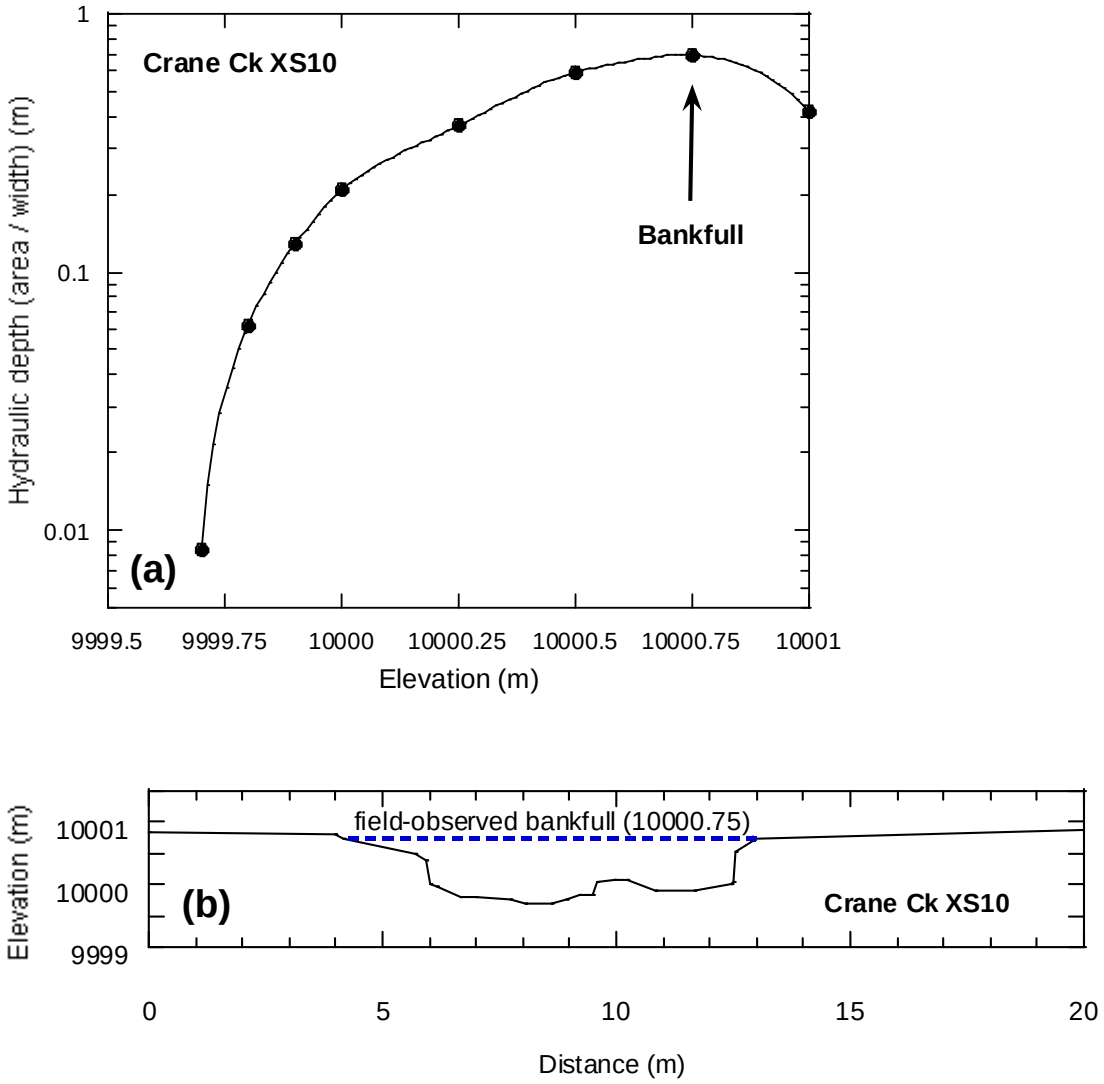

Figure 6. Example hydraulic depth function (a) for objectively defining bankfull elevation. The function maximum coincides with the active bankfull floodplain identified in the field (b, cross section). Reported elevations are for an arbitrary coordinate system and are not georeferenced.

Results

First Terrace Elevation and Bankfull Identification

With the exception of one outlier (Bridge Creek, PXS2), the first-terrace elevations derived from the LiDAR DEMs differed from those of the total station surveys by 0–40 cm (table 3), with a RMSE of 15 cm (complete dataset, including the above outlier, yields an RMSE of 34 cm). In some cases, the first terrace corresponded with the bankfull elevation identified in the field (fig. 8, Trail Creek), while in other cases, it underestimated the actual bankfull surface (fig. 8, Crane Creek; bankfull is the second terrace, while the first "terrace" is a bar top). Hence, while the first-terrace elevations are comparable between the LiDAR-derived data and the total station data, remote predictions of bankfull geometry may have errors and will likely require field observations to guide extraction of this feature from the LiDAR data.

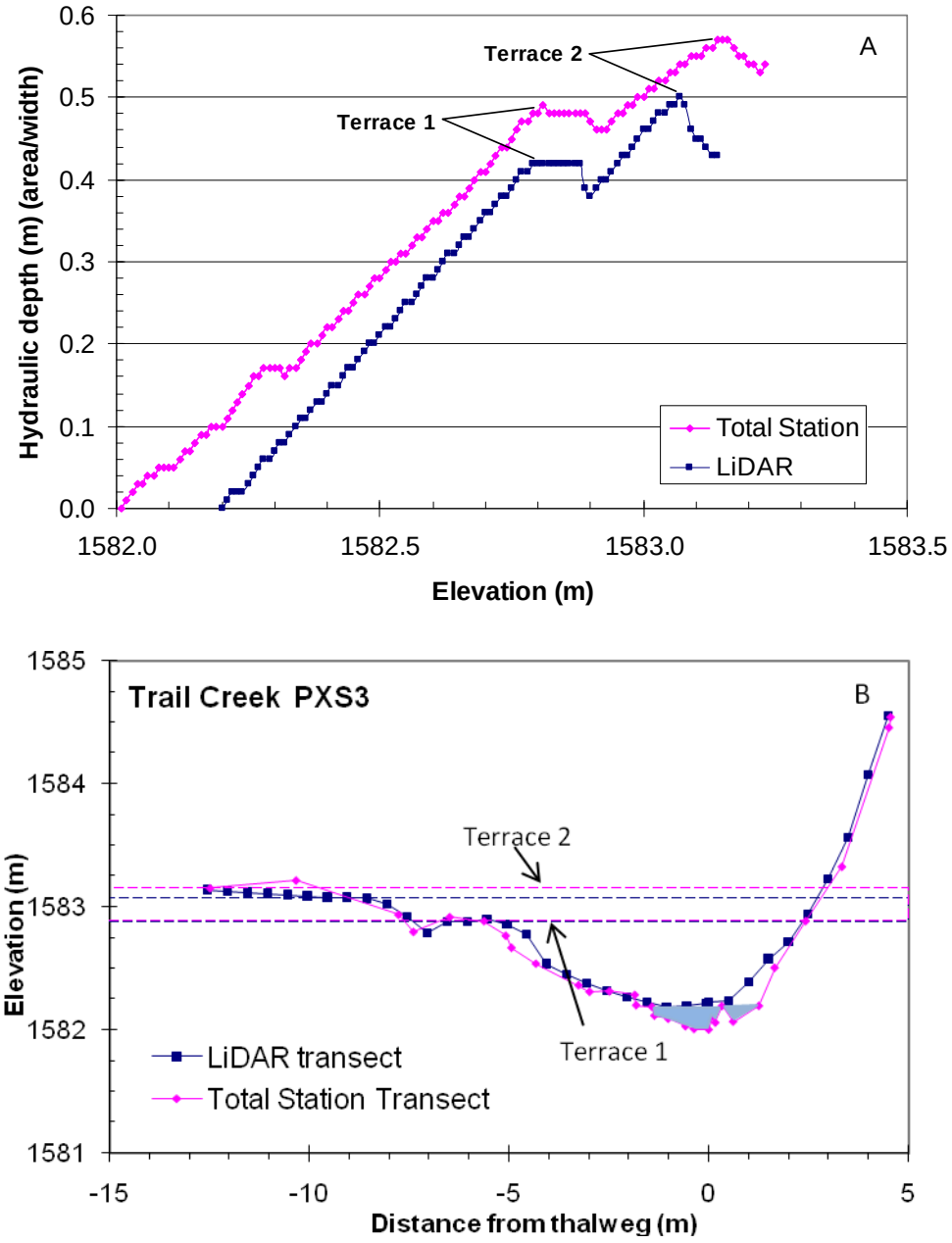

Figure 7. Example hydraulic depth function (a) and underlying cross section (b) for a channel showing two terraces. Dashed lines in (b) indicate terrace locations determined from (a).

Channel Widths

Comparisons between the LiDAR- and field-derived values of channel width at the first terrace of each cross section are shown in table 3. For plane-bed streams, a median difference of 0.87 m in channel width was observed between the two datasets. The LiDAR model overestimated channel width by 0.59–7.89 m (4–167 %) on four of the six measured cross sections, with an overall median error of 0.87 m (16%). The largest difference (7.89 m) was observed on Bridge Creek (PXS2) where the LiDAR-derived profile generalized the first terrace break and hence overestimated bankfull width. Excluding this cross section, the range of width overestimation decreases to 0.59–1.05 m (4–29%). At two of the six cross sections, the LiDAR model underestimated channel width by 0.35–2.34 m (8–13%).

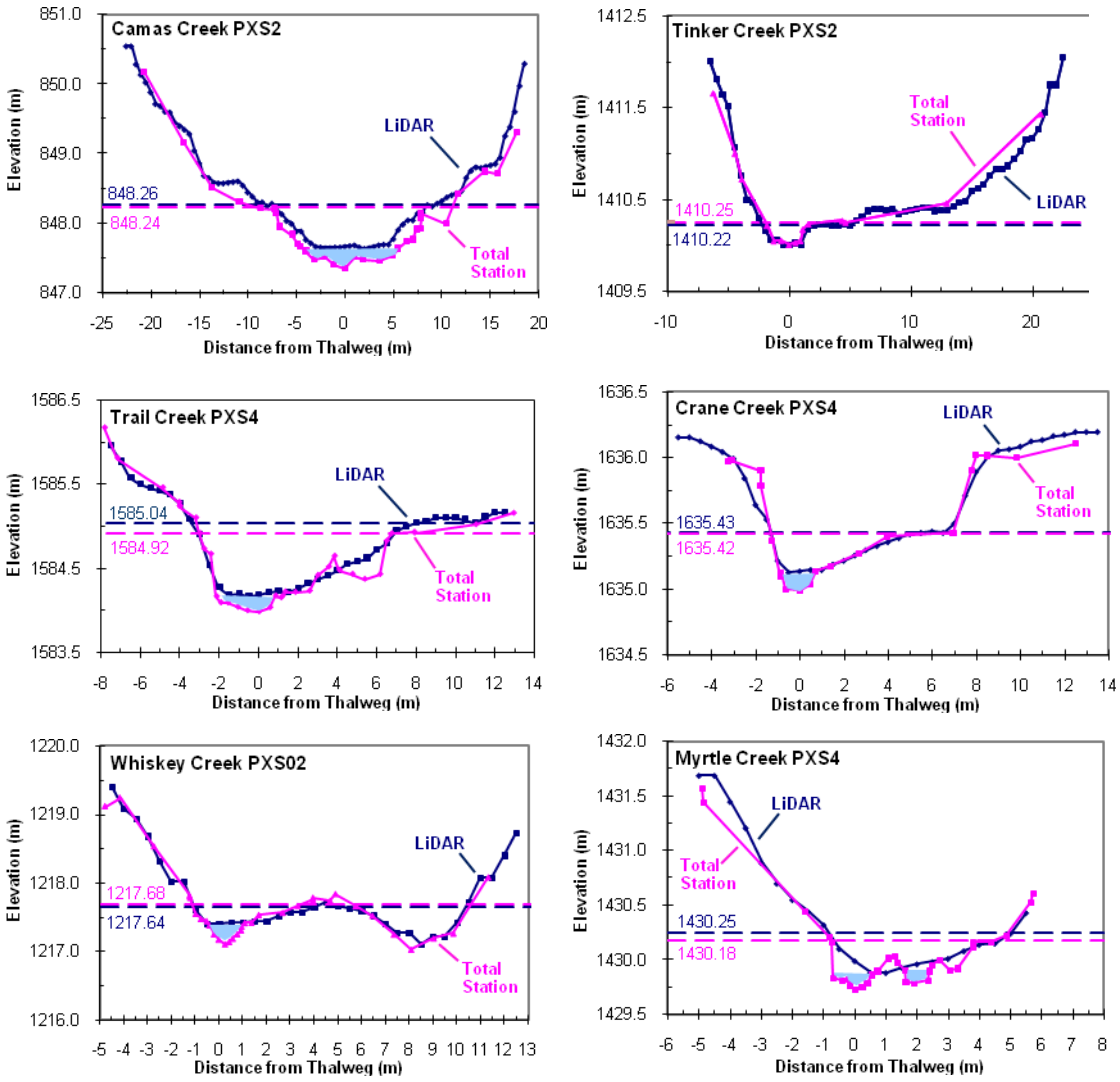

Figure 8. Comparison of LiDAR-derived and total station cross sections for plane-bed (top), pool-riffle (middle), and step-pool channels (bottom). Dashed lines are first-terrace elevations determined from the hydraulic depth method. The wetted channel is represented on the profile in blue and is based on field measurements. The water-surface topography is interpolated from the LiDAR DEM, which includes LiDAR returns from both the water surface and exposed channel topography.

For the pool-riffle streams, the comparison of LiDAR and field-derived values yielded a median difference in channel width of 1.57 m and a median error of 23%. The LiDAR model overestimated channel width by 0.40–1.89 m (4–76 %) for all four cross sections. Step-pool channels exhibited a median difference in channel width of 1.80 m and a median error of 43%. However, the frequency of over-versus under-estimation was equal in this channel type (3 overestimated and 3 underestimated).

These findings suggest that the accuracy of LiDAR-derived channel widths varies with channel type (progressively greater median errors across plane-bed, pool-riffle, and step-pool channels). The larger error in step-pool channels also may reflect limitations of the hydraulic depth approach for defining bankfull in confined streams. In several cases, plots of hydraulic depth versus elevation did not reveal a distinct local maximum. Consequently, a more robust approach or combination of methods should be considered for remote sensing of bankfull elevation across the range of stream types present in mountain rivers (e.g., Rosgen, 1994; Montgomery and Buffington, 1997).

Table 3. First-terrace elevations and widths determined from LiDAR versus total station data.

Stream	XSection	Terrence elevations (m)			Channel width (m)		
		LiDAR	Field	Difference	LiDAR	Field	Difference
Pool-Riffle Streams							
Trail	PXS2	1,581.31	1,581.31	0.00	9.91	9.51	0.40
Trail	PXS4	1,585.04	1,584.92	0.12	11.32	9.73	1.59
Crane	PXS2	1,634.31	1,634.21	0.10	4.39	2.50	1.89
Crane	PXS4	1,635.43	1,635.42	0.01	6.79	5.24	1.55
Plane-Bed Streams							
Camas	PXS2	848.24	848.26	-0.02	16.27	18.61	-2.34
Camas	PXS4	852.46	852.41	0.05	16.81	16.22	0.59
Tinker	PXS2	1,410.22	1,410.25	-0.03	4.18	3.49	0.69
Tinker	PXS4	1,412.19	1,412.24	-0.05	4.09	4.44	-0.35
Bridge	PXS2	660.17	658.94	1.23	12.63	4.74	7.89
Bridge	PXS4	660.19	660.01	0.18	4.68	3.63	1.05
Step-Pool Streams							
Whiskey	PXS2	1,217.64	1,217.68	-0.04	2.67	7.90	-5.23
Whiskey	PXS4	1,223.47	1,223.66	-0.19	3.45	5.57	-2.12
Myrtle	PXS2	1,423.62	1,423.37	0.25	4.62	2.90	1.72
Myrtle	PXS4	1,430.25	1,430.18	0.07	5.75	3.79	1.78
Crawfish	PXS2	1,797.46	1,797.06	0.40	7.24	5.43	1.81
Crawfish	PXS4	1,803.59	1,803.68	-0.09	5.47	5.70	-0.23

Channel Cross Sections

While the width predictions varied, the shape and topography of the cross-section profiles above the water-surface elevation were correlated between the two datasets, even for streams with channel widths of less than 5 m (fig. 8). In only one instance (Bridge Creek; PXS2) did the LiDAR DEM miss the first terrace, resulting in a significant overestimation of channel width (table 3). Inspection of the LiDAR DEM of Bridge Creek shows that the first terrace was visible as a continuous linear feature in the data and that the generalization of this terrace at PXS2 may have been the consequence of vegetation along the right bank rendering fewer ground returns. This finding suggests that sampling discrete cross sections in isolation from the spatially continuous dataset might be misleading.

We expected the LiDAR DEM to more precisely map the larger channel geometries due to a higher number of ground returns per cross section, with greater variability in results observed for smaller channel widths and fewer ground returns. Theoretically, the Nyquist frequency (twice the grid cell size) represents the minimum size of topographic features that can be delineated using a grid-based DEM (Warren et al., 2004; James et al., 2007). However, the LiDAR DEM described the channel geometry (in terms of terrace elevations and shape) of some of the smallest streams in the study (i.e., widths of 2–3 m). For example, the LiDAR DEM closely matched the field measured bank full elevation (within 3 cm) and width (within 70 cm) on Tinker Creek (PXS2), which had a field measured bankfull width of only 3.5 m. As expected, the DEM generally interpolated or missed features that were less than 1 m2 in planar surface area (i.e., less than 2× the DEM grid cell size; 0.5 m).

The accuracy of the LiDAR DEM depends on both the quality of the ground-point classification and the achieved ground return density. While the degree to which vegetation influences the LiDAR returns depends on season and species composition, heavily vegetated areas generally will result in fewer ground returns and the potential for more interpolation errors in the resulting DEM. This effect was evident in cases where the LiDAR DEM interpolated over fine-scale cross-sectional features and banks located under heavy vegetation. Landscape features such as downed logs also contributed to noise in the ground model. The largest inaccuracies were

observed when a combination of these factors contributed to the error budget. For example, permanent cross section 4 (PXS4) on Myrtle Creek contained both vegetation and downed logs near the streambank (fig. 9). Myrtle Creek also had one of the steepest gradients (table 1) and a confined channel. The DEM at this location generalized the steep terrace break along the left bank and completely missed the small channel split in the center of the stream, which appeared due to a mixture of relatively small channel width (<4 m) and downed logs/vegetation in the stream (fig. 9).

Stream Gradient

Stream gradients determined from the two data sets are in close agreement (table 4), with median errors of 3.87, 5.75, and 0.16 percent for pool-riffle, plane-bed, and step-pool channels, respectively. The difference in slope measurements between the two approaches generally decreases with channel gradient, with step-pool channels showing the least error (fig. 10).

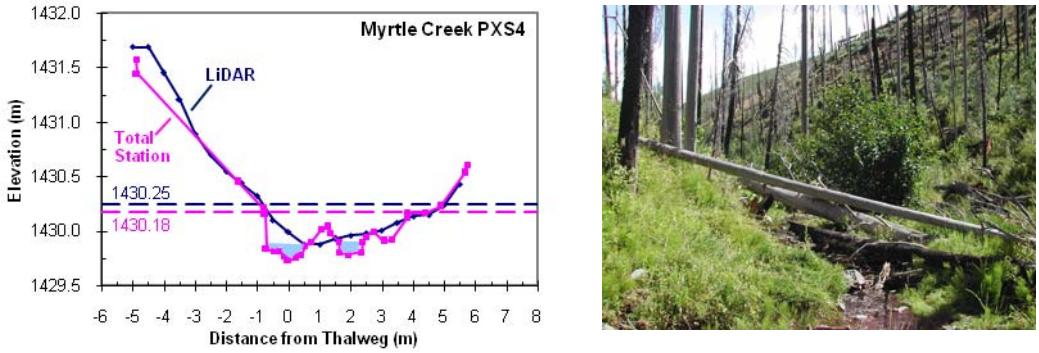

Figure 9. Example of fine-scale topography obscured by large woody debris and riparian vegetation in a LiDAR-derived cross section compared to that surveyed in the field with a total station. The ground-level photograph shows general channel conditions in Myrtle Creek.

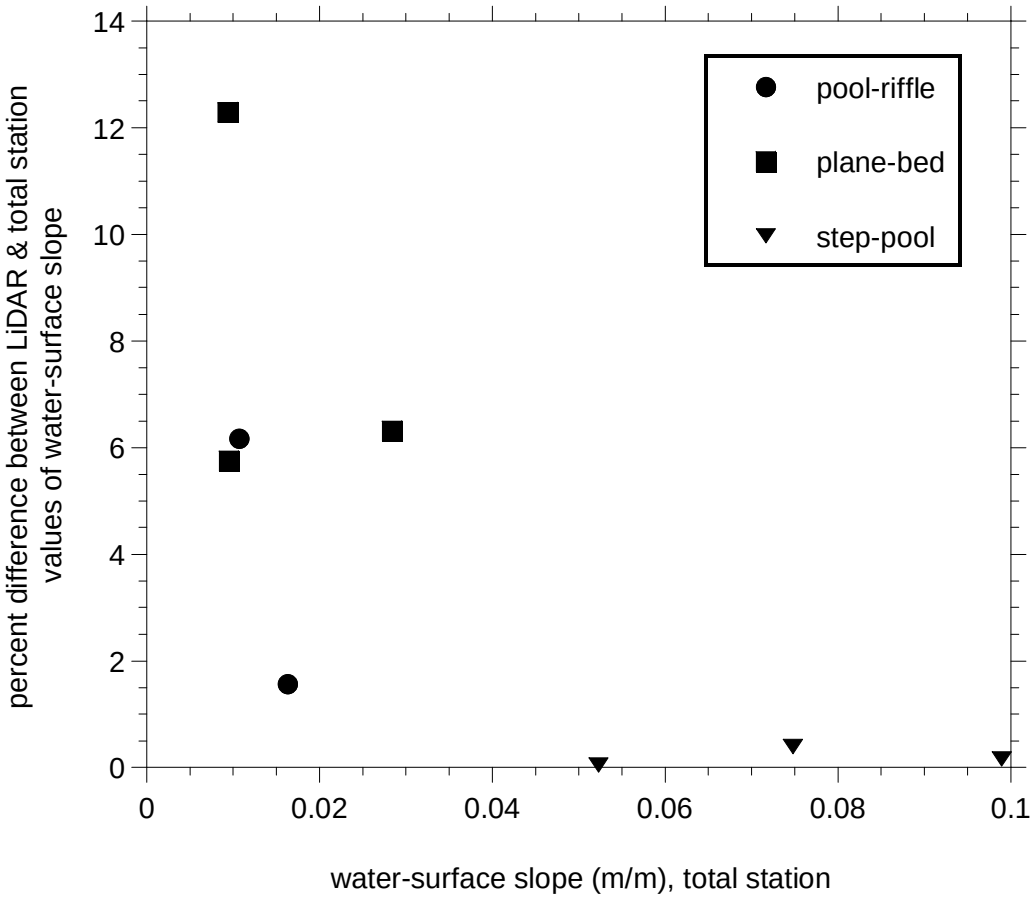

Figure 10. Scatter plot of percent difference in water-surface slope between LiDAR and total station measurements for different stream types.

While the gradient comparisons were based on a limited number of water surface measurements in the total station data, water surface elevations can be sampled from LiDAR data at any user defined interval (fig. 11). Dense sampling of the water-surface topography potentially can be used to locate pools and riffles (low-gradient, smooth surface areas relative to that of steeper-gradient, rough surface areas indicative of riffles and steps).

Table 4. Comparison of reach-average water-surface gradient between the total station data and the LiDAR DEM.

	Water-surface gradient (m/m)		
	LiDAR	Total station	Percent difference
Pool-Riffle Streams			
Trail Creek	0.0160	0.0163	1.56
Crane Creek	0.0101	0.0107	6.17
Plane-Bed Streams			
Camas Creek	0.0089	0.0095	5.75
Tinker Creek	0.0266	0.0284	6.32
Bridge Creek	0.0105	0.0094	-12.29
Step-Pool Streams			
Whiskey Creek	0.0745	0.0748	0.40
Myrtle Creek	0.0988	0.0990	0.16
Crawfish Creek	0.0523	0.0523	0.05

Discussion

Overall, the LiDAR approach tended to overestimate channel widths (69% of the time), with errors systematically varying with channel type (progressively greater median error across plane-bed, pool-riffle, and step-pool channels). Overestimation of channel width likely is due to the resolution of the LiDAR DEM and interpolation of streambank topography in locations where the density of ground returns is reduced by riparian vegetation. Some error also may be due to the native resolution of the data (section, “LiDAR Data Quality”). The geo-positioning of the field data could not be quantified, but inevitably introduced additional uncertainty due to small differences in the position or angle of the cross section.

Results also showed that remote sensing of the bankfull elevation and width using LiDAR may be prone to errors in channels with multiple terraces. However, these errors could be reduced with limited field observations that allow data training for selection of the terrace corresponding with the active floodplain.

While differences in width were observed between LiDAR-derived cross sections and those measured in the field, LiDAR offers a means to apply a consistent sampling method to all sites in a watershed and to reduce or eliminate observer variability in field sampling sites. Among observers, estimated bankfull dimensions have been shown to vary by as much as ±15 % (Roper et al., 2002). Furthermore, because the LiDAR data are geographically precise, temporal changes in channel geometry can be evaluated at the same location using the same

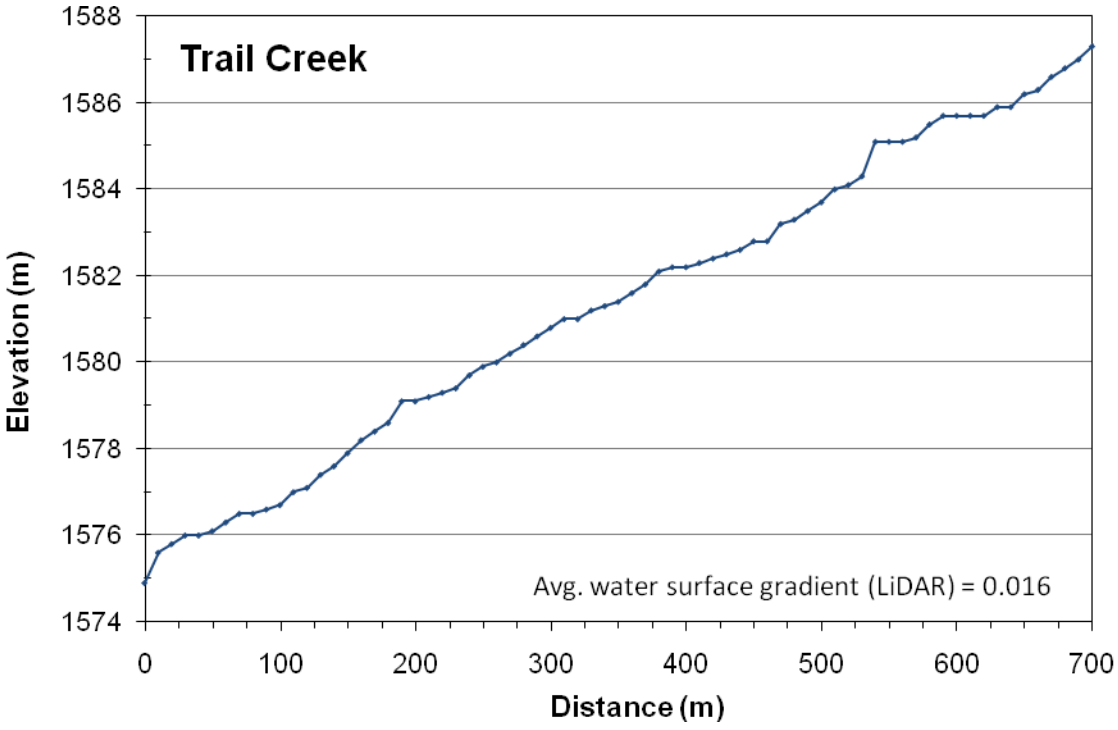

Figure 11. Example of water-surface elevations sampled from the LiDAR DEM at 1-m intervals longitudinally along Trail Creek (a pool-riffle stream).

methods. LiDAR-derived models have continued to improve through technological advances in pulse densities, GPS accuracy, and ground classification methods. Consequently, multi-temporal analysis should consider the contribution of differences in the precision and resolution of the underlying data when interpreting results.

Field crews typically measure channel cross sections at discrete locations along the channel. Although these survey points are accurate, even the most rigorous surveys are inherently limited due to time and resource constraints. Consequently, field measurements typically quantify physical habitat indicators at discrete locations, but often fail to accurately capture the variability of these parameters at the watershed or even reach scale. For example, Young et al. (2006) showed that quantifying the variability of large wood debris may require sampling over much longer stream lengths than typically measured during monitoring surveys. In contrast, LiDAR DEMs are spatially continuous and can be used to measure a variety of channel characteristics at user defined intervals along the stream, better quantifying the spatial variability of conditions. For example, first-terrace widths varied from 3.3–23.4 m over a 3-km segment of Trail Creek, showing a greater range of variability than would have been detected by the five monumented cross sections at this site (fig. 12). LiDAR mapping of these physical parameters provides an unprecedented ability to quantify channel characteristics and associated habitat at multiple spatial scales (e.g., McKean et al., 2008).

LiDAR Data Quality

The quality of results obtained from LiDAR will be strongly controlled by the native resolution and accuracy of the LiDAR data and derived products (table 2). A lower resolution data acquisition (expressed as pulse densities for raw LiDAR) may produce different results in terms of how well the DEM represents the channel geometry. James et al. (2007) showed that LiDAR data processed at 2-m grid cells were not suitable for detailed morphologic analysis or for subtle change detection in monitoring gullies in headwater streams in South Carolina. The number of ground returns can be improved by collecting data at higher pulse densities and flight planning that maximizes penetration through the canopy. In the Pacific Northwest, the Oregon LiDAR Consortium (OLC) and Puget Sound LiDAR Consortium (PSLC) are currently collecting data at pulse densities of >8 pulses/m^2 (PSLC has collected data at ≥4 pulses/m^2 since 2005). The collection of data during winter months also helps minimize the influence of broad-leaf riparian vegetation on ground return density. Finally, the LiDAR instrument has to be well calibrated with good relative consistency.

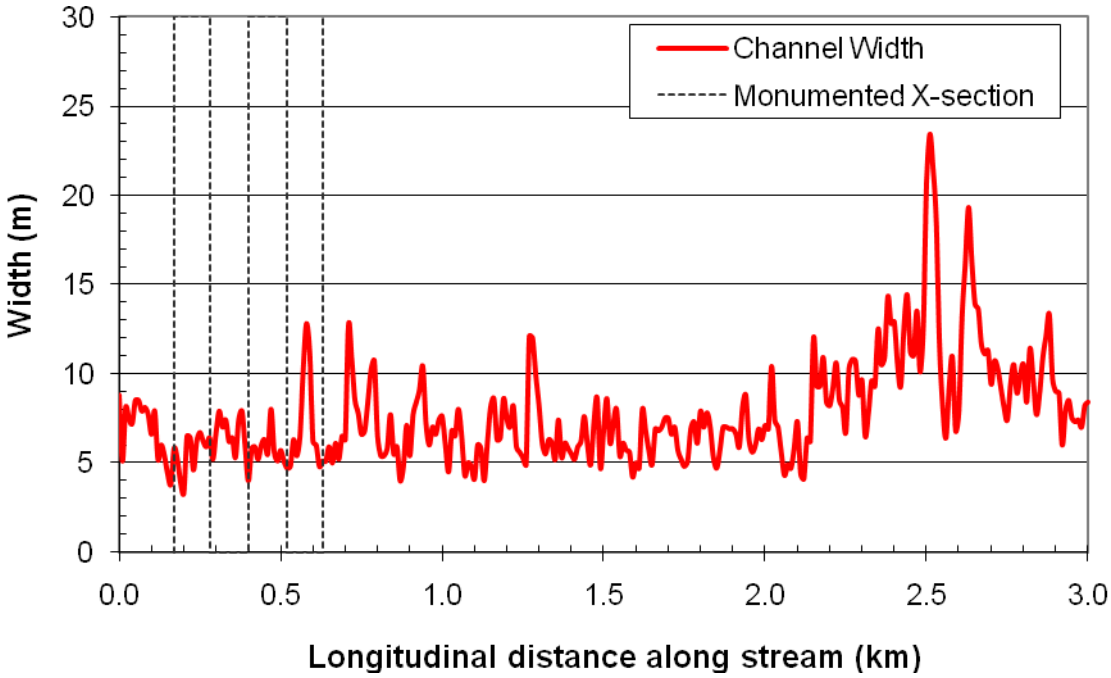

Figure 12. Plot showing first-terrace widths measured at 5-m intervals over three km of Trail Creek derived from the LiDAR data. The locations of the five monumented cross sections (fig. 5) also are shown on the plot.

Costs and Capabilities

With the increasing availability of high-resolution, quality-controlled LiDAR data through statewide initiatives and regional consortiums, natural resource managers can benefit by utilizing publicly available data and/or contributing to regional consortiums to collect data from new areas of interest. Large initiatives offer a pre-defined price structure that realizes an economy of scale by combining contributions from multiple entities. Current pricing through the Oregon and Puget Sound LiDAR Consortiums is $0.78/acre for contiguous areas greater than 250 mi^2 (Puget Sound LiDAR Consortium, 2008).

Although there are many potential benefits of using LiDAR (e.g, increased spatial sampling, elimination of observer variability), LiDAR measurements provide a subset of the attributes currently collected by aquatic habitat monitoring programs (table 5). Other attributes can be partially measured or inferred depending on scale and the availability of corresponding imagery. As technology continues to advance (e.g., increased pulse densities, small footprint green-wavelength LiDAR, etc.), the number of attributes that can be reliably measured also will advance. Currently, the benefit of LiDAR data products will be to enhance, but not replace, field monitoring programs.

Table 5. Near-infrared LiDAR capabilities for measuring channel and habitat attributes.

[**Measurable**: Y, parameter measurable with minimal error; WL, parameter measurable to some degree, with limitations under some circumstances; N, parameter can not be measured]

Parameter	Measurable	Comments
Channel characteristics		
- Reach length	Y	
- Sinuosity	Y	
- Connectivity	Y	Includes mapping inactive/paleo-channels
- Terrace Elevations	Y	
- Bank Incision	Y	Bank elevation/channel elevation
- Cross Sections	WL	Measured down to water surface
- Bankfull Depth	WL	Provides a reasonable estimate on small streams at base flow.
- Bank Angle	WL	Scale and ground-return density may be a factor on small streams in terms of how well bank topography can be identified.
- Bank Type	WL	
- Bank Stability	WL	
- Partial blockages to salmon migration	WL	Improved with digital imagery, but features that represent a real blockage may be open to interpretation.
- Water Surface Elevation	Y	
- Pool Frequency/Length	WL	Water-surface topography can be used to locate pools (low-gradient, smooth surface areas relative to that of steeper-gradient, rough surface areas indicative of riffles and steps). This capability will be a function of stream size and discharge (smoothness of water-surface profile), and can be facilitated with multi-spectral images.
- Pool Depth	N	
- Bed Topography	N	
- Substrate	N	
- Bank Materials	N	
Valley/Upslope		
- Valley cross section	Y	
- Landslides	Y	
- Road Density	Y	
- Stream Crossings	Y	
- Impervious Surfaces	Y	Improved with digital imagery.
Riparian		
- Vegetation Height	Y	
- Large Woody Debris	WL	The availability of large wood can be derived from LiDAR-derived vegetation models, but can be greatly improved with digital imagery.
Biological		
- Water Chemistry	N	
- Biology (fish, invertebrates, etc.)	N	

Conclusions

High-resolution LiDAR data and derived DEMs present an opportunity for resource managers to expand the amount and quality of information available for aquatic habitat monitoring. This paper specifically looked at the ability of LiDAR to describe the geometry and slope of mountain channels in northeastern Oregon. The LiDAR data offers the means to apply a consistent and repeatable approach for sampling and analysis of physical characteristics within the watershed. The elimination of errors introduced by observer interpretation will improve a manager's ability to compare results between streams and/or between years on the same stream.

Ultimately, the broader utility of LiDAR data is in the ability to develop higher-order topographic metrics (e.g., area, volumes, curvature, and topology) of homogeneous units rather than measuring point or line samples common to existing protocols. Because near-infrared LiDAR does not penetrate the water surface, the DEM does not contain information about the channel depth, bed topography, and substrate size. As a result, near-infrared LiDAR data are more useful for understanding riparian, floodplain, and upslope characteristics. The need for in-channel data for habitat monitoring and modeling fluvial processes warrants continued technological development and deployment of high-resolution bathymetric (green wavelength) LiDAR. In both cases, the increased availability of these data will allow field crews to focus more time on studying the biological processes occurring within the wetted channel and to sample over larger spatial areas for the remaining parameters that can not be determined remotely with LiDAR.

LiDAR-derived DEMs additionally provide the potential for extending decision support processes to include spatially explicit information that is not well represented in existing protocols. For example, stream slope, sinuosity, channel complexity, and LWD retention could be mapped continuously along the stream length, capturing the overall variability in the system (fig. 13). Although not explicitly addressed in this study, the LiDAR data inherently contain information on upslope factors that influence habitat quality, such as road location, landslides, and riparian vegetation. In short, the availability of high-resolution LiDAR data may move our view of physical habitat monitoring away from discrete subsamples to a watershed-scale view that captures more of the complexity and variability of the ecosystem condition.

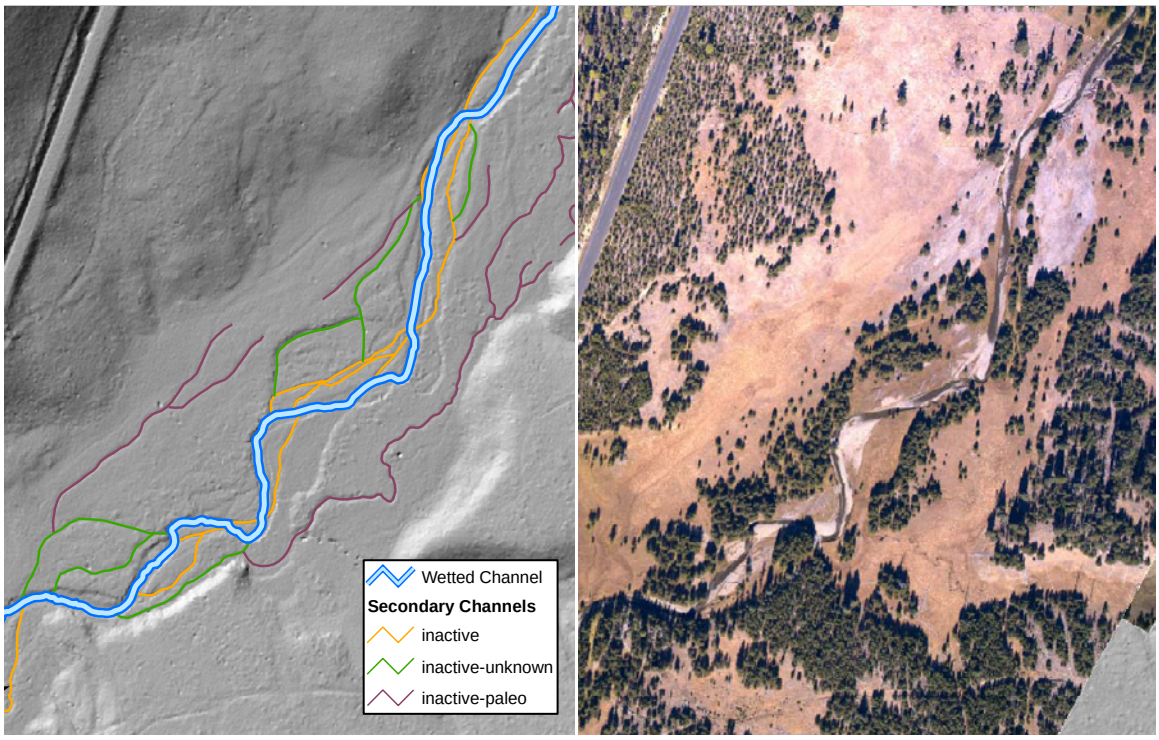

Figure 13. Example showing the mapping of side and secondary channels along a section of Trail Creek. Mapping of side-channel and floodplain elevations can provide measures of aquatic and riparian habitat suitability that extend beyond traditional monitoring parameters.

Acknowledgments

Funding for the LiDAR data acquisition and analysis was provided by NOAA Fisheries, Conservation Biology Division, Montlake Blvd East, Seattle, WA. We thank Rick Champion, Tom Frost, Jim McKean, and Keith Wolf for comments that improved the manuscript. Special thanks also to the Pacific Northwest Aquatic Monitoring Partnership for their support of this project.

References

Boyd, M., and Kasper, B., 2005, TTools program for ArcView: Oregon Department of Environmental Quality, accessed June 2008, http://www.deq.state.or.us/wq/tmdls/tools.htm

Buffington, J.M., Lisle, T.E., Woodsmith, R.D., and Hilton, S., 2002, Controls on the size and occurrence of pools in coarse-grained forest rivers: River Research and Applications, v. 18, no. 6, p. 507-531.

Cavalli, M., Tarolli, P., Marchi, L., and Fontana, G.D., 2007, The effectiveness of airborne LiDAR data in the recognition of channel bed morphology: Catena, v. 73, p. 249-260.

Dunne, T., and Leopold, L.B., 1978, Water in Environmental Planning: Freeman, San Francisco, California, 522 p.

Hardy, T., Panja, P., and Mathias, D., 2005, WinXSPRO, A channel cross section analyzer, User's Manual, Version 3.0: USDA Forest Service General Technical Report RMRS-GTR-147, Rocky Mountain Research Station, Fort Collins, CO, 94 p.

Harrelson, C.C., Rawlins, C.L., and Potyondy, J.P., 1994, Stream channel reference sites: An illustrated guide to field technique: U.S. Department of Agriculture, Forest Service, Rocky Mountain Forest and Range Experiment Station General Technical Report GTR-RM-245, 61 p.

James, L.A, Watson, D.G., and Hansen, W.F., 2007, Using LiDAR data to map gullies and headwater streams under forest canopy: South Carolina, USA, Catena, v. 71, p. 132-144.

Jones, J., 2006, Side channel mapping and fish habitat suitability analysis using LiDAR topography and orthophotography: Photogrammetric Engineering and Remote Sensing, v. 72, no. 11, p. 1202-1206.

Kershner, J.L., Archer, E.K., Coles-Ritchie, M., Cowley, E.R., Henderson, R.C., Kratz, K., Quimby, C.M., Turner, D.L., Ulmer, L.C., and Vinson, M.R., 2004, Guide to effective monitoring of aquatic and riparian resources: USDA Forest Service General Technical Report RMRS-GTR-121, Rocky Mountain Research Station, Fort Collins, CO, 57 p.

Kinzel, P.J., Wright, C.W., Nelson, J.M., and Burman, A.R., 2007, Evaluation of an experimental LiDAR for surveying a shallow, braided, sand-bedded river: Journal of Hydraulic Engineering, v. 133, no. 7, p. 838-842.

Lanigan, S., Roper, B., Buffington, J.M., Archer, E., Downie, S., Faustini, J., Hubler, S., Jones, K., Merritt, G., Konnoff, D., Pleus, A., Ward, M., and Wolf, K., 2006, Pacific Northwest side-by-side protocol comparison test: 5th National Water Quality Monitoring Conference, Monitoring Networks: Connecting for Clean Water, San Jose, CA.

Leopold, L.B., Wolman, M.G., and Miller, J.P., 1964, Fluvial processes in geomorphology: Freeman, San Francisco, CA, 522 p.

McKean J.A., Isask, D.J., and Wright, C.W., 2005, Mapping channel morphology and stream habitat with a full wave-form green lidar: EOS Transactions, American Geophysical Union, v. 86, no. 52, Fall Meeting, Suppl. Abstract H34B-05.

McKean J.A., Isaak, D.J., and Wright, C.W., 2008, Geomorphic controls on salmon nesting patterns described by a new, narrow-beam terrestrial–aquatic lidar: Frontiers in Ecology and the Environment, v. 6, no. 3, p. 125-130.

Montgomery, D.R., and Buffington, J.M., 1997, Channel-reach morphology in mountain drainage basins: Geological Society of America Bulletin 109, p. 596-611.

Puget Sound LiDAR Consortium (PSLC), 2008, PSLC Documents: accessed June 2008, at http://pugetsoundlidar.ess.washington.edu/About_PSLC.htm

Reeves, G.H., Hohler, D.B., Larsen, D.P., Busch, D.P., Kratz, K., Reynolds, K., Stein, K.F., Atzet, T., Hays, P., and Tehan, M., 2004, Effectiveness monitoring for the aquatic and riparian component of the Northwest Forest Plan: conceptual framework and options: USDA Forest Service General Technical Report PNW-GTR-577, Pacific Northwest Research Station, Portland, OR, 71 p.

Roper, B.B., Kershner, J.L., Archer, E., Henderson, R., and Bouwes, N., 2002, An evaluation of physical habitat used to monitor streams: Journal of the American Water Resources Association, v. 38, p. 1637-1646.

Roper, B.B., Buffington, J.M., Archer, E., Moyer, C., and Ward, M., 2008, The role of observer variation in determining Rosgen stream types in northeastern Oregon mountain streams: Journal of the American Water Resources Association, v. 44, no. 2, p. 417-427.

Roper, B.B., Buffington, J.M., Bennett, S., Lanigan, S.H., Archer, E., Downie, S., Faustini, J., Hillman, T.W., Hubler, S., Jones, K., Jordan, C., Kaufmann, P.R., Merritt, G., Moyer, C., and Pleus, A., (in prep.), A comparison of the performance and compatibility of protocols used by seven monitoring groups to measure stream habitat in the Pacific Northwest.

Rosgen, D.L., 1994, A Classification of Natural Rivers: Catena, v. 22, p. 169-199.

U.S. Department of Agriculture, Forest Service; U.S. Department of Interior, Bureau of Land Management (USDA and USDI), 1994, Record of decision for amendments to Forest Service and Bureau of Land Management planning documents within the range of the northern spotted owl, [place of publication unknown], 74 p.

Warren, S.D., Hohmann, M.G., Auerswald, K., and Mitasova, H., 2004, An evaluation of methods to determine slopes using digital elevation data: Catena. v. 58, p. 215-233.

Whitacre, H.W., Roper, B.B., and Kershner, J.L., 2007, A comparison of protocols and observer precision for measuring physical stream attributes: Journal of the American Water Resources Association, v. 43, p. 923-937.

Williams, G.P., 1978, Bank-full discharge of rivers: Water Resources Research, v. 14, no. 6, p. 1141–1154.

Woodsmith, R.D., and Buffington, J.M., 1996, Multivariate geomorphic analysis of forest streams: Implications for assessment of land use impact on channel condition: Earth Surface Processes and Landforms, v. 21, p. 377-393.

Wright, C.W., Brock, J.C., Nayegandhi, N., and Kinzel, P.J., 2006, The NASA Experimental Advanced Airborne Research LiDAR: A cross-environment LiDAR: EOS Transactions, American Geophysical Union, v. 87, no. 52, Fall Meeting Supplement, Abstract G53E-04.

Young, M.K., Mace, E.A., Ziegler, E.T., and Sutherland, E.K., 2006, Characterizing and contrasting instream and riparian coarse wood in western Montana basins: Forest Ecology and Management, v. 226, p. 26-40.

Chapter 7.—Managing, Manipulating, and Serving LiDAR Terrain Data and Orthoimagery for Riverine Habitat Assessment and Remediation Project Design for Salmon Recovery in the Pacific Northwest[1]

By Kristin Swoboda[2], Kurt Wille[3], Mike Beaty[2], and Greg Gault[2]

Abstract

The recent advent of affordable, high quality LiDAR and orthoimagery, acquired from aircraft platforms, offers new opportunities and challenges for end users and data managers supporting riverine habitat assessment and remediation project planning for salmon recovery in the Pacific Northwest. These include: (1) handling and manipulating extremely large, highly detailed datasets, (2) data processing and delivery to meet end user needs, and (3) the use of web services technologies to improve access and performance. This paper provides an approach for managing and delivering LiDAR data (points and surfaces) and orthoimagery for use by Reclamation engineers, hydrologists, and geologists in support of hydraulic modeling, tributary and reach assessments, and engineering design.

Introduction

The Bureau of Reclamation (Reclamation) began acquiring LiDAR and high-resolution orthoimagery data in 2006 for multiple stream reaches in the Pacific Northwest to support ongoing salmon recovery activities, including: reach level habitat assessments to identify restoration and preservation project opportunities; and to support engineering designs for restoration projects and construction. Reclamation conducts these project assessment and design activities through collaborative work processes involving project teams in multiple offices.

Reclamation project teams expressed a need for LiDAR data and orthoimagery in readily useable forms compatible with their respective software applications and IT tools. The extremely large and detailed nature of LiDAR data and orthoimagery presented significant data management and delivery challenges that began to impact project schedules. Subsequently, Reclamation's Pacific Northwest Region GIS group and Denver Technical Service Center began exploring approaches for managing, processing, and delivery of these large data in ways to improve ease of access and provide compatible data formats in manageable sizes.

Data acquisition contracts specified a set of LiDAR products and orthogonal aerial photography for each stream reach. The following LiDAR data products were processed and delivered in a data structure based on a 0.9375-minute tile grid (equivalent to a quarter-quarter-quarter of a USGS 7.5-minute quadrangle):

- Point files (LAS format)
- Point files (ASCII format)
- Bare earth
- All returns
- Digital Elevation Models (Raster format)
- Bare Earth
- Highest Hit
- Intensity Images (Raster format)
- Contours 0.5 meter interval (AutoCAD drawing format)
- Tile Index (ESRI shapefile format)
- Study Area boundaries (ESRI shapefile format)
- Flightlines (ESRI shapefile format)

[1]See also: "Using Bathymetric and Bare Earth LiDAR in Riparian Corridors: Applications and Challenges," Robert C. Hilldale, Jennifer Bountry, and Lucy Piety, Bureau of Reclamation.

[2]Bureau of Reclamation, Boise, Idaho.

[3]Bureau of Reclamation, Denver, Colorado.

LiDAR Specifications

- Flight Altitude: 1,000 m above ground
- Overlap: 50% side-lap (100% overlap)
- Flight Line Direction: Opposing
- Acquisition Speed: 110 knots
- Swath Width: 500 m
- Laser Pulse Repetition Rate (PRF): 95 kHz (95,000 pulse per second)
- Returns per Pulse: Up to four
- Scan Angle: 14 degrees from nadir (28 degrees total)
- Laser Spot Footprint: 27 cm
- Single Swath Resolution: 35 cm spot spacing >8 laser spots per square meter
- Multiple Swath Resolution: 48 cm spot spacing >4 laser spots per square meter (8 per square meter can be expected)
- Horizontal positional accuracy: 1/3000 AGL (4–7 centimeters (1.57–2.76 inches), 95th percentile 8–10 centimeters (3.15–3.94 inches)
- Vertical (elevation) accuracy: <15 cm (5.91 inches)

In addition to the above LiDAR data products, natural color orthogonal aerial photography was acquired at 6-inch resolution. The orthoimagery products were delivered using the same tiled data structure as the LiDAR products.

Orthoimagery Specifications

- Orthoimagery will be acquired in 3 spectral bands (red, green, blue) to provide a true color palette.
- Pixel resolution will equal 6 inches.
- Orthoimagery pixels will be orthorectified to the LiDAR DEM.
- Pixel positional accuracy will be 1.5 pixels (9 inches).

Cumulatively, the delivered data products exceeded two terabytes. This presented challenging data management problems, in terms of data storage and delivery to end users. A further complication was the need to deliver data products in formats useable in hydraulic modeling software and engineering design software (i.e., ESRI ArcGIS with GeoRAS and Autodesk Civil 3D).

The approaches presented in this paper address how to deliver a comprehensive range of LiDAR data products and orthogonal aerial photography to end users. The tiled data structure of the original delivery LiDAR data products lent itself to batch processing using ArcGIS Model Builder, which facilitated the sequencing of a series of data manipulation tasks to make data more readily useable to end user software applications.

Methods

The following describes the approaches used to prepare data for delivery to end users. First, the preparation and delivery of orthogonal aerial imagery are described, followed by a description of the more involved data manipulations preformed on LiDAR data.

Ortho Aerial Imagery Processing

High-resolution aerial photography, in this case 6-inch, is notoriously difficult to organize and manage in a way that makes discovery and access of desired images easy for end users. Traditional methods refer users to image indexes and catalogs for accessing data. Relatively recent developments in web service technologies provide a more efficient method for delivering imagery to end users.

Many geospatial software vendors, including ESRI and Autodesk, support web services standards promulgated by the Open GIS Consortium (OGC). Web mapping service, or WMS, is a standard for the delivery of imagery data that is supported by both ArcGIS and Civil3D. WMS supports delivery of imagery in multiple spatial references (projections), which proved quite valuable.

An open source map server product, known as MapServer (www.maptools.org) was used to generate WMS services for imagery. The 6-inch ortho aerial photography was originally delivered as images in TIFF format in a UTM projection. The images were organized into folders that correspond to the tile scheme of the LiDAR data products. A utility program provided with MapServer was used to create shapefile image catalogs. The shapefiles contains the filename of each image tile and the absolute path to the images on stored on disk. These shapefiles are used in MapServer map configuration files along with a series of parameters required for OGC-compliant WMS services including: supported spatial references, initial extent, scale dependency, output image format, and available layers.

The resulting WMS services display two or more scale-dependent layers. A wireframe index of available images displays at full extent. As users zoom-in to an area of interest, the layer containing image tiles displays at a scale appropriate for viewing high-resolution images. Adding support for multiple spatial reference systems enabled users to work with data stored in another spatial reference. The spatial reference of delivered aerial photography was UTM Zone 10 or UTM Zone 11. WMS services were configured to allow users to select a preferred spatial reference, in this case, NAD83 Washington StatePlane North 4601 Feet.

LiDAR Processing

Shortly after taking delivery of the LiDAR data products, it became apparent to end users that some of the data products in their native structures were not readily useable in their desktop applications. The tiled data structure also presented issues for discovery and access of LiDAR data tiles by end users. The example in figure 1 illustrates LiDAR data tiles for one subbasin in Washington.

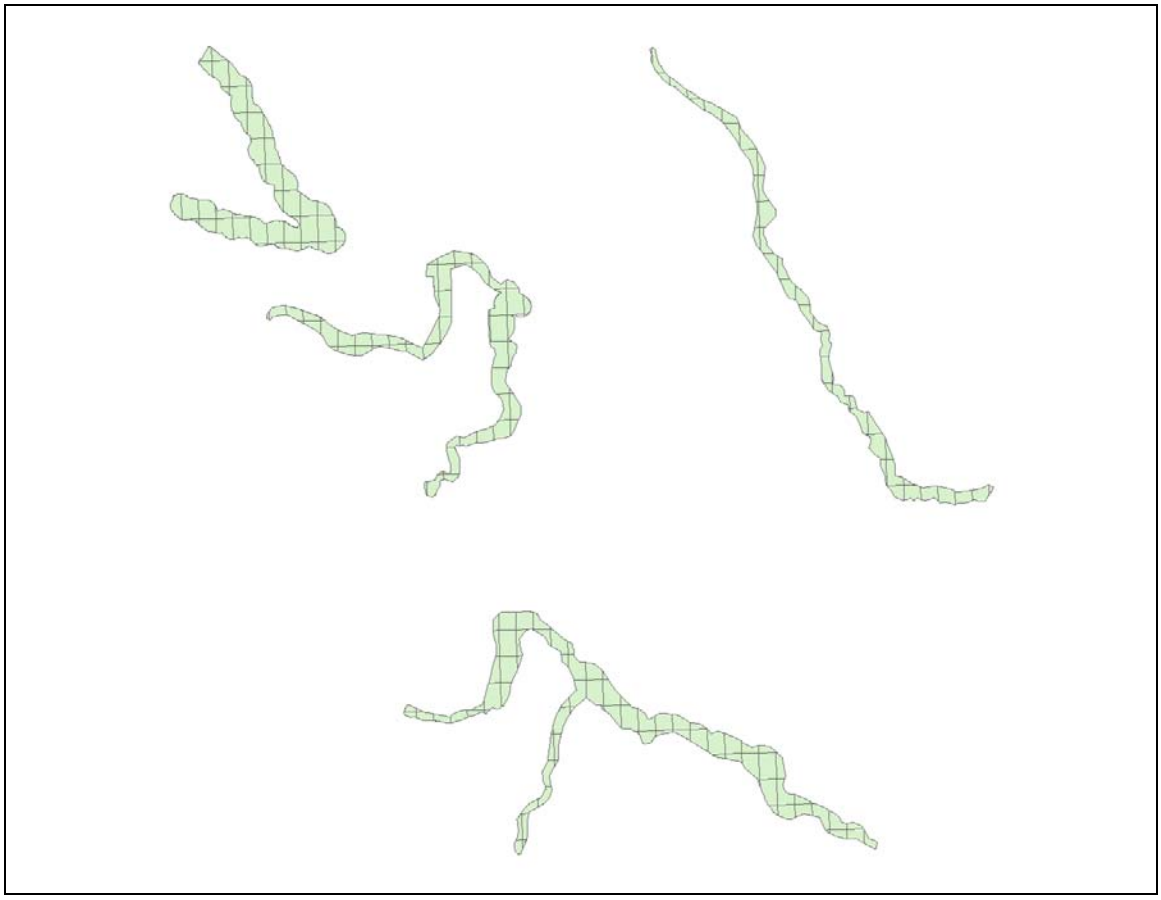

Figure 1. LiDAR data tiles for a subbasin.

Areas of interest defined by end users typically crossed parts of multiple tiles. Users found themselves working with a great deal more data than needed, which impacted performance and usability. ArcGIS rendering of LiDAR data in ASCII format was extremely slow. Although performance was much better when the LAS format was used, end users reported limited capability to perform operations when using this format.

After working with a number of engineers and hydrologists, it quickly became evident that the assistance of a GIS Analyst was necessary to create and perform a series of data manipulation tasks on their behalf. The following describes data manipulation process devised to improve the usability and performance of LiDAR data products.

The first step requires the end user to delineate the Area of Interest (AOI) as a polygon feature (in shapefile format). The AOI polygon is then used to identify, from Tile Index, the LiDAR data tiles needed. The identified data tiles (ASCII format) were then imported into 3D Feature Classes in file geodatabases (an ESRI data format). The tiled data structure was preserved in this step to permit efficient batch processing using ArcGIS Model Builder scripts.

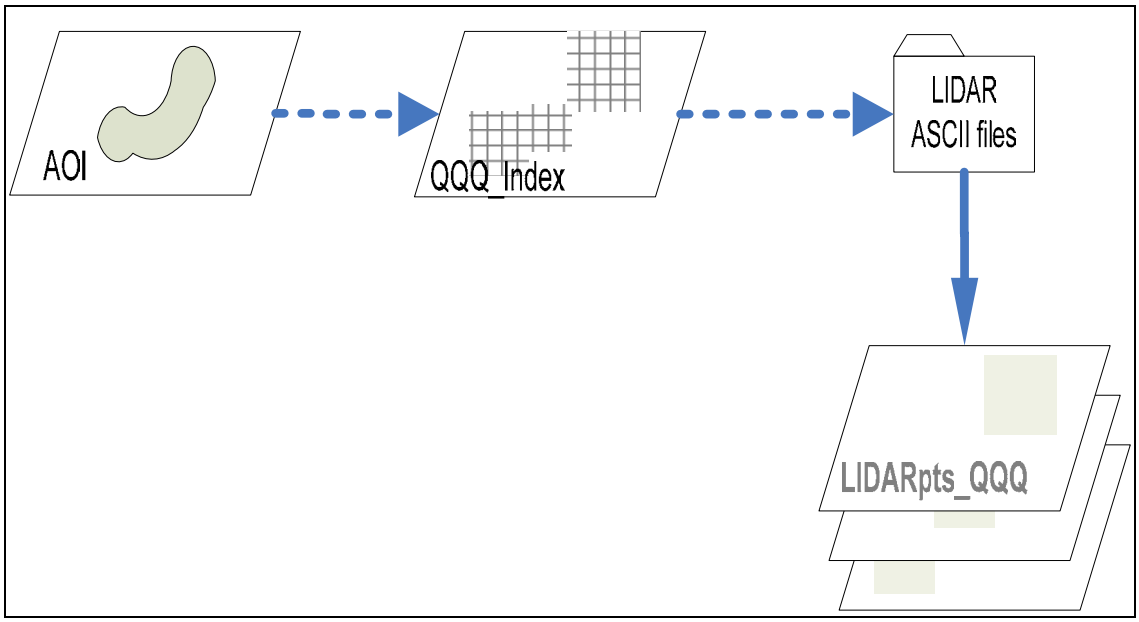

The next step, which was added when it was discovered that most users of the LiDAR data products in Reclamation preferred to work in a State Plane projection to incorporate field surveyed data collected in wetted areas with scattered LiDAR returns. Field survey data include the stream thalweg and controlling cross sections, along with additional break lines and mass points to be integrated into the final terrain model.

In this step, the 3D Feature Classes are transformed to the desired spatial reference. The process re-calculated X, Y coordinate values in the desired State Plane coordinate system for the attribute tables of the new 3D Feature Classes. Elevations values (Z) were also recalculated to convert metric units of UTM coordinate system to elevations in U.S. Standard feet. The AOI polygon is then used to perform a spatial selection of LiDAR points in each of the 3D Feature Classes (of tiles) to produce a set of interim 3D Feature Classes of LiDAR points within the AOI. This step significantly reduces the amount of unneeded data.

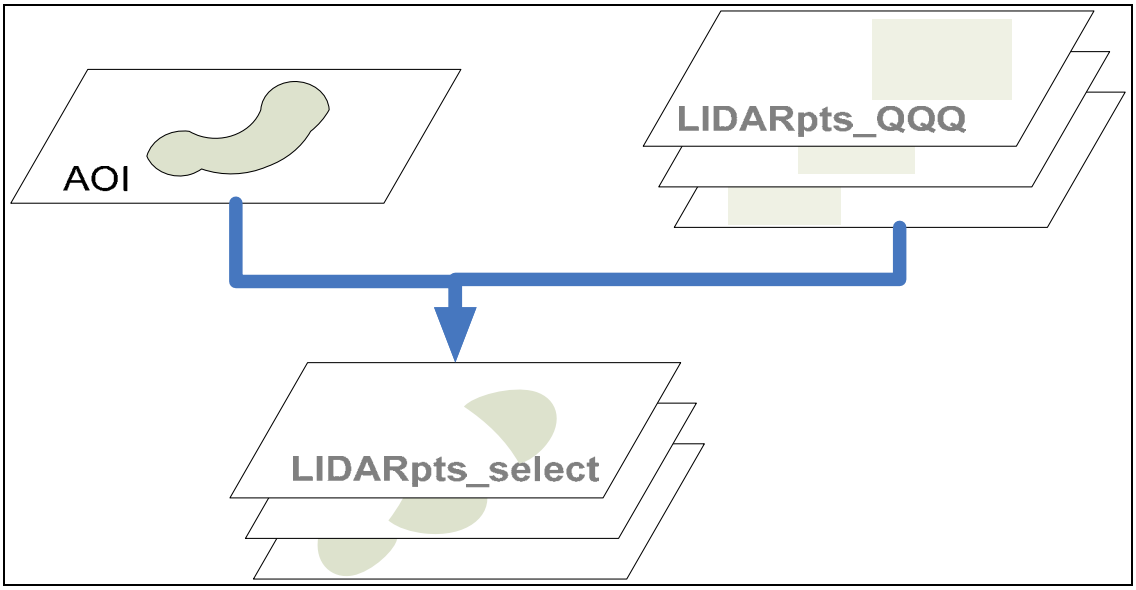

The next step in the process requires another input from the end user to produce a set of polygon features that delineate wetted area, as defined by streambanks and island shorelines. These polygon features were delineated by using the previously described orthogonal aerial imagery WMS services and LiDAR intensity grids to mask unwanted LiDAR points within the wetted area of a stream reach where LiDAR returns are suspect due to presence of water. The user-produced wetted area polygons were then used to perform another spatial select that yields another set of interim 3D Feature Classes.

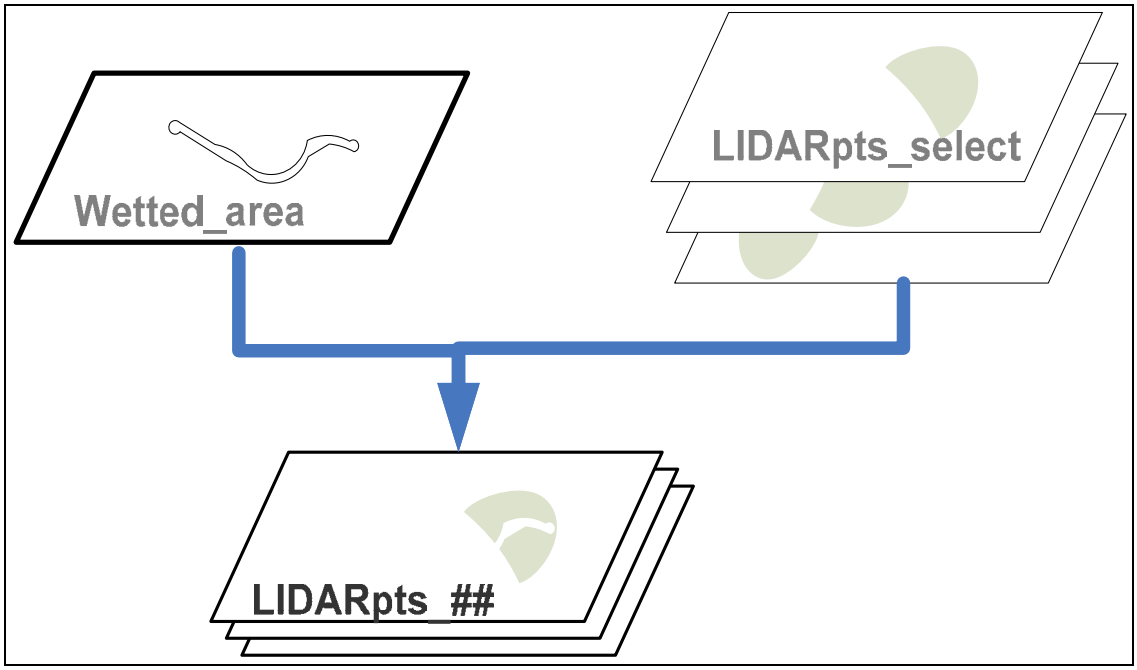

This final set of 3D Feature Classes was then appended together into a single composite 3D Feature Class. Depending on the specific needs of the end user, the composite 3D Feature Class for the AOI may be merged with field surveyed data to replace points eliminated from the wetted area in the previous step. In addition, streambanks (from wetted area delineation) and thalweg points can be merged to impose break lines or meet other needs of hydraulic models or engineering design.

The result of the described data manipulation process are a set of 3D Feature Classes ready for processing by users as inputs for building TIN surfaces, analysis in surface-water models, and manipulation in design software. Refer to the diagram on the following page.

Conclusions

Engineers, hydrologists, and geologists report that LiDAR data provide the necessary detail essential to identify and delineate riparian and riverine features that were not previously identifiable using other digital terrain data products. More precise delineation of geomorphologic features, such as floodplains, historic channel segments, streambanks, and similar features, informs reach assessments with the information necessary to efficiently facilitate river restoration project planning.

Users of LiDAR data and high-resolution orthoimagery web services report that the process described in this paper results in substantial time savings by providing data in ready-to-use forms and manageable sizes that are more efficient to use and improve system performance. Recognizing the relative ease of access and performance of the web services used to deliver orthoimagery, users requested the delivery of LiDAR data through a web-based service technology. Further, users want to perform the LiDAR data manipulation processing themselves, that is, the capability to extract LiDAR data based on user-defined Areas of Interest.

Although the nature of LiDAR data present some challenges for handling and delivery in a web services context, the potential benefits to the scientists and engineers clearly warrant further investigation. Future research of web-based technologies should be pursued to further improve the management, manipulation, delivery, and use of orthoimagery and LiDAR data.

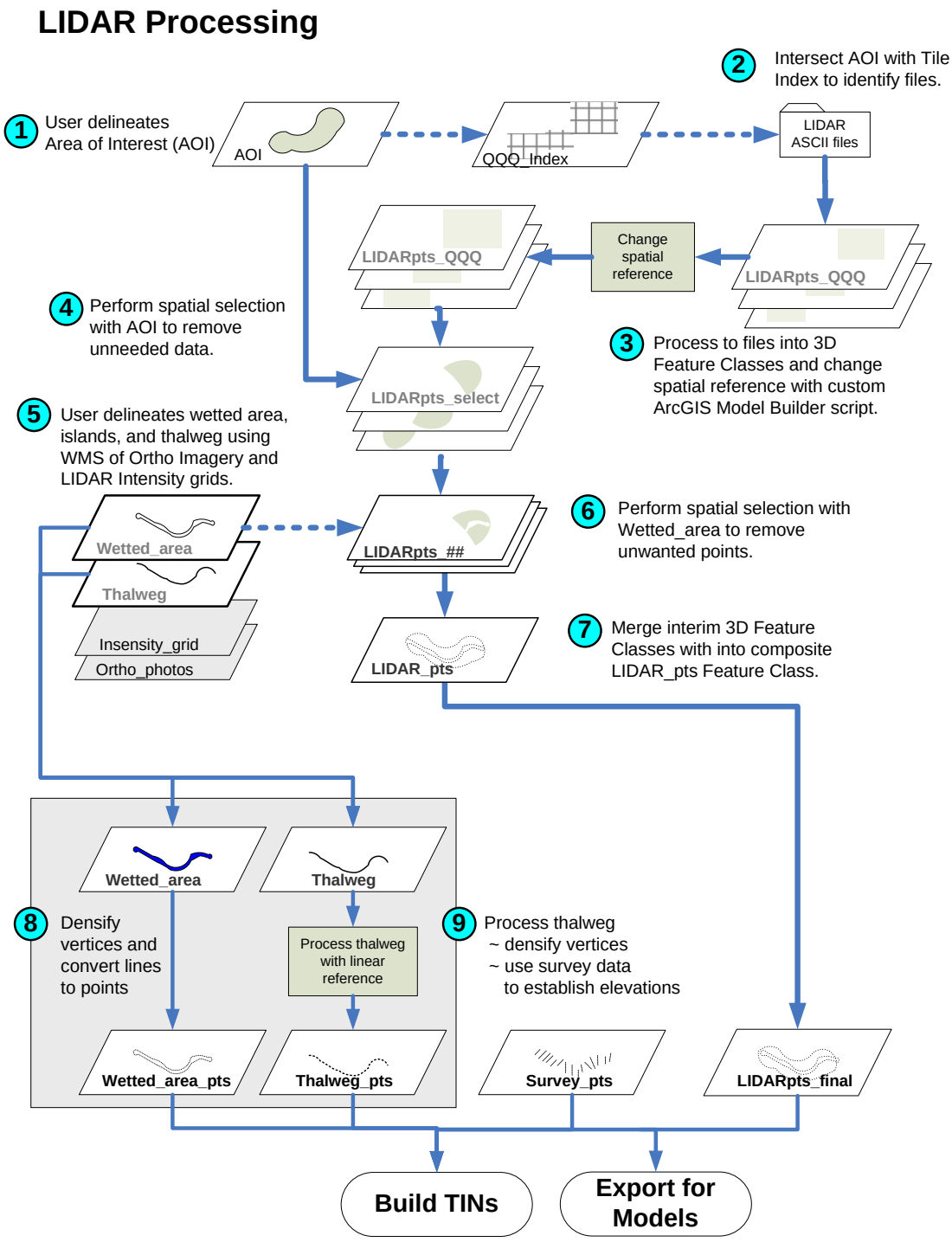

This page left intentionally blank

Chapter 8.—Mapping Intertidal Eelgrass Landscapes in Hood Canal (WA) Using High Spatial Resolution Compact Airborne Spectrographic Imager (CASI) Imagery

Ralph J. Garono[1], Charles A. Simenstad[2], Robert Robinson[1], Chris Weller[3], and Steve Todd[3]

Abstract

Intertidal eelgrass (*Zostera marina*) beds are a vital resource for many Pacific Northwest estuarine organisms including juvenile chum salmon (*Oncorhynchus keta*) and an important indicator of estuarine condition. Consequently, there is a need for current information describing eelgrass abundance and distribution. Recent studies suggest some eelgrass populations in Puget Sound may be declining. Remote sensing methods commonly are used to develop data sets describing the location and extent of landscape features, such as eelgrass beds, for large areas; however, there are a number of challenges that limit the use of remote sensing to map intertidal eelgrass beds in Pacific Northwest estuaries. We selected Compact Airborne Spectrographic Imager (CASI) to map intertidal eelgrass beds in Hood Canal because it gave us precise control over acquisition time, and spatial and spectral resolution. Controlled timing of image acquisition was necessary to collect imagery from intertidal eelgrass beds exposed during low tide. A high degree of spectral resolution was necessary to separate spectrally similar cover classes (e.g., green macroalgae and eelgrass). During June and July 2000, we collected 19-band CASI imagery with a pixel size of 1.5 m. We used a combination of unsupervised/ supervised classification to classify imagery for about 1,100 ha shoreline. We mapped 12 cover classes using training data collected from 174 sites. We found good agreement between classified eelgrass cover classes and existing eelgrass beds during our accuracy assessment. We concluded that 19-band CASI data were adequate to map eelgrass beds and to separate them from spectrally similar cover classes.

Introduction

Eelgrass (*Zostera marina*) is an important estuarine resource. Juvenile chum salmon (*Oncorhynchus keta*) use intertidal eelgrass beds in Pacific Northwest estuaries as corridors for movement, feeding, and cover during their seaward migration (Simenstad and Salo, 1982; Simenstad et al., 1982; Simenstad, 1994). As an indicator organism, eelgrass population changes have been used to evaluate estuarine condition and the impact of disturbances (Phillips, 1984; Short and Burdick, 1996; Dowty et al., 2007). Much of the spatial data on estuarine and nearshore habitat in Puget Sound is of limited scope and is more than 20 years old (Phillips, 1984; Thom and Hallum, 1991). Recent studies in Hood Canal (WA) and elsewhere in Puget Sound describe areas where eelgrass populations are stable; however, these studies also have identified areas of eelgrass decline (Berry et al., 2003; Dowty et al., 2005; Gackle et al., 2007). Consequently, there is a need for current, detailed information describing the abundance and distribution of eelgrass in Puget Sound as scientists and natural resource managers develop protection and restoration plans.

Remote sensing and geographic information system (GIS) technology are analytical and visualization tools that allow scientists and resource managers to examine landscape patterns in datasets collected over relatively large geographic areas. GIS maps derived from remotely sensed imagery can be a cost effective way to produce uniform, regional-scale datasets. However, coastal clouds and fog, and relatively large tidal amplitudes may limit the use of remote sensing imagery in mapping Puget Sound intertidal eelgrass beds. Other challenges include collecting relatively high spatial resolution data (about 1–2 m) over hundreds of kilometers of shoreline at sufficient spectral resolution to separate spectrally similar cover types (e.g., distinguish green macroalgae from eelgrass).

In 1999, we brought together an interdisciplinary team of researchers to map intertidal eelgrass beds in Hood Canal. The team included experts in remote sensing, estuarine ecology, geomorphology, geographic information systems (GIS), and Pacific Northwest salmonid ecology. In selecting an approach, our team identified several key data requirements for this study: (1) collected data must be spatially explicit and of the best possible positional accuracy because later studies would link eelgrass bed distribution to other spatial datasets (see Simenstad et al., 2008); (2) eelgrass landscape patterns must be resolved (spatially) at a scale appropriate

[1]Earth Design Consultants, Inc., 230 SW 3rd, Suite 212, Corvallis, OR 97333

[2]School of Aquatic and Fishery Sciences, University of Washington, Seattle, Washington 98195

[3]Point No Point Treaty Council, 7999 N.E. Salish Lane, Kingston, WA 98346

for juvenile salmon; (3) the approach had to be capable of distinguishing between spectrally similar intertidal cover classes; and (4) timing of data acquisition had to be precisely controlled to occur during maximal low tides.

Compact Airborne Spectrographic Imager (CASI) is a two-dimensional, charge couple device array-based push broom imaging spectrograph that can be operated in either a spatial or spectral mode. Operated in the spatial mode, this airborne remote sensing platform can produce multiple band images at a spatial resolution of 1–2 m. CASI seemed well-suited for remote sensing of Pacific Northwest intertidal eelgrass beds because it gave us precise control over image acquisition time, and spatial and spectral resolution.

Methods

We acquired 19-band CASI hyperspectral imagery for about 250 km of the Hood Canal and eastern Strait of Juan de Fuca shoreline during the spring low tide series in June and July 2000 (fig. 1). Generally, bands were set to a width of 10 nm except for band 1 (30 nm) and band 19 (20 nm), which were larger in order to increase the instrument's sensitivity (table 1). The CASI sensor, operated by Hyperspectral Data International, Inc. (HDI), was mounted in a factory-installed camera port on a DeHavilland Beaver, operated by Ecotrust (Portland, OR). All imagery was collected in spatial mode. By flying the aircraft at an altitude of 1,140 m above ground level at approximately 176 km hr^{-1} to 183 km hr^{-1}, we achieved a pixel size of 1.5 m and a ground track of approximately 768 m. Effects of downwelling light were removed from the CASI data by HDI using measurements from the incident light sensor. HDI also geometrically corrected CASI data using filtered attitude data. CASI data were supplied in ERDAS LAN format. Imagery was reviewed at the end of each day for data gaps and image quality (primarily illumination and shadows). Following review, we prioritized flight lines for processing based on image quality and we grouped flight lines into seven focal areas (FA) that represented the best quality imagery.

Spatial error is not distributed uniformly in imagery collected using airborne push broom-type imagers because the image is built up one scan line at a time while the attitude of the aircraft is constantly changing. We planned for the imagery to be spatially accurate to within 2–3 pixels (in this case 3–5 m); however, in pilot studies we conducted with CASI, we found some areas in the imagery to be greater than 10 m from their real world position. Therefore, our field teams placed 3×3 m plastic tarps, visible in the CASI imagery, along the shoreline as Ground Control Points (GCP); the position of each tarp was measured with a Trimble® Pathfinder Pro XR real-time differential Global Positioning System (GPS). In addition to tarps, we located permanent features (i.e., building corners, piers, road crossings, etc.) visible in the CASI imagery and used digital orthoquads (DOQs) to improve geocorrection. For several flight lines, we returned to the field with the CASI imagery to measure locations of additional GCP visible in the imagery with a GPS with submeter accuracy. We used ERDAS® Imagine software to geometrically correct the CASI imagery by fitting the imagery to the control points using a 1st order polynomial model. Root mean square error (RMSE) was measured using 7 to 21 GCPs for each flight line.

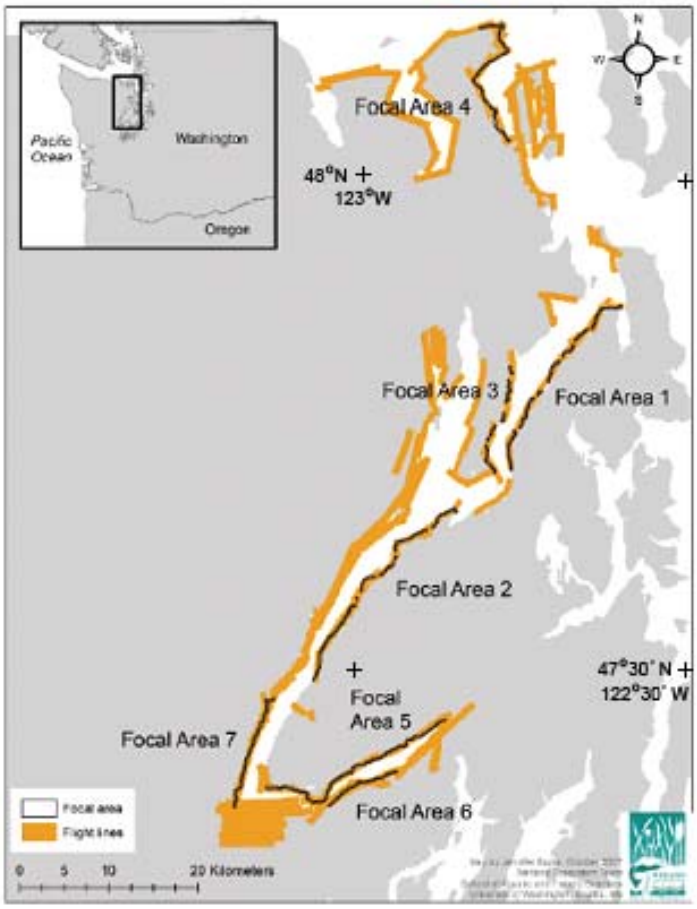

Figure 1. Location of the Hood Canal (WA) study area (inset). Shown are the locations of the flight lines (orange) and the seven FAs: (1) Northeast Hood Canal, (2) Central Hood Canal, (3) Northwest Hood Canal, (4) Admiralty Inlet, (5) Northern Southeast Bend of Hood Canal, (6) Southern Southeast Bend of Hood Canal, and (7) Southwest Hood Canal.

Table 1. Band settings for CASI hyperspectral sensor used to map intertidal cover of Hood Canal, WA shoreline in July 2000.

[Band settings were based, in part, on measurements made with a hand held radiometer (see Garono et al., 2004). Bands were selected to maximize separation of spectrally similar vegetation]

CASI band	Upper (nm)	Lower (nm)
1	460	490
2	520	530
3	530	540
4	540	550
5	550	560
6	560	570
7	620	630
8	630	640
9	640	650
10	650	660
11	690	700
12	700	710
13	720	730
14	730	740
15	755	765
16	765	775
17	775	785
18	785	795
19	800	820

In preparation for classifying the CASI imagery, we constructed a spectral library of common cover classes using a Photo Research, Inc.® PR-650 hand held radiometer. We collected both reflectance spectra and plant community composition data from representative, relatively monotypic patches of intertidal cover class categories, based on five random (1.5×1.5 m) samples taken from within 6×6 m sampling grids. Percent cover of eelgrass and other associated vegetation or oysters was estimated both visually using the sample grid and, at a later time, from projected digital camera images. We analyzed the grid cell digital photographs by superimposing a 100-point grid on the image and then counting the intertidal cover class categories intersecting each point. Data on eelgrass shoot density (shoots per 0.1 m quadrat) also were collected from each of the five randomly selected quadrat plots.

We classified the CASI imagery using a combination of unsupervised-supervised classification. Initially, we performed an unsupervised classification (ISODATA, 12 iterations, 95% convergence, 100 classes) on the 19-band, georeferenced imagery using ERDAS® Imagine® software, which resulted in 100 spectral categories. Following the collection of signatures in ISODATA, the 100 spectral classes were subjected to a Maximum Likelihood Classification. During a 1999 pilot study, we found that we could only use a maximum of four or five CASI bands in a supervised classification when extracting spectral signatures from training site grids. When we included more than five CASI bands, we found that computer processing time was long and the resulting classification was unsatisfactory due to the training grid size relative to our 1.5 m pixel imagery. We reduced the number of bands to shorten processing time of the images and to optimize the classification using the bands that best distinguished between cover classes. The supervised classification was performed on spectral signatures extracted from training site grids for four CASI bands (2, 8, 16, and 18) (table 1). We selected these bands based, in part, on spectral information collected with the hand-held radiometer. We excluded deepwater and upland areas from the classification. The supervised classification produced a new set of spectral signatures for eelgrass cover classes on which the Maximum likelihood procedure was used to group pixels that shared spectral characteristics. Smoothing algorithms were not used to aggregate classified pixels; therefore, the minimal mapping unit was equal to the pixel size (i.e., 1.5 m).

Weather, flight line quality, and the project budget made it necessary to select a subset of the flight lines for classification. Classified flight lines were grouped into seven focal areas: (1) Northeast Hood Canal; (2) Central Hood Canal; (3) Northwest Hood Canal; (4) Admiralty Inlet; (5) Northern Southeast Bend of Hood Canal; (6) Southern Southeast Bend of Hood Canal; and (7) Southwest Hood Canal (fig. 1). Although we collected training data from 174 training sites, only 54 training sites were located within the flight lines classified. Spectral information from the remaining training sites was used indirectly in the supervised classification.

We assessed classification accuracy by revisiting areas from all flight lines and comparing our classified image with existing eelgrass beds and other cover classes. We were careful to assess only those intertidal cover classes that were not expected to have changed over the winter (table 2: all classes except green, brown, and mixed macroalgae classes). We also compared our results to the results of an independent investigation of eelgrass in a small area around the Hood Canal Bridge.

Table 2. Mean total area (m^2 ha^{-1}) of each cover classes in the seven intertidal focal areas (FA).

[Note that the mixed macroalgae, sand, mud and *Salicornia* cover classes were not classified in FA1-FA3. See figure 1 for identification of focal areas. ---, not measured]

Focal area	Dense eelgrass	Sparse eelgrass	Dense green macro-algae	Sparse green macro-algaae	Brown macro-algae	Mixed macro-algae	Sand	Mixed sand-gravel	Mixed gravel-cobble	Mud	Oysters	*Salicornia*
1	1,298.88	138.47	159.04	354.08	18.11	---	---	968.11	406.57	---	88.42	---
2	212.53	176.58	114.30	192.19	239.28	---	---	749.38	663.53	---	211.85	---
3	642.65	55.49	196.05	155.12	0.00	---	---	693.49	511.02	---	123.65	---
4	939.26	355.37	181.99	220.74	144.51	73.57	1,508.46	579.19	148.37	0.00	0.00	0.00
5	200.16	299.40	113.89	365.00	5.97	186.88	109.26	455.12	834.26	1,004.99	239.05	116.97
6	65.50	35.74	221.30	185.80	48.73	86.48	288.30	296.38	771.74	0.00	365.43	0.00
7	203.12	360.46	177.45	235.12	186.42	151.08	28.23	280.40	878.71	145.16	117.86	0.00

Results and Discussion

We collected imagery along 145 overlapping flight lines varying in length from 0.9 to 20.0 km. Although the CASI data were reviewed as they were collected in the field, the quality of the imagery varied considerably due to data gaps, cloud shadows, and differences in illumination. We classified imagery from 26 of 145 total flight lines and eventually mapped 12 intertidal cover classes, including two eelgrass cover classes, over 1,100 ha of shoreline along Hood Canal (table 2).

Although the 26 flight lines were initially geometrically corrected by HDI with data collected onboard the aircraft, we verified that tarps and other features visible in the CASI imagery could be used with GCPs collected by field teams and DOQs to improve geocorrection. The average RMSE (both X and Y) was 9.3 m (range was 2.0 to 24.7 m). By returning to the field and to collecting additional GCP to improve the spatial accuracy of the CASI imagery, we reduced the spatial error (RMSE) by an additional 1 to 2 m per flight line; however, we concluded that the RMSE was not improved sufficiently to warrant the added expense of collecting additional field data. Therefore, we decided that geocorrection was adequate using the initial set of GCPs and DOQs for the remaining flight lines.

We found that mean dense eelgrass (203 to 1,299 m^2 ha^{-1}) and the unvegetated beach sediments, sand (28 to 1,508 m^2 ha^{-1}), mixed sand gravel (280 to 968 m^2 ha^{-1}) and mixed gravel-cobble (148 to 879 m^2 ha^{-1}), typically accounted for the broadest total intertidal coverage in the FAs (table 2). Unvegetated substrate (sand, mixed sand and gravel, mixed gravel-cobble) typically dominated coverage in most FAs except the Northeast; sand was not discretely classified in the Northeast, Central, and Northwest Hood Canal FAs. Sand or mixed sand-gravel covered a mean of between ~693 m^2 ha^{-1} (Northwest Hood Canal) and ~2,090 m^2 ha^{-1} (Admiralty Inlet) in the northern FAs, but less than ~565 m^2 ha^{-1} in the southern three FAs. Mixed gravel-cobble increased from less than ~664 m^2 ha^{-1} in the northern FAs to between ~772 and ~879 m^2 ha^{-1} in the southern FAs. Mud was classified only in Northern Southeast Bend FA (~1,005 m^2 ha^{-1}). Combined, macroalgae cover averaged ~573 m^2 ha^{-1} over all FAs combined, but tended to be dominated by a mixture of sparse or dense green macroalgae (most likely *Ulva* spp. and *Enteromorpha* spp. in most areas) covering ~410 m^2 ha^{-1} in all FAs combined. The highest green algae coverage appeared in Northeast Hood Canal (~513 m^2 ha^{-1}) and Northern Southeast Bend of Hood Canal (479 m^2 ha^{-1}). Brown algae (e.g., Laminariales) and other seaweeds (e.g., Fucales) were only present in any abundance in Central Hood Canal (~239 m^2 ha^{-1}), Admiralty Inlet (~145 m^2 ha^{-1}) and Southwest Hood Canal (~186 m^2 ha^{-1}), but were not detected in Northwest Hood Canal. Because most of the kelps in this group only occur at the lowest intertidal elevations, the tide elevation at the time of image acquisition could bias these estimates and also explains why coverage typically is lower than the other algae, which may occur throughout the intertidal zone. The euhaline-mesohaline salt marsh plant *Salicornia virginica* (pickleweed) was only classified from the Northern Southeast Bend of Hood Canal (~117 m^2 ha^{-1}), but that was the only FA in which we had post-image acquisition of applicable training data. We know *Salicornia* occurs in other salt marshes included in the imagery. Oysters covered the greatest intertidal area in Central (~212 m^2 ha^{-1}), Northern Southeast Bend (~239 m^2 ha^{-1}) and Southern Southeast Bend (~365 m^2 ha^{-1}) of Hood Canal but there was no detectable coverage in Admiralty Inlet. There was a tendency for the coverage of oysters to correspond to the coverage of mixed gravel-cobble, which would likely relate to the relative availability of hard substrate attachment sites and the fact that oysters are directly attached to and integrated with the gravel and cobbles.

During the post-classification accuracy assessment, we found good agreement between areas classified as eelgrass and existing eelgrass beds. This also was true for other habitat classes except for the oyster bed cover class. However, our classification failed to accurately distinguish oyster beds from wet sand–gravel–cobble. We attribute the inability of the classification to separate these two habitat classes to the low number of oyster bed training sites. Because mapping oyster beds was not a primary objective of this study, we combined oysters with the gravel-cobble class.

Coincidentally, an independent investigation of eelgrass in a shallow subtidal segment of our study area was completed for a small area around the Hood Canal Bridge in January 2001. In this area, we were able to quantitatively assess the accuracy of our eelgrass classification on a point-by-point basis using a data set collected with a towed underwater video system (Woodruff et al., 2002). The Woodruff et al. study produced a GIS coverage of shallow subtidal eelgrass over a 2 km length of shoreline. For the area where the two datasets overlapped, we compared the video trackline data to the classified CASI imagery by creating a 1.5×1.5 m grid from 1,950 video points. Although we expected seasonal differences and differences in the position of the eelgrass blades (flat at low tide versus upright in the water column at high tide) at the time of each survey, we found very good agreement (>90% of the points identified as eelgrass common to both datasets) in the eelgrass classification where the two studies overlapped.

Although our eelgrass classification matched up well with our knowledge of the study area, sites that were re-visited by field teams, and other available data, we recommend that a more complete and quantitative assessment of classification accuracy be performed.

Summary and Conclusions

Our results illustrate the feasibility of using high spatial and spectral resolution CASI imagery to map extensive regions of intertidal landscapes. Our results can be summarized as follows:

1. Intertidal eelgrass can be accurately identified and distinguished from macroalgae and other cover classes using CASI;

2. CASI can be used to delineate complex intertidal landscapes in the Pacific Northwest at high spatial resolution; and,

3. Eelgrass is a common cover class throughout the intertidal regions of Hood Canal and east Admiralty Inlet, but varies considerably in areal extent and distribution.

During this study we learned the following lessons:

- This study was successful because the image acquisition and analysis team worked closely with estuarine ecologists to select appropriate imagery and spatial analysis techniques.

- Our 1999 pilot study exposed important issues that were addressed in the fully implemented 2000 study. Specifically, the 21-band 1.5 m CASI data collected during the pilot study resulted in extremely long processing times and unsatisfactory outcomes.

- Consideration should be given to the number and arrangement of the GCP in flight lines. We found that increasing the number of GCP would improve spatial accuracy; however, budget and field resources need to be weighed against those improvements.

- We found that digital photographs of the training sites were invaluable to our interpretation of the CASI data. We recommend using a standardized protocol to take and analyze digital photographs.

- Review of CASI data every day following the flights did not eliminate areas of poor image quality; however, our daily review provided us with the opportunity to re-fly critical areas, if necessary.

- Finally, we used CASI data to map intertidal cover classes in relatively linear landscapes. We found that variability in lighting and image quality would require considerably more effort to merge (side-by-side) and classify adjacent flight lines like those shown at the southern tip of Hood Canal in figure 1.

Acknowledgments

We gratefully acknowledge the financial and logistical support of the Point No Point Treaty Council. G. Dockray (our pilot), of ECOTRUST, was a valuable partner in the CASI image acquisition. An incredible cadre of 40-50 individuals, too many to name but all greatly appreciated, contributed immensely to the intensive vegetation training site data gathering and geocontrol point collection. We also thank the following individuals for their valuable consultations and advice: H. Shipman (DOE); H. Berry, P. Dowty, T. Mumford, et al. (DNR); H. Ripley (HDI); T. Labbe; and A.C. Mortimer.

References

Berry, H.D., Sewell, A.T., Wyllie-Echeverria, S., Reeves, B.R., Mumford, T.F., Jr., Skalski, J.R., Zimmerman, R.C., and Archer, J., 2003, Puget Sound submerged vegetation monitoring project: 2000-2002 monitoring report: Nearshore Habitat Program, Washington State Department of Natural Resources, Olympia, WA. 60 p. plus appendixes.

Dowty, P., Reeves, B., Berry, H., Wyllie-Echeverria, S., Mumford, T., Sewell, A., Milos, P., and Wright, R., 2005, Puget Sound submerged vegetation monitoring project, 2003-2004 monitoring report: Washington State Department of Natural Resources, Nearshore Habitat Program, Aquatic Resources Division, Olympia, WA, 95 p.

Dowty, P., Schanz, A., and Berry, H., 2007, Eelgrass Stressor-Response Project 2005-2007 Report: Washington State Department of Natural Resources, Nearshore Habitat Program, Aquatic Resources Division, Olympia, WA, 228 p.

Gaeckle, J., Dowty, P., Reeves, B., Berry, H., Wyllie-Echeverria, S., and Mumford, T., 2007, Submerged Vegetation Monitoring Project 2005 Monitoring Report: Washington State Department of Natural Resources, Nearshore Habitat Program, Aquatic Resources Division, Olympia, WA, 93 p.

Garono, R.J., Simenstad, C.A., Robinson, R., and Ripley, H., 2004, Using high spatial resolution hyperspectral imagery to map intertidal habitat structure in Hood Canal, WA, US: Canadian Journal of Remote Sensing, v. 30, no. 1, p. 54-63.

Phillips, R.C., 1984, The ecology of eelgrass meadows in the Pacific Northwest: a community profile: U.S. Fish and Wildlife Service, Washington, D.C. Biological Services Program FWS/OBS-84/24. 85 p.

Short, F.T., and Burdick, D.M., 1996, Quantifying eelgrass habitat loss in relation to housing development and nitrogen loading in Waquoit Bay, Massachusetts: Estuaries, v. 19, no. 3, p. 730-739.

Simenstad, C.A., Fresh, K.L., and Salo, E.O., 1982, The role of Puget Sound and Washington coastal estuaries in the life history of Pacific salmon: An unappreciated function, in Kennedy, V.S. (ed.), Estuarine Comparisons: Academic Press, New York, p. 343-364.

Simenstad, C.A., and Salo, E.O., 1982, Foraging success as a determinant of estuarine and nearshore carrying capacity of juvenile chum salmon (*Oncorhynchus keta*) in Hood Canal, Washington, *in* Melteff, B.R., and Neve, R.A. (eds.), Proceedings of North Pacific Aqua¬culture Symposium, August 18-27, 1980, Anchorage, Alaska and Newport, Oregon, Alaska: Sea Grant Rep. 82 2, University of Alaska, Fairbanks, AK, p. 21-37.

Simenstad, C.A., 1994, Faunal associations and ecological interactions in seagrass communities of the Pacific Northwest coast. Seagrass science and policy in the Pacific Northwest: proceedings from a seminar series: Wyllie-Echeverria, S., Olson, A.M., and Hershman, M.J., Seattle, U.S. Environmental Protection Agency, SMA 94-1, v. 63.

Simenstad, C.A., Garono, R.J., Labbe, T., Mortimer, A.C., Robinson, R., Weller, C., Todd, S., Toft, J., Burke, J., Finlayson, D., Coyle, J., Logsdon, M., and Russell, C., 2008, Assessment of intertidal eelgrass habitat landscapes for threatened salmon in the Hood Canal and eastern Strait of Juan de Fuca, Washington State: Technical Report 08-01, Point No Point Treaty Council, 7999 N.E. Salish Lane, Kingston, WA 98346, 152 p.

Thom, R.M., and Hallum, L., 1991, Historical changes in the distribution of tidal marshes, eelgrass meadows and kelp forests in Puget Sound *in* Proceedings of Puget Sound Research, 1991: Puget Sound Water Quality Authority, Olympia, Wash., p. 302–313.

Woodruff, D., Borde, A., Williams, G., Southard, J., Thom, R., Simenstad, C., Garono, R., Robinson, R., and Norris, J., 2002, Mapping of subtidal and intertidal habitat resources: Hood Canal Floating Bridge, Washington, Research Project T1803, Task 46, Washington State Department of Transportation, Olympia, WA. 15 p. plus appendixes.

Chapter 9.—Using Remote Sensing to Assess Anthropogenic Influences on Stream Temperature

Mimi D'Iorio[1] and Carol Volk[2]

Abstract

In-stream water temperatures are regulated by a variety of intrinsic and extrinsic environmental variables dictated by the natural and anthropogenic state of a fluvial stream system. To evaluate how landscape scale processes relate to in-stream conditions, this study applies an integrated remote sensing and GIS-based approach to compare *in situ* measured stream-water temperatures with remotely derived proxies for land cover and land use in the John Day basin of east-central Oregon. Preliminary findings suggest that stream temperatures correlate more strongly with landscape variables assessed at the watershed level than at the reach scale, suggesting that instream conditions may be regulated by watershed characteristics present well beyond the traditional riparian corridor. This research lends insight to fish habitat modeling strategies by testing the utility and application of remotely derived landscape variables as proxies for stream habitat function, fish performance, and restoration potential.

Introduction

Rivers and streams flow through landscapes in constant contact with surrounding habitat. The ever changing landscape through which the stream flows is shaped by a plethora of natural and anthropogenic processes. Whether a stream flows in a straight channel through miles of continuous grassland, or it sweeps in a meandering path through intermingled patches of wetlands, urban areas and industrial parks, the relationship between the structure of the stream and the complexity of the landscape through which it flows are linked to the streams potential for rearing and maintaining healthy fish populations. In this conceptual model, the stream integrates landscape information, communicating the complexity of the watershed to fluvial system (see fig. 1). Evaluating the relationships between the landscape and the stream habitat is often confounded by this landscape complexity and the means by which it is traditionally represented in models designed to predict habitat suitability. Critical for relating landscape scale variables to in stream ecological indicators is an understanding of how the landscape communicates with the stream across varying spatial scales.

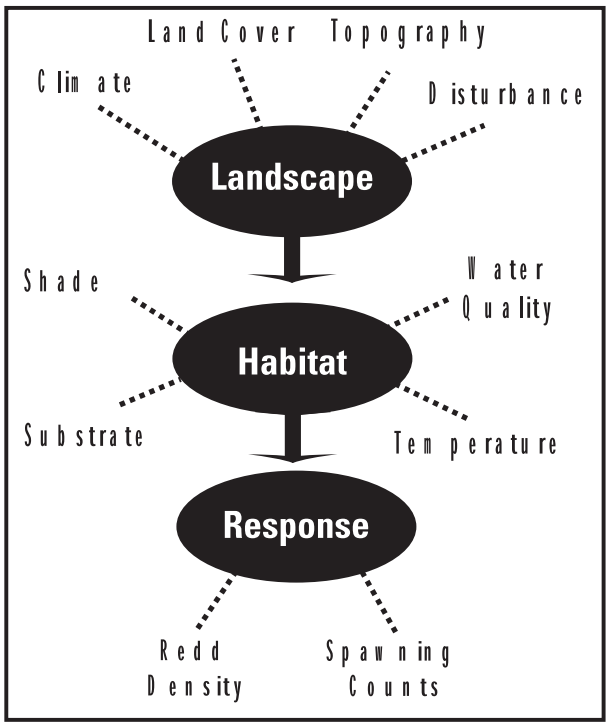

Figure 1. Conceptual model illustrating the connectivity between between parameters used to evaluate landscape, riparian habitat and the suitability (response) of that habitat for fish productivity.

Water temperature has direct and indirect effects on nearly all aspects of stream ecology and function. Changes in riparian vegetation, irrigation water-management practices and channel engineering are all potential human influences on water temperature. Understanding how stream water diversions (e.g., through culverts and irrigation canals), removal of stream buffers (e.g., through riparian clear cut harvests), and decoupling of the stream channel from the floodplain (e.g., through channelization and bank-hardening) relate to measured in-stream water temperatures is important for modeling fish habitat, for developing habitat restoration strategies, and for understanding overall human impacts on stream condition. Most management actions do not adequately consider the myriad environmental processes that drive stream temperature regimes nor do they acknowledge the wide variety of pathways by which human activities may affect stream temperature (Poole and Berman, 2001).

[1]1NOAA Marine Protected Areas Center, 99 Pacific Street Suite 100F, Monterey, CA, 93940, 831-645-2703, mimi.diorio@noaa.gov

[2]NOAA Northwest Fisheries Science Center, Seattle, WA, carol.volk@noaa.gov

We use satellite image-derived measures of vegetation that define the spatial and temporal variability in riparian buffer extent and floodplain wetness in concert with GIS hydrography layers that characterize and define the spatial extent of channel alterations and engineering to apply GIS-based spatial analysis tools to compare in situ measured stream-water temperatures with remotely derived proxies for water withdrawals from irrigation, loss of riparian vegetation from grazing and land use, and alterations to channel complexity. With an integrated remote sensing and GIS-based approach, we evaluate how remotely sensed landscape variables, namely Normalized Difference Vegetation Index and related metrics, correlate with measured in-stream water temperatures in the Middle Fork of the John Day River in east central Oregon (see fig. 2).

This study explores the overall utility of satellite data for deriving landscape variables that can be used to evaluate the impacts of irrigation, clear cutting, wildlife grazing and channel alterations on habitat suitability and restoration efforts. The findings will lend insight to how remote sensing can improve the predictive capabilities of habitat models with regards to stream function, fish performance and restoration potential.

Study Region

This research focuses on the Middle Fork John Day (MFJD) of the John Day River in Grant County of east-central Oregon. Covering more than 500,000 acres, this watershed primarily is publicly owned forest (60%) with the remainder held privately as range and pastureland. Through the mid-1800s, the landscape of the MFJD was a largely untouched wilderness until the 1862 Canyon Creek gold strike brought thousands of placer miners and homesteaders to the region. The basin subsequently underwent various alterations as stream bottoms were cleared and planted to hay or grain, and stream courses were channelized and diverted for irrigation (Oliver, 1962). In the early mid-1900s, the drainage had been further developed for agriculture and more large-scale gold dredging that overturned spawning beds, altered stream configuration, and nearly decimated riparian vegetation. These and other historical and current land-management practices including placer mining, livestock overgrazing, irrigation withdrawals, land clearing, road building, logging and stream canalization have all changed the dynamics of the present day MFJD watershed (Stuart and Williams, 1988). Many of these changes are still evident in the modern landscape,

Figure 2. Map of the John Day subbasin in east-central Oregon, showing the trace of the John Day River and the study region along the Middle Fork (highlighted). Upper right corner schematic shows the basin's geographic location relative to the State border between Washington and Oregon.

rendering riparian habitat degradation the most serious anadromous fish habitat problem in the John Day River basin with approximately 660 degraded stream miles (Columbia River Inter-Tribal Fish Commission, 1995). Specifically, high seasonal water temperatures are commonly considered to be one of the major anadromous limiting factors in the John Day Subbasin (Columbia-Blue Mountain Resource Conservation and Development Area, 2005).

This specific region was chosen for study due to its land-use history, the relatively low impact of urbanization, the availability of remote sensing thermal data, (i.e., thermal infrared), and its potential for salmonid habitat modeling and restoration.

Data

The datasets used in this analysis include remotely sensed spectral satellite data (Landsat 5 Thematic Mapper), airborne thermal infrared imagery (FLIR), and various geospatial anthropogenic datasets collected by the Bureau of Reclamation (see fig. 3). The Landsat 5 Thematic Mapper dataset, captured in September 2000, is used to run a Normalized Difference Vegetation Index (NDVI) for evaluating landscape variability. The NDVI algorithm provides a continuous numerical statistic related to vegetation potential or greenness of each pixel in the image and is derived from the values of the red and near infrared spectral bands of the satellite data. With this algorithm, each pixel within the watershed is attributed with a value that represents its potential to be green, healthy vegetation, as represented on a scale from 0 (low) to 200 (high). For this study, the NDVI metric is the primary landscape scale variable representing the state of the surrounding watershed at various spatial scales.

The FLIR thermal data were employed as the response variable representing in-stream temperature and its variability within the stream channel. The airborne thermal infrared (TIR) surveys were flown by Watershed Sciences, Inc. of Corvallis, Oregon, in August 2004 and were subsequently provided for this study as processed GIS point data. The continuous raw data images were sampled by querying pixel temperature values from the center of the stream channel and then calculating and exporting the median value of a 10-point sample of adjacent pixels. Note that each pixel covers approximately 812 m^2 in area and represents 28.5 m in distance from the stream channel. The temperatures of detectable surface inflows (i.e., surface springs, tributaries) also were sampled at their mouth. The resulting data layer followed the trend of the stream channel yielding point temperature summary statistics for the 10 pixels analyzed.

Additional data used in this research included geospatial information related to anthropogenic alterations to stream dynamics, including stream diversions, pumps, and water rights withdrawal sites. These data were collected by the Bureau of Reclamation (Pacific Northwest region) through the interpretation of high resolution aerial imagery and review of historical records. Point locations for these features were incorporated into the GIS and used to explore potential spatial relationships with in stream temperature patterns.

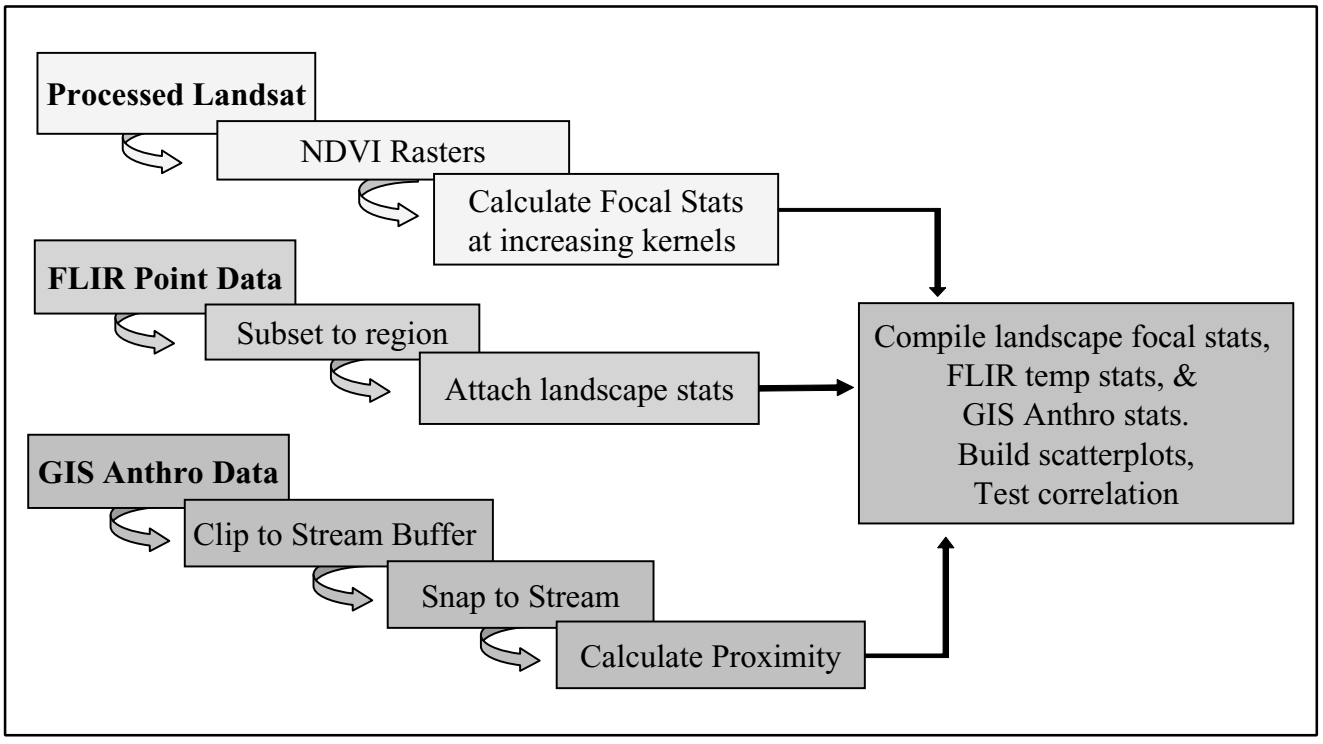

Figure 3. Workflow for processing the three main datasets used in this study. Each dataset was processed separately and then spatially joined for pair-wise regression.

Methods

The three above described datasets were processed and analyzed to explore the role that spatial scale plays in driving in stream habitat conditions, namely temperature. We first calculate summary statistics (maximum, minimum, standard deviation, median, average) on the NDVI data at varying spatial extents across the surrounding watershed. Using this approach, every stream pixel is attributed with watershed scale information through a GIS-based focal algorithm that calculates and associates surrounding landscape metrics to the stream pixel based on a user-defined kernel or analysis window (see fig. 4). A kernel is defined as a moving analysis window whose center pixel is attributed depending on the metric being analyzed (in this case NDVI values). The smallest kernel calculated metrics for a 3×3 pixel window to evaluate the landscape variables at a radius of 1 pixel around the stream channel on all sides. The stream channel itself was converted to null prior to running the model to exclude the water-based spectral signatures from the analysis. The kernel size was then increased incrementally up to a 19×19 pixel window.

The attributed stream pixels that were coincident with FLIR temperature data points were then extracted from the data layer and further attributed with the associated FLIR temperature data value. Pair-wise regression was then calculated between the landscape statistics and the temperature values to test how they co-vary as kernel size is increased.

The GIS point locations for water withdrawals and diversions was similarly processed to test against the in-stream temperature patterns. The point data were first subset to the area within 1,000 m from the centerline of the stream channel. Upstream distance and direction was calculated and attributed to each withdrawal point feature before it was spatially joined to the nearest downstream FLIR data point. Each FLIR data point that was linked to a withdrawal location was then extracted and used to run pair-wise regression between its standard deviation in temperature (from adjacent pixels) and the distance upstream of the water withdrawal/structure feature.

Results

The initial results from this study suggest that the condition of the landscape upland from the riparian corridor does indeed relate to measured in-stream water temperatures. The strength of the relationship between the in-stream temperature and the landscape variables (specifically the NDVI) appears to increase with kernel size (see fig. 5). That is, correlation appears to be strongest between landscapes evaluated at larger kernels (19×19), which capture more of the surrounding watershed composition and variability than kernels that simply evaluate the near-stream adjacent pixels of the riparian corridor. This preliminary conclusion implies that

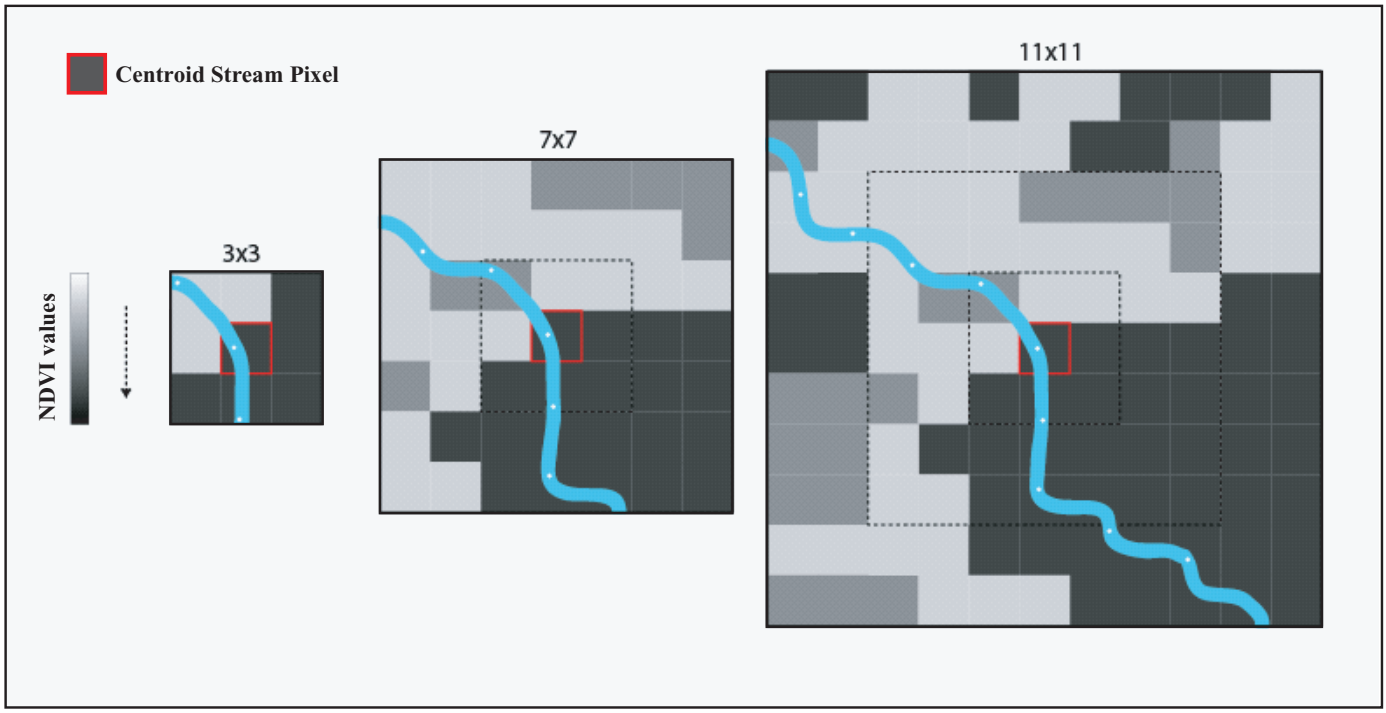

Figure 4. Schematic diagram illustrating a sample of the kernel analysis used in this study. The centroid stream pixel (outlined in red) is attributed with values that represent the statistics of NDVI for all the surrounding pixels in the kernel window. As the kernel size increases, more pixels are evaluated in the analysis and the resulting values represent a larger extent of the watershed.

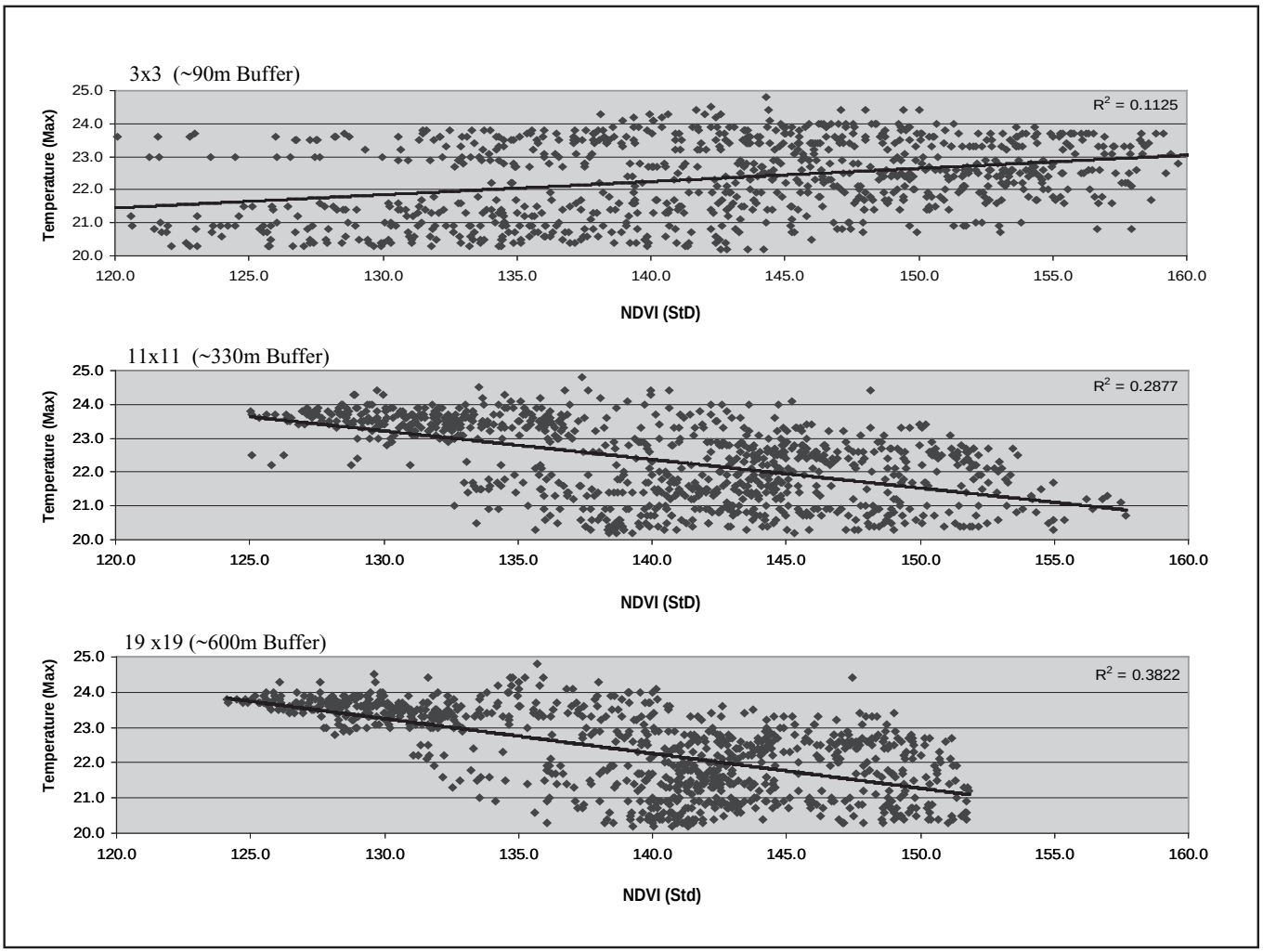

Figure 5. Results of pair-wise regression for kernel analysis showing the standard deviation in NDVI in NDVI pixels against the maximum temperature value for each pixel. Note how the coefficient of determination (r-squared) increases with increasing kernel size, indicating that the regression equation explains more of the variance in temperature as the kernel is increased.

the traditional riparian corridor setbacks designed to mitigate anthropogenic impacts on fluvial systems may be too narrow to adequately buffer streams from these external influences.

The proximity of water withdrawals, pumps, and diversion structures to the stream channel also appears to show correlation to in-stream water temperature (see fig. 6). Subsampling the original data to within 1 km of the stream channel, found there are 65 structures near or adjacent to the stream at varying distances. When spatially joined to the nearest downstream temperature data point, the scatterplot of the distance versus recorded temperatures indicate that the closer the structures are to the channel, the higher the standard deviation of the recorded in-stream water temperatures. These initial results suggest that notable downstream fluctuations in water temperatures may be linked to the presence of water withdrawal and other anthropogenic structures present near the stream channel.

Conclusions

This study has shown that there is value in utilizing landscape scale satellite imagery for assessing the role of watershed conditions with respect to in stream habitat conditions. The availability of reliable GIS and remote sensing data regarding the presence and location of near stream structures, and other anthropogenic alterations to the landscape can even further the potential for modeling stream habitat and understanding the role that humans play in regulating the availability of suitable fish habitat. In summary, this study has shown that:

- Streams respond to the landscape beyond the traditionally recognized narrow riparian buffer;
- Vegetation metrics derived at the landscape level can be correlated with habitat conditions measured in the stream, specifically temperature;

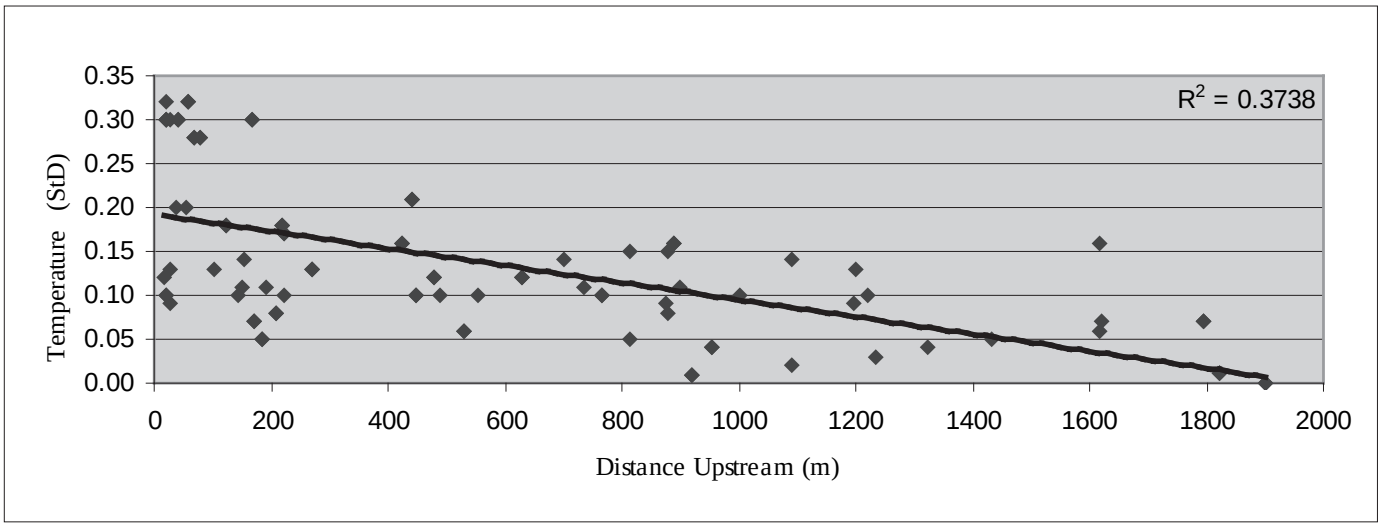

Figure 6. Preliminary pair-wise correlation results for geospatial analysis of water diversion, withdrawal and pump data as they relate to in-stream temperature. Nearly 38% of the variance in downstream water temperatures can be explained by the presence and proximity of a water diversion, pump or withdrawal structure.

- Watershed land use and disturbance plays an important role in driving local stream habitat conditions;
- Water rights and stream diversions impact local temperature regimes, however to what extent is unclear;
- Accurate mapping of the locations of these diversions will assist in more accurate modeling of local temperature fluctuations.

The initial findings of this research are preliminary and will continue to be verified and expanded upon to include other remote sensing data (e.g., Advanced Spaceborne Thermal Emission and Reflection Radiometer), additional stream channel alteration information, ground truth validation, correlation outlier analysis, and multivariate regression. However, these results in their present form do lend valuable consideration to how remote sensing can be applied to inform watershed management and stream habitat restoration strategies.

Acknowledgments

This study has been a collaborative effort between the Pacific Northwest Region of the Bureau of Reclamation and NOAA's Northwest Fisheries Science Center. We especially thank Michael Beaty, Michael Newsom, and Kristin Swoboda of BOR and Chris Jordan, Blake Feist, and Steve Rentmeester of the NWFSC. Thanks to Watershed Sciences, Inc. and specifically Russ Faux for the FLIR data and related technical support.

References

Poole, G.C., and Berman, C. H., 2001, An ecological perspective on instream temperature: Natural heat dynamics and mechanisms of human-caused thermal degradation: Environmental Management 27, p. 787–802.

Columbia-Blue Mountain Resource Conservation and Development Area, 2005, John Day Subbasin Plan: Prepared for the Northwest Power Conservation Council, Portland, OR.

Columbia River Inter-Tribal Fish Commission, 1995, Wy-Kan-Ush-Mi-Wa-Kish-Wit Spirit of the Salmon: Columbia River Anadromous Fish Plan of the Nez Perce, Umatilla, Warm Springs and Yakima Tribes. Portland, Oregon.

Oliver, H., 1962, Gold and cattle country, Portland, Oregon: Binfords and Mort, 312 p.

Stuart, A., and Williams, S.H., 1988, John Day River Basin Fish Habitat Improvement Implementation Plan: BPA Project Number 84-21, Bonneville Power Administration, Portland, Oregon.

Chapter 10.—Modeling Watershed Condition and Trend—How the Aquatic Riparian Effectiveness Monitoring Program (AREMP) is Evaluating Watershed Condition and Trend in the Pacific Northwest

Peter Eldred[1] and Kirsten Gallo[1]

The Aquatic and Riparian Effectiveness Monitoring Program (AREMP) is a multi-Federal agency program developed to assess the effectiveness of the Northwest Forest Plan (NWFP) in maintaining or restoring the condition of watersheds in the NWFP area. The NWFP encompasses the range of northern spotted owl habitat, about 58 million acres in western Washington, western Oregon, and northwest California. AREMP's goal is to evaluate the status and trend of watershed condition at the 6th-field subwatershed scale. To do this, a random sample of 250 subwatersheds was selected from 1,400 subwatersheds that have at least 25% Federal ownership along the stream channels. About 30 subwatersheds a year are visited to collect field data from 4 to 8 randomly selected stream reaches in each subwatershed. GIS and remotely sensed data are used to evaluate the upslope and riparian condition in the 250 sample subwatersheds, along with field data where available. This information was aggregated with a decision-support model to produce a watershed condition score for each subwatershed. The watershed condition was evaluated at time 1 (1994) and time 2 (2004) to assess trends. The results of the status and trend for the first 10 years was published in 2004. The program is now evaluating the trend and condition for the next 5-year period for a report update. This paper gives an overview of the analysis process and how the program is evolving.

Watershed condition and trend is evaluated using decision-support models. Decision-support models document decision processes and allow the same process to be applied consistently across time and space. The models developed by the monitoring program are used to evaluate whether the subwatersheds are in good condition, meaning the physical and biological processes are intact to create and maintain salmonid habitat. Decision support models work by evaluating individual attributes (such as road density) and calculating an evaluation score for each attribute that ranges between -1 and 1, with -1 being poor and 1 being good. The model then aggregates the evaluation scores of all attributes into a single watershed condition score. To account for the ecological diversity within the NWFP area, a decision-support model was constructed for each of the seven different physiographic provinces. The models were built in workshops attended by local agency professionals. Lacking onsite instream measurements, surrogates for watershed condition must be used, such as number of road and stream crossings. The workshops consisted of an informal group process through which participants came to consensus on how the model evaluated individual attributes and aggregated the scores of individual attributes. Each attribute has a "fuzzy curve" associated with it. The curve defines the values at which the attribute scores a 1 or a -1 and the shape of the transition between the two scores. The transition may be abrupt, such as water temperature reaching a lethal threshold, or gradual as the density of roads increase the habitat score gradually decreases. Following the workshops, models were constructed and run, and the results returned to the workshop participants. Participants compared the model results with their knowledge of the condition of watersheds and suggested refinements to the model as necessary.

Some of the watershed parameters evaluated in the model are road and stream crossings, road densities inside riparian areas, road miles by slope position, miles of road on unstable slopes, percentage of large conifers in riparian areas, percent of urban and agricultural areas, and area by fire condition class. These parameters rely on GIS data. The GIS layers for streams, roads, and vegetation did not exist in a continuous uniform layer for the Forest Plan area. Continuous layers were assembled from various sources. Compiling data from multiple agencies and sources is problematic because data standards (and therefore data layers) are not consistent between agencies. Available data for private lands generally are at a lower resolution than data for public lands. A Pacific Northwest hydrography framework layer exists for Oregon

[1]USDA Forest Service, Aquatic and Riparian Effectiveness Monitoring Program, Corvallis, Oregon.

and Washington, but stream density on the layer varies greatly across ownerships, with a wide range of standards and mapping intensities being used. For vegetation, the interagency vegetation mapping project (IVMP) layer was used. This is a uniform layer for the Oregon and Washington portion of the NWFP area developed from Landsat satellite imagery. For California, a vegetation layer derived from a combination of Landsat imagery and aerial photograph interpreted polygons was developed (CALVEG). BLM, Forest service, and USGS map data (DLGs) were used for the GIS road layer. The GIS parameters were used with in-channel physical, chemical, and biological data where they were available in the decision-support models.

The watershed status and trend evaluation is expanding from the original sample of 250 to all 1,400 6th-field subwatersheds with at least 25% Federal ownership in the NWFP area. Because of the high cost of field visits and the large extent of the project area, the program is only able to visit a very small number of subwatersheds each year. So far about 170 subwatersheds have been visited since 2002. To determine the status and trend of all subwatersheds, the program will be relying on GIS and remotely sensed data. A new vegetation layer, the Interagency Mapping and Assessment Project (IMAP), is being developed from Landsat imagery. IMAP uses the Gradient Nearest Neighbor method to assign plot information to every pixel. IMAP rasters will be created for they entire NWFP area for 1994 and 2006. This method provides a wide range of vegetation attributes in a 30-m grid. Consequently, we can use more detailed information in evaluating vegetation and compare current attribute levels with the historic range of variability. Change detection overlays will be created by looking at all intervening years instead of just comparing 2 years as was done in the past. This creates a complex series of changes that can be thought of as a life history of a pixel. Subtle changes can be picked up with more confidence, and variation due to clouds and shadows become less important. The resulting change layer will have attributes not just for whether a pixel has experienced a stand replacing event, but also for how it is recovering and subtle changes such a thinning can be picked up.

A landslide model developed by Dan Miller calculates landslide susceptibility for each pixel of a watershed area using topography derived from DEMs, vegetation, and roads. To develop the parameters for the landslide model, landslides digitized from aerial photographs in 14 watersheds were combined with field data. Landslide polygons were overlaid with topography, vegetation, and road buffers to determine how these three factors influenced the occurrence of landslides. Because of the small sample size, it was not possible to tease out different parameters for different regions, so one parameter file is used for the whole NWFP area. Three rasters are created, the landslide susceptibility just for the topography, topography and vegetation, and landslide susceptibility with topography vegetation and roads. The effect of vegetation is portrayed by multiplying the landslide grid for topography by 0.5 for DBH greater than 4 in. and 1.48 for DBH less than 4 in.. The effects of roads can be overlaid on top of the vegetation and topography by multiplying landslide susceptibility within 100 m of a road by 2.73.

One way of addressing the problem of inconsistent stream mapping is to develop a new stream layer base on 10-m DEMs. This would provide a more consistent stream layer and allow the mapping of stream intrinsic potential based on topography and streamflow. Intrinsic potential is a measure of a stream's capacity to provide high-quality habitat for salmonids based on channel gradient, valley constraint, and mean annual discharge. Having streams that match the DEMs allows the calculation of catchment size for stream reaches (required to model mean annual discharge) and stream gradient. We would like to combine this information in future watershed condition assessment to evaluate how much of high-quality habitat may be blocked by barriers.

We are currently rebuilding all our decision-support models and adding new attributes. This will allow us to take advantage of new information that has become available and incorporate the opinions of a new group of workshop participants. The more the program relies on GIS and remotely sensed data, the more important the quality of these data becomes. Acquiring and updating quality data for such a large area has always been a problem. The DEMs that are currently available were interpreted off old USGS topography maps. Looking to the future, the program would like to improve the quality of the data used. LIDAR is potentially a source of vastly improved DEMs that could be used for determining stream channels, streamflow, stream gradient, and topography. Improved topography will improve our landslide model and improved stream information will increase the quality of many of our decision-support model parameters for evaluating watershed condition. The size of our study area has made LIDAR data cost prohibitive, but hopefully through cooperation and increased usage of LIDAR, it will be possible to have complete coverage in the near future. LIDAR or some other remotely sensed imagery may be used to improve our road layer, especially on private land. As our program relies more on remotely sensed data, we will have to strive to remain aware of new technologies as they become available.

Chapter 11.—Projecting Watershed Condition with Interagency Mapping and Assessment Project (IMAP) Vegetation Data and Landscape Models

Melinda Moeur[1], Janet Ohmann[2], Miles Hemstrom[3], Theresa Burcsu[3], and James Merzenich[1]

Abstract

The Interagency Mapping and Assessment Project (IMAP) is a collaboration between Federal, State, and non-government partners in Washington and Oregon to build a collection of landscape-level data and state-and-transition models for conducting mid-scale assessments (5th-field hydrologic code watersheds and larger). IMAP data and models can be used for analyzing resource decisions and their effects on important regional programs like forest health and restoration, watershed condition, species' habitats, and long-term timber supply. The state-and-transition models are initialized with current vegetation data developed from Landsat ETM satellite imagery and other spatial data. Output from the landscape models provides a means for comparing likely outcomes of alternative management strategies and disturbance regimes on forested landscapes over time horizons from one to several centuries. In this paper, we provide an overview of the IMAP program and refer the reader to original publications for additional detail. We also present examples of IMAP data and models for assessing the vegetation component of watershed condition.

Introduction

The diverse landscapes of the Pacific Northwest are managed by different owners for different objectives. However, certain key forest management questions shared by all owners include managing fire risk, wildlife habitats, old-growth forest ecosystems, rangeland conditions, supply and demand of forest products, biomass supplies and carbon budgets, and others. State and Federal agencies in Washington and Oregon are currently conducting assessments and updating forest plans. For example, Oregon Department of Forestry (ODF) plans to publish a state-wide assessment of forest conditions in 2010, and to evaluate various policy scenarios and their implications for indicators of forest sustainability, timber supply and demand, conversion of wildland forest to residential use, and water quality (http://www.oregon.gov/ODF/RESOURCE_PLANNING/Sustainable_Forest_Indicators_Project.shtml). On National Forest lands, long-term planning strategies are being focused on opportunities for improving forest health through active management in the face of increasing fire risk and insect and disease damage. Effects of management practices also are being focused on for old-growth forests, habitat for northern spotted owls, marbled murrelets, and aquatic habitat quality—monitoring of these elements is a legal requirement under the Northwest Forest Plan for lands in the range of the spotted owl.

Policymakers and the managers who implement policy objectives need tools to both evaluate alternatives and to display potential outcomes, while accurately accounting for the wide variety of values people expect from both public and private lands. The most helpful tools are easy to use and provide a robust representation of the social, economic, and environmental implications of vegetative succession, management, and natural disturbances. The Interagency Mapping and Assessment Project (IMAP) is a multi-partner collaborative effort to develop consistent vegetation data, models, and analytical tools for conducting landscape-scale mapping and projections useful for assessing current and future landscape conditions. The objective is to enhance the capability of land managers and policymakers to understand likely outcomes of future management and disturbance scenarios, for the purpose of comparing the effects of alternative policy regimes and prioritizing treatment opportunities.

The purpose of this paper is to provide an overview of the IMAP project—its organization and objectives; the vegetation data—how it is developed and applied by IMAP, and how it can be acquired for use; and to show examples of the IMAP models and data for landscape-scale watershed assessment. The reader who wants additional IMAP design details should refer to the original sources referenced throughout this paper.

[1] USDA Forest Service, Pacific Northwest Region, Portland, Oregon

[2] USDA Forest Service, Pacific Northwest Research Station, Corvallis, Oregon

[3] USDA Forest Service, Pacific Northwest Research Station, Portland, Oregon.

IMAP Organization and Objectives

IMAP is a program for building integrated datasets, models, and tools for conducting landscape-scale assessment, monitoring, and planning in the Pacific Northwest Region, supported by current vegetation maps and associated spatial data. The IMAP project is being implemented in Oregon and Washington. The project is led by the USDA Forest Service Pacific Northwest Research Station (PNW), and at present includes as partners USDA Forest Service Region 6 (R6), Oregon Department of Forestry (ODF), Washington Department of Natural Resources (WDNR), USDI Bureau of Land Management (BLM), Oregon Department of Fish and Wildlife (ODFW), and The Nature Conservancy (TNC).

The concept of an interagency partnership was born from a need to foster cooperation on important landscape management issues affecting different agency entities and landowners at different scales. Ideally, planning efforts on lands with a variety of management objectives would all share a common collection of landscape data and models, to help ensure comparable answers to common resource questions. For virtually all landowners, a singular resource perspective is no longer suitable (Barbour et al., 2007a). The IMAP vision is to provide data and models capable of representing a variety of important management and policy scenarios, with sensitivity to both current and potential disturbance agents. The ability to model changes in regional fire risk under climatic warming scenarios, with attendant impacts on timber supply and carbon emissions is an example. Furthermore, a landscape perspective recognizes that regardless of which entity is conducting resource planning, analyses need to be landscape-level, multi-resource, and multi-owner in nature (Lettman and Hemstrom, 2008).

Landscape Modeling Approach

IMAP is designed for mid- to broad-scale assessment (individual 5th-field hydrologic code watersheds and larger). It uses wall-to-wall current vegetation data to populate an initial landscape, from which projections of future landscape conditions are made.

IMAP uses a state-and-transition modeling approach for projecting the effects of disturbance and management on landscape vegetation dynamics. This model type treats vegetation as combinations of broad cover types and seral states linked together by transition pathways resulting from natural disturbances, management actions, or growth and development. State and transition models are fairly easy to understand and use, are applicable at multiple spatial scales, and provide a reasonable representation of vegetative dynamics and responses to management and disturbance.

We use the Vegetation Dynamics Development Tool (VDDT) developed by ESSA Technologies (Beukema and Kurz, 1995; ESSA Technologies Ltd., 2005) to project how forest vegetation transitions between states in reaction to management and disturbance. A VDDT model simulates the probability of each acre being affected by natural succession or disturbance, moving each acre between linked states. The vegetation cover type/structure state classes, pathways describing movement between states, and transition probabilities (the stochastic frequency with which movement between states occurs in the model) are parameters established through expert knowledge and empirical data and models. Movements between states result either from changes due to successional dynamics such as regeneration, growth, and competition, or changes driven by disturbances—human management such as harvest activities and land use conversion, or natural disturbances such as wildfire and insect attack. Model projections are performed in a Monte Carlo environment for evaluating, displaying, and comparing outcomes on the landscape due to alternative management and disturbance scenarios.

Vegetation Data

For modeling purposes, a landscape is divided into environmental strata called potential vegetation types (PVTs) that describe particular combinations of environment, disturbance agents, and growth potential (Hemstrom et al., 2007). A VDDT model is designed for each single PVT within a study region (example, table 1).

Using a map of existing vegetation, the landscape to be modeled is initialized by assigning each acre within a PVT into state classes defined by cover type (defined by dominant tree species) and structural stage (defined by the average diameter of the dominant tree canopy, percentage canopy coverage, and whether single- or multi-storied) (table 2). In IMAP, consistent vegetation data are created using Gradient Nearest Neighbor (GNN) imputation. GNN uses tree-level data collected on Forest Inventory and Analysis (Forest Inventory and Analysis Program, 2006) and Current

Table 1. An example of the set of VDDT models defined by potential vegetation type. This one is in the 14-million acre Blue Mountains project area of northeastern Oregon.

Potential vegetation type	Predominant cover types
Xeric ponderosa pine	ponderosa pine; western juniper
Dry ponderosa pine	ponderosa pine
Dry Douglas-fir	ponderosa pine; Douglas-fir
Dry grand fir	ponderosa pine; Douglas-fir/grand fir
Cool moist mixed conifer	Douglas-fir; grand fir/Engelmann spruce; western larch/lodgepole pine
Cold dry mixed conifer	grand fir; Engelmann spruce/subalpine fir; lodgepole pine/western larch
Whitebark pine	whitebark pine

Table 2. Standard structure classes that along with disturbance history, define states in the IMAP VDDT models.

Tree size (DBH—inches)	Class description
1.0 to 4.99	Young tree
5.0 to 9.99	Pole tree
10.0 to 14.99	Small tree
15.0 to 19.99	Medium tree
20.0 to 29.99	Large tree
30.0 and larger	Giant tree
Canopy closure (percent)	**Class description**
0 to 9.9	Non-stocked
10 to 39.9	Open
40 to 69.9	Medium
70 to 100	Closed
Canopy Layers	**Class description**
1	Simple
2 or more	Multiple

Vegetation Survey (Max et al., 1996) inventory plots on forested lands, coupled with satellite imagery and other spatial data to populate 30-m raster maps with plot data (Ohmann and Gregory, 2002). The resulting vegetation map, along with other spatial layers used to stratify the study region by ownership and land allocation, define the initial conditions that assign acres to state classes for VDDT modeling.

Component processes of a GNN model are as follows (fig. 1).

1. Vegetation data in the form of live tree lists by species, heights, and diameters, snags, logs, understory, and fuels collected in the field on regional inventory plots.

2. The plot data are coupled with spatial data from remotely sensed and other sources. Along with Landsat ETM spectral bands and transformations, environmental and disturbance gradients used as explanatory variables include precipitation and temperature means and seasonality from climate models, ownership, geology and soils maps, and topographical attributes—slope, aspect, and elevation. At present, GNN vegetation maps are complete for Washington and Oregon using Landsat imagery from 2000 to 2001.

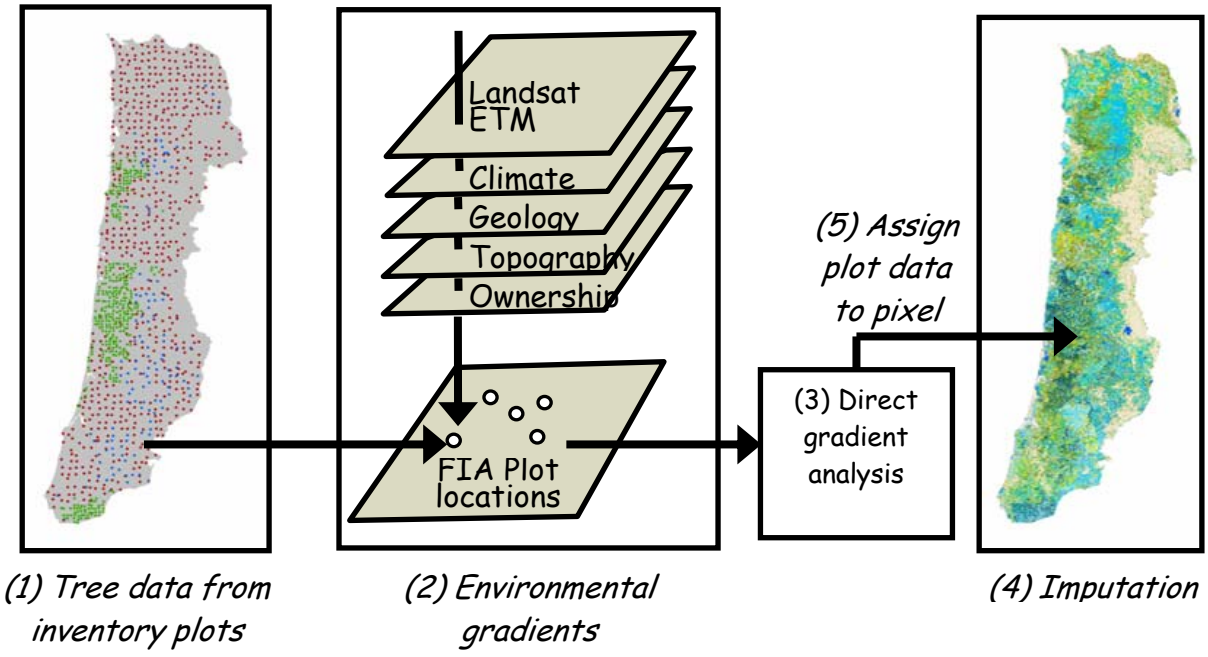

Figure 1. Overview of Gradient Nearest Neighbor (GNN) imputation approach. See text for number explanations.

3. A statistical procedure—direct gradient analysis—correlates the plot and spatial data to fit a model in multivariate gradient space.

4. For every individual 30-m pixel, the gradient model is used to identify the unique field plot that is the best "match", given its combination of explanatory attributes. This plot is assigned, or "imputed," to the pixel.

5. All vegetation attributes of the plot are then assigned to the pixel. The end result is a map where each pixel is attributed with all vegetation measures collected on its matching field plot.

Because all field data from the inventory plot is assigned to the pixel, the resulting map data are rich in vegetation attributes. The pixel data can be summarized spatially and thematically to meet various analysis needs. Data joined to each pixel can be any value that can be computed or summarized from the plot data. Many attributes are stored as core values in a GNN pixel attribute table accompanying the vegetation map. Others attributes can be computed by the user from tree data in the plot database. Examples include basal area, trees per acre, percent cover, species composition, large woody debris pieces and volume per acre, indicator species presence, and many others. All GNN data are accompanied by accuracy assessments conducted at the pixel, plot, and landscape scales, and intended to guide the end user toward appropriate use of the data.

For modeling purposes in IMAP, the 30-m existing vegetation pixels are aggregated upward to watershed units (5th-field hydrologic code, units averaging about 100,000 acres). Within watersheds, strata are developed using owner/land allocation spatial data. This stratification is useful for defining and modeling different management goals. Examples are timber-suitable Federal lands, Federal wilderness or species habitat reserves, and private industrial lands managed for intensive wood production. Summarizing the acres and outputs for these owner/allocation strata within 5th-filed watersheds generates useful information about the spatial distribution of landscape characteristics, without implying pixel or stand-level accuracy. This is necessary because IMAP vegetation data are simply not sufficiently accurate at the scale of individual 30-m pixels for most analyses.

Example 1: Examining Landscape Response to Active Fuel Treatment in Central Oregon

In an IMAP analysis, the regional landscape is divided into local geographic project areas that roughly represent physiographic provinces or ecoregions. After initializing the vegetation state classes for the project area landscape, and parameterizing the state-and-transition model for the potential vegetation type, we then simulate vegetation development over one or more centuries for comparing likely outcomes of alternative management and disturbance scenarios.

IMAP data and models have been used to examine the ecological consequences of thinning and prescribed fire on reducing the risk of large, severe wildfires in eastern Oregon (Wales et al., 2007). In a similar example in the 3.8 million acre Central Oregon Landscape Analysis (COLA), public workshops were held to develop modeling scenarios that reflect current management, as well as alternative scenarios testing various levels of active fuels treatments to move Federal forests towards historical conditions, in which single-story, old-growth forests were more prevalent than at present. The proposed treatment regime included periodic reduction of stocking by pre-commercial and commercial thinning, and regular prescribed fire. Treatment objective was to reduce vertical canopy structure and understory fuels while retaining large diameter trees. For the active fuels treatment compared with no treatment scenarios, we plotted the projected proportion of open-canopied stands dominated by large trees on the landscape, as well as timber harvest levels, and susceptibility to catastrophic wildfire (Hemstrom and Merzenich, 2006).

There are 36 HUC5 watersheds within four subbasins in COLA (fig. 2). We simulated each treatment scenario with 30 Monte Carlo simulations over 300 years, and then examined the results for the area as a whole, and for three of the individual watersheds. Under active fuels treatment, HUC 206 developed the largest percentage of area in old-growth forest having an open canopy (fig. 2). HUC 307 had much more area in medium and dense canopy, and very little open-canopy, large forest. H101 was intermediate between the other two. This example is used to help the reader envision how simulation results like these might be used to guide treatment priorities across watersheds. Forest managers also might be interested in overall differences in key attributes for the entire modeled landscape—for example, proportion of the landscape by forest condition (fig. 3a), potential timber harvest levels (fig. 3b), and potential fire risk reduction (fig. 4).

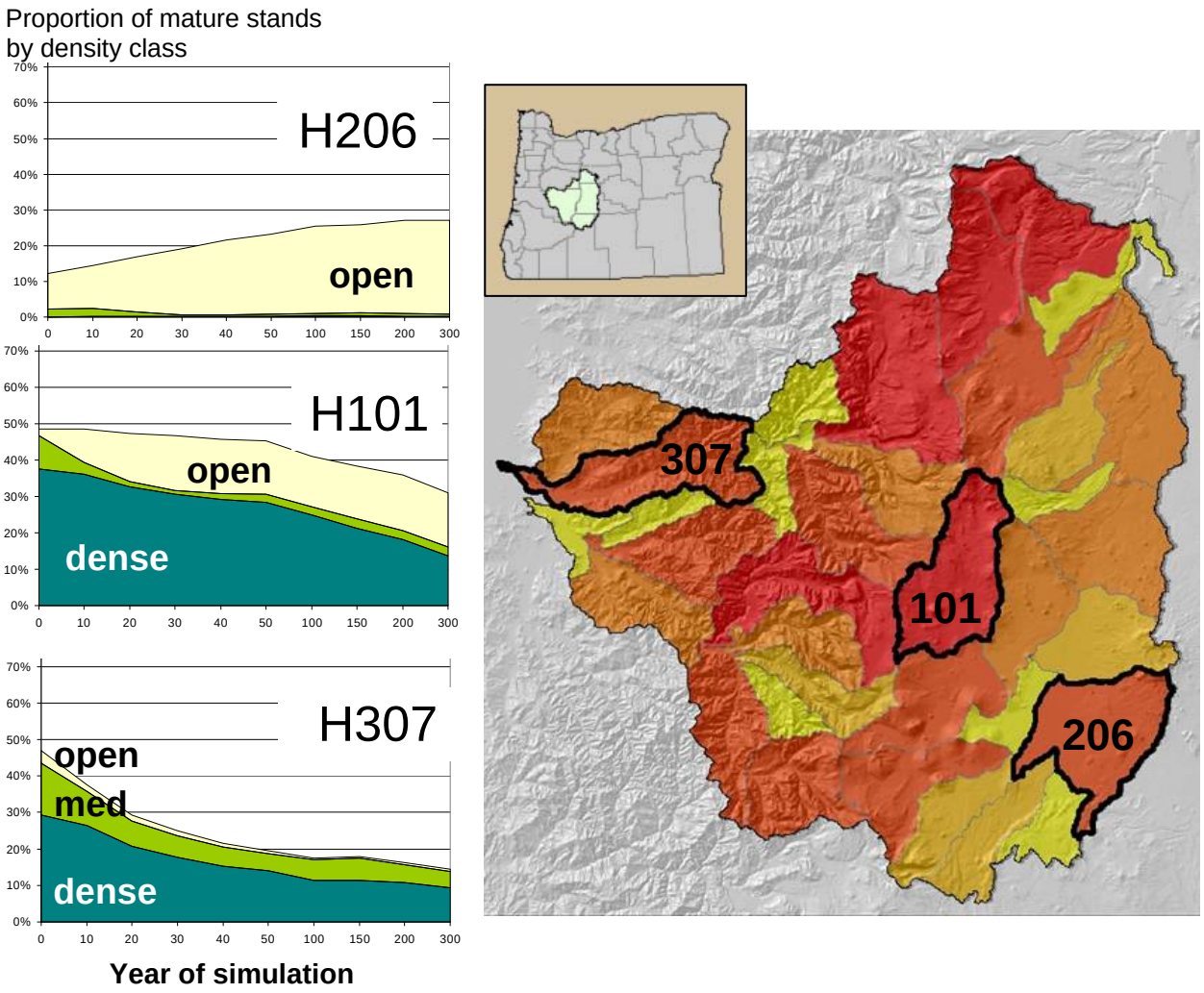

Figure 2. Simulation results for three watersheds in COLA of an active fuels treatment scenario. Shown is the proportion of mature stands in open (< 40% canopy cover), medium (40–70%), and closed (>70%) density classes after 300 years of simulated development and 30 random sequences of fire year intensity.

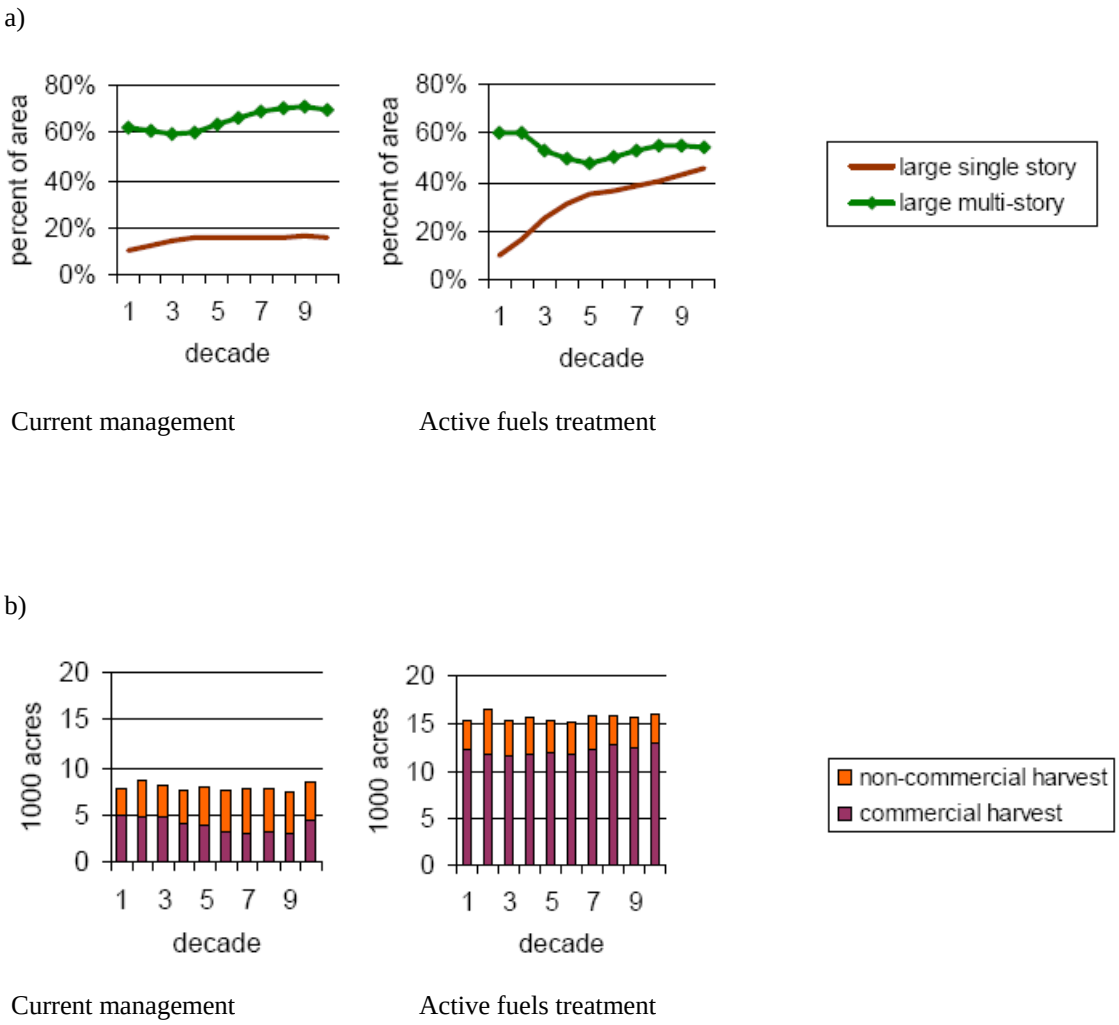

Figure 3. Summary results for COLA current management vs. an active fuels treatment scenario outlined in the text as Example 1. a) Percent of the COLA landscape occupied by single-storied and multi-storied old forest. b) Acres of timber harvested.

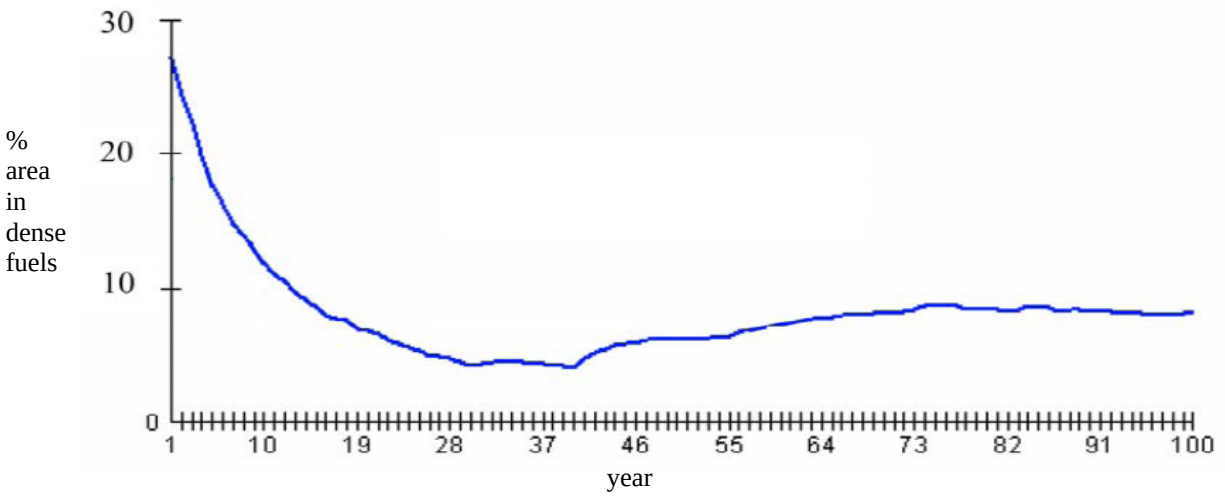

Figure 4. Change in dense fuels over time with aggressive fuel treatment. Based on simulation results for COLA study.

Example 2: Estimating Amounts and Distribution of Large Woody Debris

Large woody debris data are standard inventory attributes collected on FIA and CVS inventory plots and stored as core attributes of the GNN pixel database. In this example from the Oregon Coast Range, Ohmann et al. (2007) used the current vegetation data to summarize the amount of large woody debris by 5th-field HUC. They found that the distributions of large woody debris in this landscape were strongly correlated with disturbance history and ownership patterns, and only weakly with environmental gradients such as climate. Snag volume was most abundant in older forests, and diminished in young managed forests (fig. 5). Furthermore, although down wood volume was persistent in all age classes, log volume was highest in the oldest forests. The GNN vegetation data supported an assumption of increasing snag and log densities as seral condition moves from youngest to oldest forest.

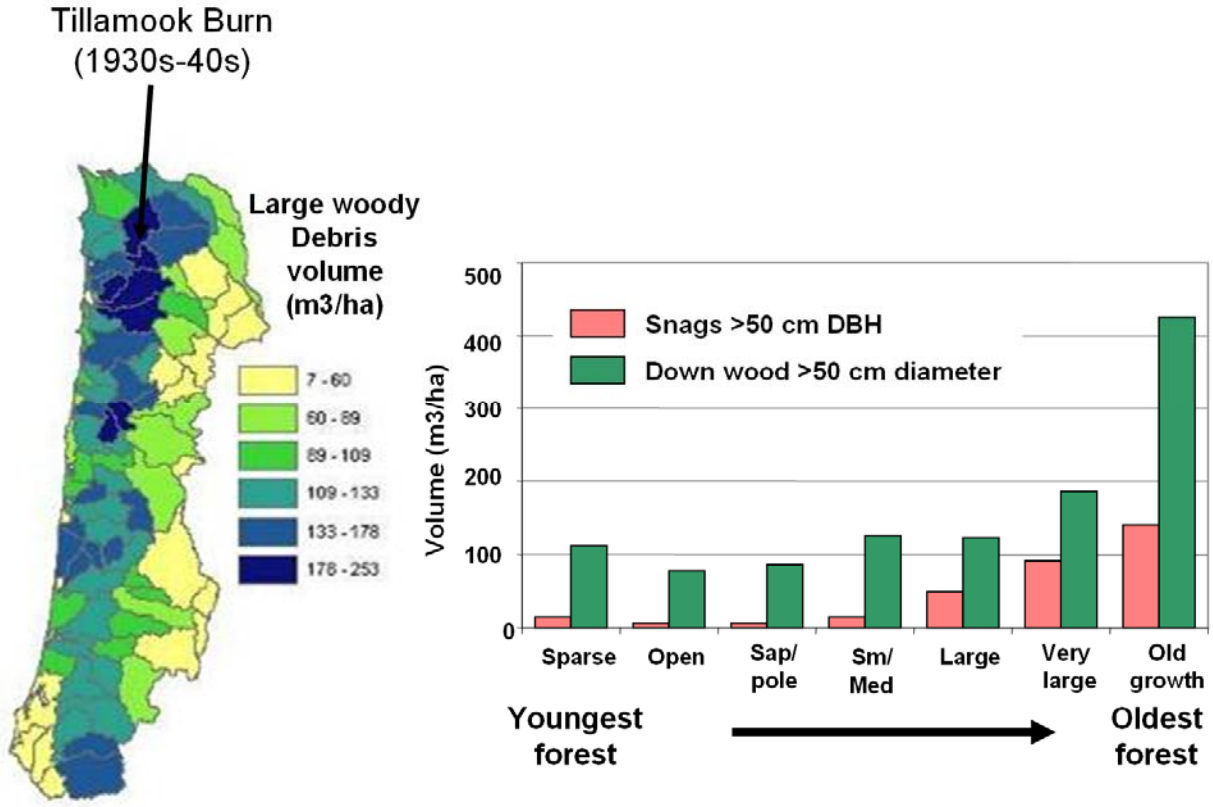

Figure 5. (left) Volume of large woody debris in the Oregon Coast range, by HUC5 watershed. (right) Large woody debris volume by forest age and structure.

Additional IMAP Examples from Published Literature

Wondzell et al. (2007b) used the IMAP state and transition model approach to evaluate the effects of disturbance and management on channel morphology and riparian vegetation in the Grand Ronde River basin in eastern Oregon. Their results linked declines in habitat quality for Pacific salmonids with degradation in riparian vegetation and channel conditions associated with Euro-American settlement. Other linked projects include an economic analysis of restoration projects (Barbour et al., 2007b), and the influence of native and non-native ungulate herbivores on forest structure (Vavra et al., 2007). Wondzell et al. (2007a) have summarized these studies as an integrated research package around riparian and stream ecosystems in the Upper Grand Ronde River watershed.

Acquiring the GNN Data

IMAP data for Washington and Oregon and supporting information can be downloaded from PNW's website (http://www.fsl.orst.edu/lemma). In Oregon, all map data available at the time of this writing are based on 2000–2001 imagery. In Washington, map data for NE Washington are based on 2000 imagery. In addition, GNN maps based on 1996 and 2006 imagery will be available in early 2009 for western Washington and western Oregon, and for 1994 and 2007 imagery for northwestern California (in the range of the Northern spotted owl).

The plot databases, data dictionary of the detailed attributes, map metadata, and accuracy reports are posted along with the GNN vegetation coverages. Map quality is reported using a number of quantitative assessments at the pixel, plot, and landscape scales. These include cross-validation, confusion matrices, kappa statistics, root mean square errors, observed vs. predicted value scatterplots, map vs. plot sample area distributions, map vs. plot sample area variation, and error maps. All these quality measures are intended to guide the end user toward appropriate use of the data.

Conclusion

IMAP data and models are continuing to be developed by the interagency IMAP partners. Data, models, and results for Oregon will be complete in 2010 and policy scenarios evaluated for a state-wide assessment to be published by ODF. Concurrently, IMAP data and models for Washington are proceeding and planned for completion around 2012. Please contact any of the authors for additional information on current IMAP projects.

References

Barbour, R.J; Hemstrom, M.A., and Hayes, J.L., 2007a, The Interior Northwest Landscape Analysis System: a step toward understanding integrated landscape analysis: Landscape and Urban Planning, v. 80, p. 198-211.

Barbour, R.J., Maguire, D., and Singleton, R., 2007b, Evaluating forest product potential as part of planning ecological restoration treatments on forested landscapes: Landscape Urban Planning.

Beukema, S.J., Kurz, W.A., 1995, Vegetation dynamics development tool user's guide, Vancouver, B.C., Canada: ESSA Technologies Ltd., 51 p.

ESSA Technologies Ltd., 2005, Vegetation Dynamics Development Tool user guide, Version 5.1. Prepared by ESSA Technologies Ltd., Vancouver, BC. 188 p. (http://www.essa.com/downloads/vddt/reppub.htm)

Forest Inventory and Analysis Program, 2006, Field instructions for the annual inventory of Washington, Oregon, and California, 2006: Portland, OR, U.S. Department of Agriculture, Forest Service, Pacific Northwest Research Station. 188 p., plus appendixes. http://www.fs.fed.us/pnw/fia/publications/fieldmanuals.shtml

Hemstrom, M.A., Merzenich, J., Reger, A., and Wales, B.C., 2007, Integrated analysis of landscape management scenarios using state and transition models in the upper Grande Ronde River Subbasin, Oregon, USA: Landscape and Urban Planning, v. 80, p. 198-211.

Hemstrom, M.A., and Merzenich, J., 2006, Results of scenario modeling—Bend and Klamath Falls workshops:. Draft report on file, Pacific Northwest Reseach Station, Portland, OR.

Lettman, Gary, and Hemstrom, M.A., 2008, Interagency Mapping and Assessment Project Study Plan: Draft dated July 1, 2008, on file at Oregon Department of Forestry, 140 p.

Max, T.A., Schreuder, H.T., Hazard, J.W., Oswald, D.D., Teply, J., and Alegria, J., 1996, The Pacific Northwest Region vegetation and inventory monitoring system: Research Paper PNW-RP-493, Portland, OR: U.S. Department of Agriculture, Forest Service, Pacific Northwest Research Station, 22 p.

Ohmann, J.L., and Gregory, M.J., 2002, Predictive mapping of forest composition and structure with direct gradient analysis and nearest-neighbor imputation in coastal Oregon, USA: Canadian Journal of Forest Research, v. 32, p. 725-741.

Ohmann, J.L., Gregory, M.J., and Spies, T.A., 2007, Influence of environment, disturbance, and ownership on forest vegetation of coastal Oregon: Ecological Applications, v. 17, no. 1, p.18-33

Vavra, M., Hemstrom, M.A., and Wisdom, M., 2007, Modeling the effects of herbivores on the abundance of forest overstory states using a state-transition approach in the upper Grande Ronde River Basin, Oregon, USA: Landscape Urban Planning, v. 80, p. 212-222.

Wales, B.C., Suring, L.H., and Hemstrom, M.A., 2007, Modeling potential outcomes of fire and fuel management scenarios on the structure of forested habitats in northeast Oregon, USA: Landscape Urban Planning, v. 80, p. 223-236.

Wondzell, S.M., Burnett, K.M., and Kline, J.D., 2007a, Landscape analysis: Projecting the effects of management and natural disturbances on forest and watershed resources of the Blue Mountains, OR, USA: Landscape Urban Planning, v. 80, p. 193-197.

Wondzell, S.M., Hemstrom, M.A., and Bisson, P.A., 2007b, Simulating riparian vegetation and aquatic habitat dynamics in response to natural and anthropogenic disturbance regimes in the Upper Grande Ronde River, Oregon, USA: Landscape Urban Planning, v. 80, p. 249-267.

This page left intentionally blank

Chapter 12.—Discussion on Remote Sensing for Aquatic Monitoring

Ralph A. Haugerud[1]

Introduction

The special session on Remote Sensing for Aquatic Resource Monitoring concluded with an expert panel discussion. Panel members were Jennifer Bountry (hydraulic engineer, Bureau of Reclamation), Mimi D'Iorio (GIS analyst and database manager, National Oceanic and Atmospheric Administration), Russ Faux (president, Watershed Sciences, Inc.), Steve Lanigan (team leader, Aquatic and Riparian Effectiveness Monitoring Program, U.S. Forest Service), and Amar Nayegandhi (computer scientist, Jacobs Technology, contracted to U.S. Geological Survey). The panel was moderated by Ralph Haugerud (geologist, U.S. Geological Survey) and there were significant contributions from the audience. The dialogue is summarized below in question and answer format. This summary is followed by discussion of what we learned in the course of the special session and identification of some next steps for the Pacific Northwest aquatic monitoring community.

A Note on LiDAR Technology

Presentations in the special session, the panel discussion, and papers in this volume addressed three types of airborne LiDAR (LIght Detection And Ranging) instrument: discrete-return IR LiDAR, high-energy, full-waveform green LiDAR, and EAARL. Essential aspects and differences between these various LiDAR are summarized here, as some readers may not be familiar with them.

Discrete-return infrared (IR) LiDAR instruments use a laser that operates at 1,064 nm wavelength (near infrared), pulses at rates of 10 to 150 kHz, and records the returned signal as one or more discrete returns. These returns are simplifications of a continuous waveform into constituent peaks that correspond (ideally) to reflections from discrete surfaces in the target area. On-ground laser beam diameter typically is on the order of 15 cm. Pulse densities (the basic measure of data quantity and the limiting factor for XY resolution) commonly are in the range of 1–12/m^2 (0.3–1 m spot spacing). Flying height commonly is 800 m or greater. There are many discrete-return IR LiDAR instruments in commercial operation. Surveys by such instruments can be contracted with relative ease. Airborne1, Sanborn, Terrapoint, Watershed Sciences, and many other firms provide discrete-return IR LiDAR surveys. The CLICK (Center for LiDAR Information Coordination and Knowledge) website (http://lidar.cr.usgs.gov) provides a useful entry to the world of IR LiDAR. Swoboda and et al. (2009, chapter 7, this volume), Faux and et al. (2009, chapter 6, this volume), and Hilldale and et al. (2009, chapter 4, this volume) discuss data obtained with discrete-return IR LiDAR. Infrared light does not penetrate water and therefore these instruments can not survey beneath the water surface.

A handful of high-energy, full waveform, green LiDAR instruments are in operation, used primarily for navigational charting in shallow water. These instruments use a laser that operates at 532 nm wavelength and pulses at 0.8–4 kHz. On-ground laser beam diameter is on the order of 2 m and typical pulse densities are 0.05–0.25/m^2 (2–4 m spot spacing). Flying height commonly is 200 m. Rather than simplifying the returned signal to one or more discrete returns, the entire waveform is recorded for later analysis. To provide enough light to return a signal from depths in excess of 20 m, the lasers consume more power and require more cooling than commercial IR systems. Consequently, the instruments are heavy, require a multi-engine aircraft for a platform, and are expensive to operate. Per-area survey costs are an order of magnitude greater than with commercial IR systems, whereas the resulting data densities (per area) are 1–2 orders of magnitude less. The great strength of these systems lies in their ability to provide good bathymetry at depths of 1–20 m in settings where hydroacoustic surveys are hazardous or prohibitively expensive. Guenther (2007) provides a useful discussion of high-energy, full waveform green LiDAR. Systems available for collecting data include:

CHARTS	http://shoals.sam.usace.army.mil/CHARTS/
HawkEye	http://www.airbornehydro.com/HawkEyeII/hawkeyeII.html
LADS	http://www.lhd.tenix.com/Main.asp?ID=30#

CHARTS (and before 2003, its predecessor SHOALS) is operated by the Joint Airborne LiDAR Bathymetry Technical Center of Expertise (JALBTCX), staffed by the Army Corps of Engineers, Naval Oceanographic Office, and NOAA National Geodetic Survey, with significant support by contracted employees of Fugro Pelagos, Inc. CHARTS surveys are available commercially from Fugro Pelagos. Tiffan and et al. (2009, chapter 5, this volume) discuss data obtained with the SHOALS system.

[1]U.S. Geological Survey c/o Dept. Earth & Space Sciences, University of Washington, Seattle, WA 98195, rhaugerud@usgs.gov

EAARL (Experimental Advanced Airborne Research LiDAR) is a very successful attempt to build a green full-waveform LiDAR with a different set of compromises. Using a smaller laser pulsed at 5 kHz and with a 15 cm on-ground beam diameter, EAARL consumes about 1/20th the power of CHARTS or LADS and can be operated from a single-engine aircraft. Consequently, it is significantly cheaper to operate than other bathymetric LiDARs. Further, the short pulse width and narrow receiver field-of-view of the EAARL allows simultaneous mapping of bare-earth topography and shallow submerged topography in coastal and riverine environments. Nayegandhi (2009, chapter 1, this volume) further describes the EAARL system. The EAARL system is operated by the USGS (formerly by NASA) and is not available commercially. Material on the Web about EAARL includes:

http://lidar.cr.usgs.gov/downloadfile2.php?file=Wright_EAARL_Overview.pdf
http://coastal.er.usgs.gov/remote-sensing/advancedmethods/eaarl.html

McKean and others (2009, chapter 2, this volume) and Kinzel (2009, chapter 3, this volume) discuss data obtained with EAARL.

Two other LiDAR technologies are worth briefly noting. In the last few years, small scanning LiDAR units designed to be mounted on a tripod have become available and are used for surveying areas with dimensions of 101–103 m with accuracies of a centimeter. The original application of LiDAR was as fixed, upward-looking instruments for measuring the height and density of atmospheric particulates.

Questions (and comments) and Answers

1. What is the best technology for surveying streams?

Airborne discrete-return infrared (IR) LiDAR—the technology used by the Puget Sound LiDAR Consortium and the Oregon LiDAR Consortium—can provide excellent descriptions of the subaerial environment. Over the last decade, airborne IR LiDAR has become the technology of choice for obtaining digital elevation models (DEMs) at XY resolution <5 m, supplanting photogrammetry, IFSAR, and ground surveys (Maune, 2007). For surveys with extents less than approximately 10 km^2 and requiring very high resolutions (XY resolution <0.3 m or Z resolution <5 cm), ground-based or photogrammetric technologies are still preferred. Airborne IR LiDAR is particularly effective at mapping topography in forested regions whereas photogrammetry and IFSAR tend to map only the canopy surface.

For the wet part of the world, possible survey techniques include hydroacoustic surveys in streams large enough for boat operations, full-waveform green LiDAR, IR LiDAR at low flow to survey the emergent part of the channel, and field crews with sticks, GPS, and(or) total-station instruments.

What is the best technology?

All these technologies have their place. Key issues include the spatial scale (extent and resolution) involved, access, weather, whether the technology is capable in the particular setting, and cost. Present technology limits green LiDAR to an XY resolution of 1 m (EAARL) to 2 m (SHOALS, CHARTS) with Z resolution on the order of a decimeter. IR LiDAR typically produces higher resolutions, as good as 0.3 m XY and a few centimeters in Z. Hydroacoustic surveys can provide excellent high-resolution data but at a limited extent, typically 2,030 km of river length. Moreover, many streams large enough to survey from a boat are not considered navigable and thus there may be legal and physical access issues exemplified by cross-stream fences. Airborne LiDAR, whether IR or green, requires the ground be clearly visible from the aircraft; where rain and (or) low cloud cover are the norm, the cost of standby time while waiting for adequate weather may favor a ground-based survey. For mountain streams, pool depths might be most accurately and cheaply obtained by a field crew, especially as CORS (Continuously Operating Reference System, e.g., Stone, 2006) GPS becomes more widely available. Deep or turbid streams can not be surveyed by green LiDAR (see below). In some settings, stream depth may be usefully inferred from hyperspectral imagery. For some streams, the combination of a hydroacoustic survey at high flow (during winter, or high tide) and IR LiDAR at low flow may be very effective.

Comparative costs are not easily estimated. At present, large-area IR LiDAR surveys cost about $1/acre and costs vary with size of surveyed area, local relief, pulse density requirements, and weather and access conditions. Small and irregular areas (e.g., stream corridors) cost significantly more. SHOALS/CHARTS are an order of magnitude more expensive. EAARL is less expensive to operate than SHOALS/CHARTS (but in deep-water settings, EAARL is less capable). However, because EAARL is not a commercial system, costs are not comparable. West of the Cascade crest, the rarity of coincident good weather, suitable ground conditions (snow absent, streams not flooding), and leaf-off conditions (to increase the fraction of LiDAR pulses that yield ground returns) is likely to significantly increase the cost, or reduce the success, of all airborne LiDAR surveys. Ground surveys almost always will be more expensive than airborne surveys for the amount of data obtained. But ground surveys typically produce much less data per unit stream length. To a first approximation, the per-area cost of hydroacoustic surveys varies inversely with water depth, as swath width is greater in deeper water.

These technologies are complementary and the best solution is often a combination of techniques depending on the physical characteristics of the stream. For example, IR LiDAR can provide wide area characterization of the floodplain morphology, riparian vegetation, and upland influences (i.e., landslides, roads, etc.) allowing ground based surveys to concentrate efforts within the wetted channel or in intensive study reaches. A small footprint, bathymetric LiDAR (EAARL or successor) may eventually offer the best solution for stream surveys, but it is not there yet.

2. How important is bathymetry? Can we get by without it?

Bathymetry of streams is expensive to acquire. For the same cost, one can survey the topography of much larger riparian and upland areas. The bathymetry of steep, high-energy mountain streams may change rapidly and surveys may have a limited useful lifetime, further increasing their relative cost.

Can we get adequate answers without the expense of bathymetric surveys?

In general, there is no simple answer to this question. A good topographic DEM, probably acquired by infrared discrete-pulse LiDAR, will be sufficient for modeling floodplain inundation. For detailed modeling of bank protection, levee removal, or design of diversion dams, good bathymetry is essential. Our experience with hydraulic modeling is "Garbage in, garbage out." We must pay the cost of collecting bathymetry to get useful results.

3. Can we survey subaquatic vegetation with waveform LiDAR?

Currently (2008), there is a great deal of research into the potential for describing the forest canopy with airborne discrete-return IR LiDAR and airborne and satellite full-waveform IR LiDAR (e.g., Lefsky and others, 2002; Andersen and others, 2005; Hyypp et al., 2008). With time, IR LiDAR is likely to prove to be the best technique for measuring many aspects of forest vegetation (with the exception of species composition) over areas of 1 to 10,000 km^2.

Is green waveform LiDAR similarly powerful in describing subaquatic vegetation (SAV)?

Describing SAV with green waveform LiDAR is a difficult problem. The SAV signal is convolved with attenuation and scattering within the water column and surface and bottom reflections to produce the return waveform. Deconvolving the SAV signal is challenging. Sea grass can be distinguished from bare sandy bottom (Nayegandhi, personal commun., 2008; see also Tuell and et al., 2005) largely because of the gross difference in albedo. There is more work to be done.

4. Did EAARL find bottom everywhere along the Boise River?

There are limitations to the settings in which green LiDAR systems can measure bathymetry.

Was EAARL everywhere effective in the recent survey of the Boise River?

No. Where the water is too turbid, or bottom reflectivity is too low, green LiDAR systems will not map the bottom. Water clarity is the biggest factor. In general, EAARL can map at depths up to 1.5x the Secchi depth. Bathymetric LiDARs use green lasers: if the bottom is dark in green light, it will be hard to map. If bottom is visible to the naked eye, it can be mapped with EAARL. If not, EAARL may or may not be capable of mapping the bottom.

Note that other bathymetric survey techniques rarely provide depths for all of a stream. Although incomplete, an EAARL survey may still be more complete than any feasible alternative.

5. Is there EAARL capacity to survey all PNW streams?

McKean and others (2009, chapter 2, this volume) indicate that EAARL can survey moderate-size stream channels at about 30 km/h. There are hundreds of thousands of kilometers of significant streams in the Pacific Northwest.

Is EAARL available for enough time to survey all Pacific Northwest streams?

Probably not. EAARL is a research system, built by Wayne Wright at NASA to map coral reefs and other coastal environments. Since EAARL was built, Wright and EAARL have moved to the USGS Coastal and Marine Geology program. There is some freedom for EAARL to work on western streams, but the primary obligation of the instrument is to the Coastal and Marine Geology program. In particular, during hurricane season on the East Coast—a large part of summer and early fall, prime time for western stream surveys—EAARL must be on the East Coast.

There are plans to build a second EAARL system to be mounted on a USGS aircraft. This should increase availability, but it is still unlikely that there would be sufficient capacity to monitor all streams of interest to the PNAMP community. Funding is a different question.

6. When will we see a commercial equivalent to the EAARL system?

Although NOAA and the USGS have supported EAARL, and the USGS may build a second EAARL, this may not provide the capacity that is needed to survey western streams. Furthermore, Federal research agencies find it difficult to staff, on a sustained basis, survey operations that depend on highly skilled operations personnel. The required capacity could be provided by the commercial sector.

When will we see a commercial equivalent to the EAARL system?

Watershed Sciences is very interested in lightweight, small-footprint green full-waveform LiDAR. They are interested in mounting a federally owned EAARL on Watershed Sciences aircraft and have approached commercial instrument manufacturers (Optech, Leica) about building a similar system. The primary concerns are the cost of the instrument and whether there will be sufficient demand to support its operation.

What if the possible market in estuarine mapping does not pan out because EAARL produces poor results on the dark bottoms of Pacific NW estuaries?

Is there a Federal incentive to operate such an instrument, or a guaranteed Federal market?

We should remind ourselves that the primary purpose of EAARL is technology development. EAARL does not exist to supplant the commercial sector, but at present is the only system available with its unique capacity to survey moderate-depth streams at moderate cost.

7. Can we promote landscape-wide LiDAR surveys?

Limited budgets and a strong focus on in-stream and riparian issues have led fisheries interests to fund LiDAR surveys of narrow corridors along streams. Yet stream health is affected by the entire drainage basin, stream-corridor LiDAR surveys are more expensive per unit area than landscape-wide surveys, other groups will use LiDAR data from upslope areas, and the benefit-cost ratio to the community as a whole is very likely greater for landscape-wide LiDAR surveys.

How can we promote landscape-wide surveys?

There is not a simple answer to this question. The U.S. Forest Service's Aquatic and Riparian Effectiveness Monitoring Program (AREMP; see Eldred, 2009, chapter 10, this volume) would benefit from landscape-wide surveys to provide a more accurate stream network, to provide a more accurate and more uniform road network, and to provide a better vegetation layer (but see Moeur et al., 2009, chapter 11, this volume, for a LANDSAT-based solution). But AREMP alone can not fund large-area LiDAR.

The Puget Sound LiDAR Consortium has been contracting large-area surveys since 1999. It has been most successful at covering the landscape when it has had significant Federal funding that is not strongly tied to a particular area. When all funding has been from partners with strong responsibilities to their own jurisdictions or immediate areas of interest, the result has been patchwork partial coverage. Despite this, the consortium may still be the best way to provide relatively coherent coverage with common specifications, deliverables, and quality control. The younger Oregon LiDAR Consortium, with significant State funding and a commitment to covering much of the State, may be more successful at landscape-wide coverage.

8. What about sensors other than airborne LiDAR?

Remote sensing comes in flavors other than airborne LiDAR: CASI (Garono and et al., 2009, chapter 8, this volume), Landsat (D'Iorio and Volk, 2009, chapter 9, this volume; Moeur and et al., 2009, chapter 11, this volume), FLIR (D'Iorio and Volk, 2009, chapter 9, this volume) IKONOS, ASTER, and many more.

What do these other sensors offer to the aquatic monitoring community?

Landsat has the particular advantage of near-global coverage at very little cost to the end user. Disadvantages are its limited spatial resolution (about 30 m) and modest spectral resolution. Landsat data may be particularly appropriate for defining a limited spatial target for analysis with a higher resolution, more expensive airborne sensor.

The CASI sensor offers greater spatial and spectral resolution and shows significant utility in mapping landcover types to better understand habitat dynamics (Garono et al., 2009, chapter 8, this volume).

9. How do we encourage data sharing?

Audience members expressed frustration, echoed by the panel, over the frequent inability of agencies to share data in a timely fashion, thus increasing the cost of monitoring and limiting the quantity and richness of science that can be done.

How do we fix this?

Discussion identified several impediments to data sharing: absence of a high-level mandate to share; licensing restraints on commercial data; fear of lost glory for failing to interpret the story first; fear of loss of credit to the entity that funded data acquisition; lack of confidence that data from another agency are of adequate quality; ignorance about what data are available.

Monitoring programs could refuse to purchase data without unlimited redistribution rights. Grants that fund data acquisition could require speedy release of data. The geospatial community could develop more complete, and stronger, standards for data quality. The monitoring community could continue to reinforce the benefits of sharing.

Better metadata would help. Necessary improvements include widely understood formats for spatially explicit metadata, routine designation of go-to individuals (not groups) for all datasets, and routine inclusion in all metadata of direct links to data.

Audience members reported experience with agencies that claim incomplete QA/QC to avoid release of data, followed by the suggestion that such data be released with a PRELIMINARY stamp. It was then observed that digital GIS data commonly do not have a place for such a stamp. The Puget Sound LiDAR Consortium is concerned that distribution of data constitutes implicit acceptance, thus the PSLC does not distribute preliminary data. But the PSLC's acquisition contracts define a short (3045 day) window in which QA/QC must be completed.

It was suggested that social scientists be included in monitoring projects with the explicit task of encouraging natural-resource scientists to share data. This was followed by an anecdote about a project that had 20% of the budget allocated to social science, yet when the social scientist talked the biologists were out in the hall having side conversations.

10. There is more to monitoring than data acquisition

Beyond data acquisition, monitoring also requires data analysis. Considerable concern was expressed about funding of data acquisition without corresponding funding of data analysis. In some cases, data acquisition contractors can perform analysis and it may be useful to include analysis in the acquisition contract.

Concern also was voiced for the need of the monitoring community—and often individual agencies—to create and conserve a pool of expertise. Too often, hard-won analytical expertise is lost as temporary employees move on.

Some concern was voiced that a disproportionate amount of available funding is directed to sensor development instead of data analysis. This did not appear to be a majority view.

11. How do we pool monitoring funds from multiple agencies?

Economies of scale, shared interests, and multiple-use data suggest that would be good to pool monitoring funds from multiple agencies for acquisition of remotely sensed data.

How do we do this?

The following suggestions were made: To collaborate in data acquisition, managers need to be convinced that collaboration will (a) save money, (b) reduce risk, and (or) (c) help make better decisions. Some agencies divide funding for natural-resource studies into inventory and monitoring components; however, both activities commonly need the same data and the division makes it more difficult to fund data acquisition. We need the secretaries of Agriculture, Commerce, Defense, Energy, and Interior to give us a mandate to collaborate. PNAMP has a role to play in solving these coordination problems.

Shared data acquisition will be easier with strong data standards. Existing standards for bathymetric mapping are oriented towards nautical charting and, in shallow-water areas, do not match well with the needs of natural-resource scientists or the capabilities of current technology. NOAA and USGS could collaborate to provide better standards for mapping of shallow-water areas. For IR LiDAR, “A proposed specification for lidar surveys in the Pacific Northwest” by Haugerud et al. (2009) should be useful.

What have we learned?

LiDAR, which is primarily geometric (position, shape) information, is qualitatively different from other remote sensing technologies that provide reflectance (Landsat, CASI) or emittance (FLIR) data, and from which geometric information is derived by photogrammetry. LiDAR data are not pictures, though we commonly make pictures from them. A growing body of experience demonstrates that such shape information is very powerful (e.g., Haugerud and et al., 2003b; McKean and et al., 2009, chapter 2, this volume).

IR LiDAR works well for describing the terrestrial environment, including riparian and upland areas. EAARL is useful for describing in-stream parts of many western aquatic systems, as well as the riparian and upland areas, although it has less resolution and is likely to be more costly than IR LiDAR.

Airborne IR LiDAR and EAARL (and its successors) are likely to revolutionize ecological studies (Vierling and et al., 2008; McKean et al., 2009, chapter 2, this volume). They provide increased ecological scope; make it feasible to acquire continuous data; establish a more accurate geometric framework for sensor fusion, correlation with ground data, and spatial analysis; and for some phenomena provide previously unattainable spatial resolution and accuracy.

Without a robust geometric framework and good geolocation of remotely sensed data, fusion of data from different sensors and correlation of remotely sensed data with ground observations is likely to produce significant errors. Analysis of a subset of the Hood Canal CASI data (Garono et al., 2009, chapter 8, this volume) by Haugerud et al. (2003a) illustrates the problem. In an attempt to understand physiographic controls on eelgrass distribution, Haugerud et al. (2003a) intersected CASI-defined landcover with elevation and local slope. Although there were significant correlations, the strongest conclusion from the analysis was that many elevations inferred for the CASI pixels were incorrect. CASI data were from the intertidal zone (minimum elevation circa -4 ft MLLW, maximum elevation circa +8 ft MLLW), yet a significant number of CASI pixels had apparent elevations outside this range. This largely reflects errors in the reference DEM, although there was some contribution from mislocation of the CASI data (with estimated RMS location errors of 5–24 m). One of the strengths of LiDAR data is that above all they are accurately located—except for the intensity values, LiDAR data are locations (x,y,z). As such they provide a robust framework for spatial correlation and analysis of other information.

Computing with and managing the large volumes of data produced by LiDAR surveys are problematic for many users. Crosby et al. (2006), Swoboda et al. (2009, chapter 7, this volume), and McKean et al. (2009, chapter 2, this

volume) suggest that the solution lies in centralized data storage and computation, with associated economies of scale and concentration of expertise. Results would be accessed via a custom web interface and file download or as a web mapping service. Such centralized storage and computation may become a locus for a growing community of expertise in analyzing these data.

Presentations at the session provided some suggestions on data density and accuracy necessary for aquatic resource monitoring. McKean et al. (2009, chapter 2, this volume) state that 0.25 pulse/m^2 (2 m spot spacing) EAARL data were not dense enough to accurately describe steep banks. Hilldale et al. (2009, chapter 4, this volume) note that poor XY resolution because of large spot size for SHOALS (and CHARTS) is a problem, and that existing mapping standards (IHO, NMAS) may not be adequate to meet the needs of the aquatic monitoring community. Hilldale et al. (2009, chapter 4, this volume) also note that stated errors for LiDAR are commonly Z errors on flat ground; XY errors on the steep slopes common in Pacific Northwest riparian zones contribute to aggregate Z errors that commonly exceed stated values.

What do we do next?

Presentations in the special session and the panel discussion illuminated some likely next steps for the Pacific Northwest aquatic monitoring community.

We need a better understanding of the capacities and associated costs of various bathymetric survey technologies, as well as a better understanding of our data needs, so that we can select the most appropriate and most cost-effective survey technology. To this end, we could use more reports on bathymetric surveys and consequent analyses that document survey methods, survey costs, the data obtained, and the results of data analysis. These reports will be most useful if they include sensitivity analyses that explore how the results depend on the quality and quantity of the survey data.

We need to share data more effectively. To do this, we need tools to facilitate sharing. These include better metadata, including a standard protocol for spatially explicit metadata; strong data standards that are appropriate for community needs; and a better data inventory. We also need to grow a culture that promotes data sharing. Grants that fund data acquisition should require timely release of data. Where we are allowed to copyright our data, we can assert copyright and license the use of our data under terms that make it freely available (see http://creativecommons.org/). We should support our professional societies as they develop policies that promote open access to data.

We need to devote more resources to validating models developed for aquatic monitoring. The use of existing datasets to model watershed health is a necessary part of the large and complex task that is aquatic monitoring. However, our ability to construct a model is no guarantee that the model is useful. Modeling needs to be verified by independent observations! Validation with the observations used to construct the model is likely to be uninformative. Models developed on the basis of observed correlations, rather than on a basis of explicit, quantitative knowledge of the relevant biological, hydrological, and geological processes, are especially likely to need validation.

We need to acquire landscape-wide LiDAR data. We know that the benefits of such data for aquatic monitoring will be great, but the costs are likely beyond the resources of this community alone. However, large-area, high-resolution LiDAR surveys also provide useful information on timber resources, forest health, wildfire fuel loads, forest carbon sequestration, landslide occurrence and susceptibility, seismic hazards, flood hazards, water resource availability, habitat for terrestrial and avian species, highway design, irrigation design, and more, and the relevant communities should be amenable to calls for collaboration. The Puget Sound LiDAR Consortium and the Oregon LiDAR Consortium are cooperatively funding large-area surveys and effectively sharing data. The USGS hosts a nascent national LiDAR initiative. The Pacific Northwest Aquatic Monitoring Partnership should encourage the aquatic monitoring community to participate in these efforts. We clearly need more research on obtaining habitat metrics from airborne LiDAR data, but our need to monitor change dictates that we acquire the best data possible now, without full knowledge of all the ways that these data will be analyzed in the future.

Acknowledgments

I thank Russ Faux, Amar Nayegandhi, and Jennifer Bayer for helpful comments on this text.

References Cited

Andersen, H.E., McGaughey, R.J., and Reutebuch, S.E., 2005, Estimating forest canopy fuel parameters using LIDAR data: Remote Sensing of Environment, v. 94, p. 441-449.

Crosby, C.J., Arrowsmith, J R., Frank, E., Nandigam, V., Kim, H.S., Conner, J., Memon, A., Baru, C., 2006, Enhanced access to high-resolution LiDAR topography through cyberinfrastructure-based data distribution and Processing: Eos Transactions American Geophysical Union, v. 87, n. 52, Fall Meeting Supplement, Abstract IN41C-04. [Slides from this talk - 5.4 MB]

D'Iorio, M., and Volk, C., 2009, Using remote sensing to assess anthropogenic influcences on stream temperature, *in* Bayer, J.M., and Schei, J.L., eds., PNAMP Special Publication: Remote Sensing Applications for Aquatic Resource Monitoring, Pacific Northwest Aquatic Monitoring Partnership, Cook, Washington, chap. 9, p. 75-80.

Eldred, P., and Gallo, K., 2009, Modeling watershed condition and trend – How the Aquatic Riparian Effectiveness Monitoring Program (AREMP) is evaluating watershed condition and trend in the Pacific Northwest, *in* Bayer, J.M., and Schei, J.L., eds., PNAMP Special Publication: Remote Sensing Applications for Aquatic Resource Monitoring, Pacific Northwest Aquatic Monitoring Partnership, Cook, Washington, chap. 10, p. 81-82.

Faux, R.N., Buffington, J.M., Whitley, M.G., Lanigan, S.H., and Roper, B.B., 2009, Use of airborne near-infrared LiDAR for determining channel cross-section characteristics and monitoring aquatic habitat in Pacific Northwest rivers: A preliminary analysis, *in* Bayer, J.M., and Schei, J.L., eds., PNAMP Special Publication: Remote Sensing Applications for Aquatic Resource Monitoring, Pacific Northwest Aquatic Monitoring Partnership, Cook, Washington, chap. 6, p. 43-60.

Garono, R.J., Simenstad, C.A., Robinson, R., Weller, C., and Todd, S., 2009, Mapping intertidal eelgrass landscapes in Hood Canal (WA) using high spatial resolution Compact Airborne Spectrographic Imager (CASI) imagery, *in* Bayer, J.M., and Schei, J.L., eds., PNAMP Special Publication: Remote Sensing Applications for Aquatic Resource Monitoring, Pacific Northwest Aquatic Monitoring Partnership, Cook, Washington, chap. 8, p. 69-74.

Guenther, G., 2007, Airborne Lidar Bathymetry *in* Maune, D.F., ed., Digital elevation model technologies and applications: the DEM users manual, 2nd edition: American Society for Photogrammetry and Remote Sensing, Bethesda, MD, p. 253-320; see http://shoals.sam.usace.army.mil/downloads/Publications/DEM_Chapter08.pdf

Haugerud, R., Finlayson, D.P., Garono, R., Greenberg, H., Logsdon, M., and Simenstad, C., 2003a, Physiographic controls on the distribution of eelgrass (Zostera marina) in Hood Canal: Puget Sound–Georgia Basin Research Conference, Vancouver, BC. [Presentation online at http://david.p.finlayson.googlepages.com/haugerud_2003.pdf]

Haugerud R.A., Harding D.J., Johnson S.Y., Harless J.L., Weaver C.S., and Sherrod, B.L., 2003b, High-resolution lidar topography of the Puget Lowland, Washington—a bonanza for earth science: GSA Today, v. 13, n. 6, p. 4–10.

Haugerud, R., Curtis, T., Madin. I., Martinez, D., Nelson, S., Nile, E., and Reutebuch, S., 2009, A proposed specification for lidar surveys in the Pacific Northwest, version 1.1: available at http://pugetsoundlidar.ess.washington.edu/links.htm

Hilldale, R.C., Bountry, J.A., and Piety, L.A., 2009, Using bathymetric and bare earth LiDAR in riparian corridors: Applications and challenges, *in* Bayer, J.M., and Schei, J.L., eds., PNAMP Special Publication: Remote Sensing Applications for Aquatic Resource Monitoring, Pacific Northwest Aquatic Monitoring Partnership, Cook, Washington, chap. 4, p. 27-34.

Hyypp, J., Hyypp, H., Leckie, D., Gougeon, F., Yu, X., and Maltamo, M., 2008, Review of methods of small-footprint airborne laser scanning for extracting forest inventory data in boreal forests: International Journal of Remote Sensing, v. 29, n. 5, p. 1339-1366.

Kinzel, P.J., 2009, Advanced tools for River Science: EAARL and MD_SWMS, *in* Bayer, J.M., and Schei, J.L., eds., PNAMP Special Publication: Remote Sensing Applications for Aquatic Resource Monitoring, Pacific Northwest Aquatic Monitoring Partnership, Cook, Washington, chap. 3, p. 17-26.

Lefsky, M.A., Cohen, W.B., Parker, G.G., and Harding, D.J., 2002, LiDAR remote sensing for ecosystem studies: Bioscience, v. 52, p. 19–30.

Maune, D.F., ed., 2007, Digital elevation model technologies and applications: the DEM users manual, 2nd edition: American Society for Photogrammetry and Remote Sensing, Bethesda, MD, 655 p.

McKean, J., Issak, D., and Wright, W., 2009, Stream and riparian habitat analysis and monitoring with a high-resolution terrestrial-aquatic LiDAR, *in* Bayer, J.M., and Schei, J.L., eds., PNAMP Special Publication: Remote Sensing Applications for Aquatic Resource Monitoring, Pacific Northwest Aquatic Monitoring Partnership, Cook, Washington, chap. 2, p. 7-16.

Moeur, M., Ohmann, J., Hemstrom, M., Burcsu, T., and Merzenich, J., 2009, Projecting watershed condition with Interagency Mapping and Assessment Project (IMAP) vegetation data and landscape models, *in* Bayer, J.M., and Schei, J.L., eds., PNAMP Special Publication: Remote Sensing Applications for Aquatic Resource Monitoring, Pacific Northwest Aquatic Monitoring Partnership, Cook, Washington, chap. 11, p. 83-92.

Nayegandhi, A., Wright, C.W., and Brock, J.C., 2009, EAARL: An airborne LiDAR system for mapping coastal and riverine environments, *in* Bayer, J.M., and Schei, J.L., eds., PNAMP Special Publication: Remote Sensing Applications for Aquatic Resource Monitoring, Pacific Northwest Aquatic Monitoring Partnership, Cook, Washington, chap. 1, p. 3-6.

Stone, W., 2006, The evolution of the National Geodetic Survey's continuously operating reference station network and Online Positioning User Service: Position, Location, and Navigation Symposium, 2006 IEEE/ION, p. 653-663, ISBN: 0-7803-9542-2, see http://ieeexplore.ieee.org/servlet/opac?punumber=10978 or http://geodesy.noaa.gov/CORS/Articles/CORS-OPUS-Stone.pdf

Swoboda, K., Wille, K., Beaty, M., and Gault, G., 2009, Managing, manipulating, and serving LiDAR terrain data and orthoimagery for riverine habitat assessment and remediation project design for salmon recovery in the Pacific Northwest, *in* Bayer, J.M., and Schei, J.L., eds., PNAMP Special Publication: Remote Sensing Applications for Aquatic Resource Monitoring, Pacific Northwest Aquatic Monitoring Partnership, Cook, Washington, chap. 7, p. 61-68.

Tiffan, K.F., Wagner, P.G., and Wolf, K.S., and Hoffarth, P.A., 2009, Application of the SHOALS survey system to fisheries investigations in the Columbia River, *in* Bayer, J.M., and Schei, J.L., eds., PNAMP Special Publication: Remote Sensing Applications for Aquatic Resource Monitoring, Pacific Northwest Aquatic Monitoring Partnership, Cook, Washington, chap. 5, p. 35-52.

Tuell, G.., Park, J.Y., Aitken, J., Ramnath, V., and Feygels, V., 2005, Adding hyperspectral to CHARTS: early results: Proceedings, U.S. Hydro 2005, The Hydrographic Society of America, March 29-31, San Diego, CA, paper 7-1, 10 p., http://www.thsoa.org/hy05/07_1.pdf

Vierling, K.T., Vierling, L.A., Gould, W.A., Martinuzzi, S., and Clawges, R.M., 2008, Lidar: shedding new light on habitat characterization and modeling: Frontiers in Ecology and the Environment, v. 6, n. 2, p. 90-98.

Publishing support provided by the U.S. Geological Survey
Publishing Network, Tacoma Publishing Service Center

For more information concerning the research in this report, contact the
Coordinator, Pacific Northwest Aquatic Monitoring Partnership
5501A Cook-Underwood Road
Cook, Washington 98605
http://www.pnamp.org/

Bayer, and Schei eds.,—PNAMP Special Publication: Remote Sensing Applications for Aquatic Resource Monitoring: Results of a Special Session at the 2008 ASPRS Annual Conference